Investigation of the Energetic Performance of an Attached Solar Greenhouse through Monitoring and Simulation

by

Osama Asa'd

Submitted in partial fulfilment of the requirements
for the degree of Master of Applied Science

at

Dalhousie University
Halifax, Nova Scotia
February 2019

Dedication Page

To:

My mother, who is always my motivation

My brothers and sisters, who are my backbone

without their support, encouragement and prayers this work could never be done

Table of Contents

List of Tables

List of Figures

Abstract

In Canada, energy costs represent a significant portion of the overall operating cost of greenhouses. This energy is mostly consumed in winter to satisfy the heating requirement of greenhouses. Therefore, it is essential to investigate energy efficient systems to reduce the heating requirements in greenhouses, and as a result, improve the overall performance. Solar greenhouses are designed to maximize the heat gain in order to reduce the heating loads in winter. This research work was conducted to investigate the energetic performance of an attached solar greenhouse connected to a rock-bed thermal storage and located in Joliette near Montreal through monitoring and simulation. A TRNSYS model was developed to analyze the energetic performance of the attached greenhouse and rock-bed thermal storage. The TRNSYS model was validated by comparing the measured greenhouse indoor temperatures and rock-bed outlet temperatures to the predicted ones for three periods. The validation results of the three periods showed a good agreement between the measured and predicted temperatures.

The optimal design of a solar greenhouse is essential to have high performance in terms of productivity and energy costs. Therefore, a parametric study using the TRNSYS validated model was conducted to investigate the effects of the heating and cooling set point temperatures, rock-bed air flow rate, cover materials, mechanical outside air ventilation, and rock-bed thermal storage size in order to improve the overall design. The parametric study results showed that the rock-bed air flow rate and the U-value of the greenhouse cover material have a significant effect on the greenhouse indoor temperatures. While changing the cooling (rock-bed charging) set-point temperature from 12°C-22°C while keeping the heating (rock-bed discharging) set-point temperature fixed at 10°C did not have a significant effect on the greenhouse indoor temperatures. As the rock-bed size increased, the amount of heat discharged from the rock-bed thermal storage increased. As a result, the greenhouse indoor temperatures increased in winter nights. Moreover, in order to avoid the undesirable high indoor temperatures especially in summer, the installation of the mechanical outside air ventilation is necessary.

List of Abbreviations and Symbols Used

A	Cross-sectional area of the rock-bed (m^2)
CFD	Computational Fluid Dynamics
C_p	Specific heat of air (kJ/kg.°C)
C_r	Specific heat of rock (kJ/kg.°C)
D-Poly	Double layers of polyethylene
EAHESS	Earth-to-air heat exchanger systems
EF	Model Efficiency
ETFE	Ethylene tetra fluoroethylene
FRP	Fiber glass reinforced polyester
HVAC	Heating, Ventilation and Air Conditioning
k	Rock conductivity (W/m.°C)
L	Rock-bed length in the flow direction (m)
low-e	Low emissivity
MAE	Mean Absolute Error
$\dot{m}$	Mass flow rate (kg/hr)
N	Number of segments
NREL's	National Renewable Energy Laboratory's
NSRDB	National Solar Radiation Data Base
P	perimeter of rock bed wall (m)
PCMs	Phase change materials
PE	Single layer of polyethylene
Poly film	Polyethylene
PV	Solar photovoltaic system

PVDF	Polyvinylidene difluoride
$\dot{Q}$	Heat gain or loss (W)
r	Sample correlation coefficient
r^2	Pearson coefficient of determination
RMSE	Root Mean Squared Error
R-value	Thermal resistance
SHESS	Soil heat exchanger-storage system
SSP	Shallow solar pond
t	Time (hr)
T	Air temperature (°C)
$T_{ambient}$	Ambient temperature (°C)
$T_{Bed\text{-}Bottom}$	Bottom temperature of the rock-bed (°C)
$T_{cooling\text{-}set\text{-}point}$	Cooling set-point temperature (°C)
TESS	Thermal energy storage system
T_{env}	Temperature of the surroundings (°C)
$T_{heating\text{-}set\text{-}point}$	Heating set-point temperature (°C)
T_{in}	Temperature of air entering the rock bed (°C)
T_{GH}	Greenhouse temperature (°C)
TMY	Typical meteorological year
TRNSYS	TRaNsient SYstem Simulation
TSSE	Total Sum of Squared Error
U-value	Thermal transmittance
U	Loss coefficient from the rock bed to surroundings (kJ/hr. m².K)
V	Volume of rock bed (m^3)
$\dot{V}$	Air flow rate (ft^3/min)

WEL	Web Energy Logger

Greek Symbols

ρ_r	Apparent rock density (accounting for voids) (kg/m^3)

Subscripts

b, r	Rocks (or bed) material
env	Environment
i	Inside
o	Outside
conv	Convection

Acknowledgements

First and foremost, I am greatly thankful to my supervisor Dr. Ismet Ugursal for his continuous support, patience, motivation and trust in me over the last two years. He encouraged and helped me to improve myself as a student and as a researcher. The priceless advices Dr. Ismet Ugursal gave me on both my research and professional career had a huge positive impact on my understanding of life and on whom I want to be in the future. He has been not just a supervisor in school but also a mentor in my life. I was honored to be his student and I could not have imagined doing this without him.

I would like to thank my co-supervisor Dr. N. Ben-Abdallah for giving me the opportunity to work on this project. I had the privilege of working with him, and his advices and comments have been always so supportive and helpful. Having him as a co-supervisor made me job easier and I am so grateful for it.

I am also thankful to my committee members Dr. J. Militzer and Dr. A.M. Al Taweel for reviewing my thesis and providing valuable feedback as members of my examining committee.

Chapter 1

Introduction

The focus on finding energy saving methods in greenhouses to reduce the heating costs started in the early seventies after the oil crisis (Critten and Bailey, 2002). Greenhouses have been used for centuries to provide an isolated environment from the outside conditions (e.g., temperature, relative humidity, wind speed) to grow plants and supply the market with a variety of products in all seasons. Greenhouses are preferred in winter to open field production in cold climates such as Canada, since they protect the plants from the cold ambient temperature. Greenhouse production is increasing worldwide, and it has higher production and irrigation efficiency than field production (Stanghellini et al, 2003; Costa et al., 2004; Van Kooten et al., 2008). Figure 1 shows the increase in the total area of greenhouses in Canada from 1996 to 2016. It can be noticed that the total area declined since 2006 due to different factors such as competition from imports, increasing of labour costs, and fluctuations in product prices.

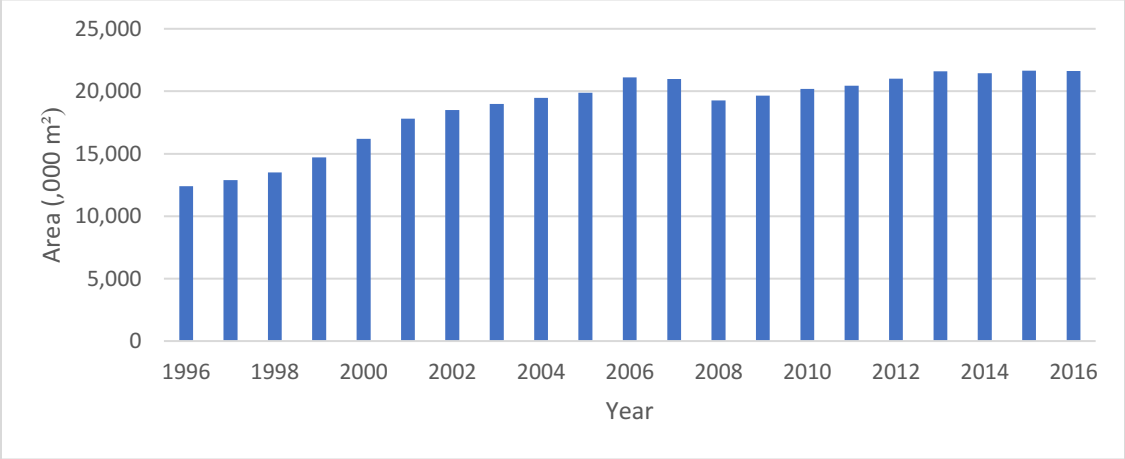

Figure 1. Total area of the Canadian greenhouses from 1996 to 2016. (Statistics Canada. CANSIM Table 001-0047)

In cold climates, the energy consumed in greenhouses is mostly for heating. Therefore, it is a requirement to seek energy efficient technologies to reduce the heating loads in greenhouses during winter. Energy costs (fuel and electricity) represent the second largest cost of the total operating cost of greenhouses as it represents 11% of the total operating expenses in 2016 as shown in Figure 2. Energy costs come second to labor costs which represent almost one-third of the total operating costs. Solar greenhouses represent an effective technique to reduce energy consumption in the agriculture sector, where the greenhouse heating requirement is mostly provided from the sun.

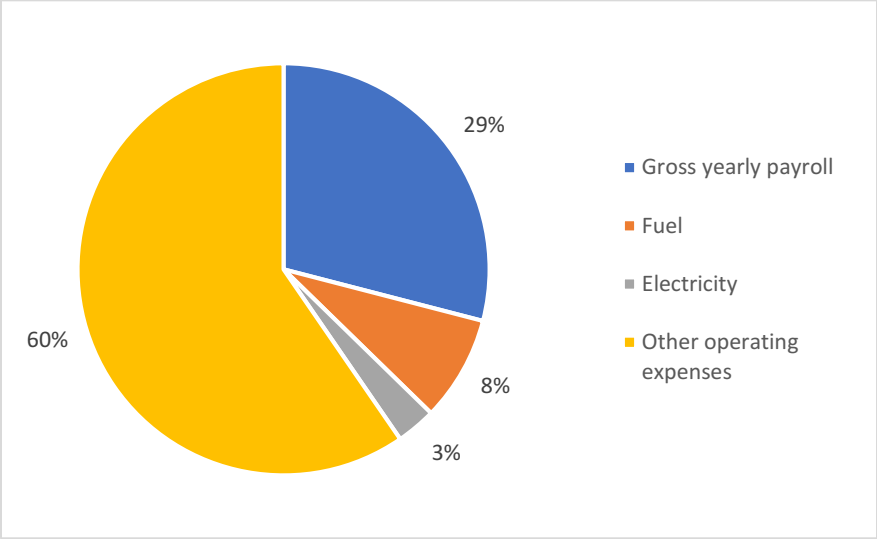

Figure 2. Total operating expenses of greenhouses in Canada in 2016. (Statistics Canada. CANSIM Table *001-0052*).

The most important characteristics which make solar greenhouses effective in cold climates in terms of productivity and energy cost are:

- The glazed walls are oriented to the south to maximize the heat gain,
- Solar greenhouses contain storage systems to store the surplus heat,
- The unglazed walls are well insulated,

- The greenhouse ventilation is mechanically controlled,

Temperature and ventilation control are important to have a high performance of the greenhouse in terms of productivity and energy cost. The ideal temperature in the greenhouse depends on the type of plant grown (Paula A. Claudino, 2016). Ventilation in greenhouses is used to provide cooling when the temperature exceeds a certain limit or to control the humidity levels (Seginer, 1997). Using mechanical ventilation instead of the natural one prevents any unnecessary ventilation, and as a result, reduces the energy requirement of the greenhouse.

Solar greenhouses can be freestanding or attached to other buildings. Freestanding greenhouses usually are for large-scale production (commercial greenhouses) while the attached greenhouses are usually just for dwelling-scale farmers. Attached greenhouses are cost-efficient solar collectors attached to the south side of dwellings and the unglazed surfaces are usually insulated to minimize the heat loss. An attached greenhouse might provide up to 50 percent of a dwelling's heat demand. (MacCullagh, 1978). Usually, solar greenhouses are connected to heat storage systems to get advantage from the surplus heat which accumulates inside the greenhouses, and they are known as passive solar greenhouses if no outside energy was included within the process. (Santamouris et al., 1994)

A variety of materials can be used as the heat storage medium, such as water, rocks, phase change materials (PCMs) or soil (buried pipes). During the day, the surplus heat is stored in the storage system and released during the night or whenever it is needed to

fulfill the greenhouse heating requirement. Rocks have high thermal conductivity, long life, availability, and they are easy to work with and maintain. The mentioned characteristics make rocks an attractive storage medium to be used in greenhouses. The application and properties of each storage medium will be discussed in detail in chapter 2.

Several software packages (e.g., TRNSYS, ESP-r or EnergyPlus) have been used to predict the performance of dynamic systems (e.g., greenhouses). TRNSYS is considered one of the most exhaustive software packages in simulating solar energy systems (Beckman et al., 1994). TRNSYS consists of a set of components, where each component is described by a number of input variables to generate desired outputs.

1.1 Objectives

In this study, an attached solar greenhouse connected to a rock-bed thermal storage located in Joliette near Montreal was instrumented and monitored to study its thermal behavior. In order to guarantee a high performance of the rock-bed thermal storage system and the greenhouse in terms of productivity and energy cost, factors which affect the performance of the greenhouse and rock-bed thermal storage such as cover materials, fan size, and rock-bed size should be studied carefully. Based on the purpose of the attached greenhouse, it is important to provide comfortable conditions inside the greenhouse in terms of light, temperature, and humidity. Therefore, monitoring the greenhouse operation should be done on a daily basis to ensure high performance.

The main objectives of this study are:

- To monitor the operation of the attached solar greenhouse,
- To analyze and simulate the energetic performance of the attached solar greenhouse,
- To study the parameters that affect the greenhouse and rock-bed performance in order to improve the overall design and operation,

1.2 Methodology

With these intended objectives, the attached solar greenhouse was instrumented and monitored to collect data. The measured data are the temperature, relative humidity (RH), and the solar radiation in several spots (to be defined in Chapter 3). Thereafter, the attached solar greenhouse was modeled using TRNSYS 17 and the simulation results were then validated and fine-tuned based on the measured data from the greenhouse. Furthermore, the daily energetic performance of the rock-bed thermal storage was investigated based on how much heat is stored and released.

After the TRNSYS 17 model of the greenhouse was validated using the collected data, factors that influence the energy performance of the attached solar greenhouse and rock-bed thermal storage were discussed and each factor was studied in order to improve the overall design.

Chapter 2

Literature Review

The aim of this review is to highlight the types of greenhouses, the parameters that influence their energy performance and the optimal control of the climatic conditions inside greenhouses. Also, the impact and effectiveness of thermal energy storage systems, rock-bed in particular, in reducing the energy cost of greenhouses will be discussed.

2.1 Greenhouses

Greenhouses operate based on the greenhouse effect. The short-wave radiation passes through the transparent cover material of the greenhouse and is absorbed by the greenhouse objects (e.g., inside wall surfaces) and then is re-radiated as long-wave radiation. The cover material is opaque to long-wave radiation; therefore, the long-wave radiation accumulates inside the greenhouse which increases the temperature. Long-wave radiation, convection, conduction, and infiltration are responsible for the most heat loss in greenhouses (ASABE, 2008). Therefore, to reduce the heat loss and thus, reduce the heating requirement of the greenhouse, each mode should be treated carefully. During the night, the temperature of the inner surfaces of the greenhouse is higher than the ambient temperature. As a result, they emit heat in the form of infrared (IR) radiation, while part of this radiated heat passes through the cover material of the greenhouse to the environment. This process is known as radiation cooling. (Goldammer, 2017)

Two types of greenhouses exist, and the comparison between them is summarized in Table 2.1:

- Freestanding greenhouses,
- Attached greenhouses.

Table 2.1 Comparison between attached and freestanding greenhouses (Sharon M. Rudnitski, 1987).

Type	Freestanding greenhouses	Attached greenhouses
Advantages	• Flexible design and orientation • The sunlight can enter from all sides of the greenhouse • Can be located anywhere • The capability of expanding the size of the greenhouse whenever it is needed	• Low cost • More energy efficient • Convenient access to water, electricity, and to the greenhouse itself • Can be considered as an extra living space • Heat can be exchanged between the residential house and the attached greenhouse whenever it is needed
Disadvantages	• More expensive • Less energy efficient • Less convenient access to water, electricity, or to the greenhouse itself	• The amount of sunlight entering the greenhouse is limited • The size and orientation of the greenhouse are critical • The temperature control sometimes is more difficult

Conduction heat loss exists at mostly between the greenhouse ground floor and the soil, also through the greenhouse covering material (Vadiee, 2013). This mode of heat loss can be addressed by having a high R-value of the ground floor and cover material of the greenhouse. However, it is more difficult to increase the R-value of the greenhouse cover material without reducing its light transmissivity, which affects the energy performance of the greenhouse. Therefore, selecting the optimal window is a complicated aspect.

Bot et al., (2005) used plastic foils, especially PVDF (polyvinylidene difluoride) and ETFE (ethylene tetra fluoroethylene), which can be used in double or triple layers with light transmissions similar to single layer conventional covers. The obtainable energy savings due to using these kinds of films were found to be around 40%.

Convection heat transfer in greenhouses occurs mainly by natural and mechanical ventilation besides infiltration. Ventilation is used in greenhouses to modulate the inside temperature and humidity levels (Vadiee, 2011). Mechanical ventilation works by using fans or blowers to move the air. Alternatively, natural ventilation is achieved using vent openings. A study of greenhouses in Marmara/Turkey found that 70% of the evaluated greenhouses had problems regarding ventilation. (Kendirli, 2006)

Flores-Velazquez et al. (2009) investigated the effect of mechanical and mixed (mechanical and natural) ventilation on the inside climate of a three-span greenhouse located in Spain, using Computational Fluid Dynamics (CFD). They found that mechanical ventilation is more effective and important than natural ventilation in greenhouses. Thus, in comparison to mechanical ventilation, the effect of natural ventilation on the inside conditions of greenhouses was found to be insignificant. However, as the length of the greenhouse increased, natural ventilation became more important than mechanical. Therefore, they concluded that mixed ventilation might be more effective for longer greenhouses.

Kittas et al. (2005) studied the effect of mechanical ventilation on the inside temperature of a rose crop greenhouse located in Greece. The results showed that mechanical ventilation was an efficient tool in improving the indoor climate of the greenhouse as it caused a reduction in overheating and alleviated the excess solar radiation in the greenhouse in the summer. Fernandez and Bailey (1994) found that adding fans to the greenhouse improves the indoor climate. Adding insect screens across the ventilation openings causes a significant reduction on the inside air velocity and increases the inside temperature and humidity. (Boulard, et al., 2008), (Molina-Aiz et al., 2004)

2.1.1 Attached solar greenhouses

Attached solar greenhouses, also referred to as attached sun-spaces, can be used to provide a controlled environment for growing plants or for reducing the heating requirement of the attached building (e.g., a residential house). Monge-barrio and Sánchez-ostiz (2015) simulated the energy performance of an attached sunspace located in Spain. They found that in summer, the attached sunspace is very efficient in reducing the energy requirement of the attached house. Also, they concluded that sunspaces should be used in cold climates especially in winter, to reduce the heating requirements of the attached houses. Owrak et al., (2015) investigated heating a room by an attached sunspace located in Karaj (Iran). They concluded that the impact of the sunspace on heating the room was positive, as the temperature inside the sunspace was higher than the room and ambient temperatures.

The sunspace cost can be considered as an additional cost for residential houses. However, for the long term performance, the energy savings caused by the sunspace can overcome this cost (Bakos & Tsagas, 2000). Oliveti et al., (2012) noticed that locating the sunspace in the east or west reduces the solar heat gains. This is caused by the reduction in the incident energy and the effective absorption coefficient of the sunspace. Bataineh and Fayez (2011) studied the energy performance of a sunspace attached to a living room located in Jordan. They noticed that the sunspace reduced the heating requirement of the living room in winter; however, it caused overheating during summer. The same conclusion was observed by Mihalakakou (2002) for a southern European climate like Athens. Figure 3 shows a schematic of the main energy fluxes in attached solar greenhouses.

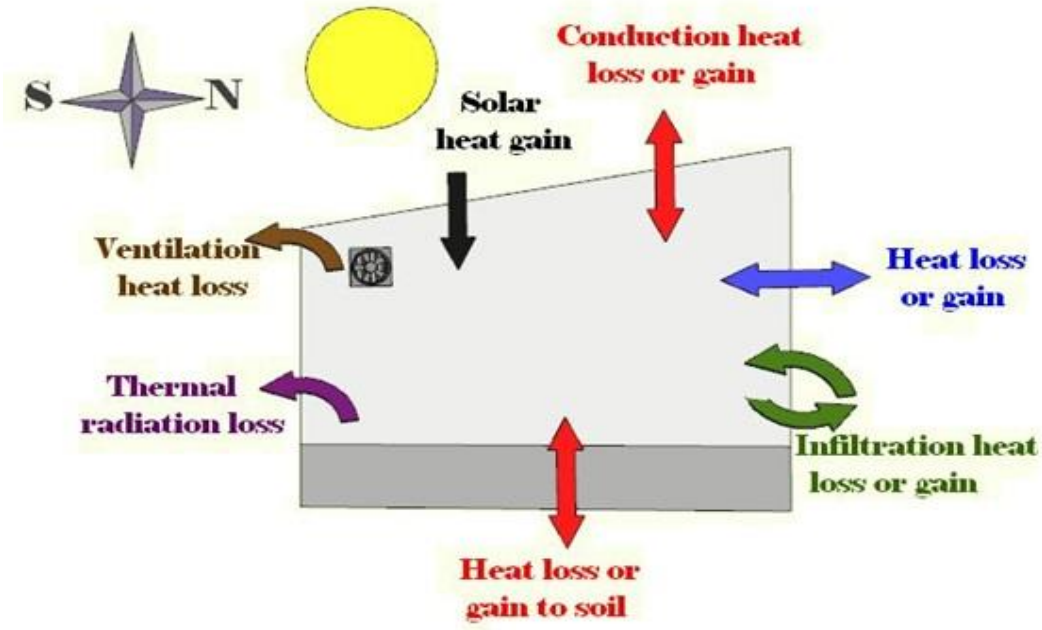

Figure 3. Heat loss and gain fluxes in attached solar greenhouses

2.2 Factors affecting the energy performance of greenhouses

The environment inside greenhouses is complicated and dynamic. A set of parameters describe and affect this environment. In order to accomplish high performance of the greenhouse in terms of energy and productivity, these parameters and their effects should be studied carefully. In this review, the focus will be on two parameters:

- Shape and orientation of greenhouses,
- Covering material of greenhouses,

2.2.1 Shape and orientation of greenhouses

The shape and orientation of a greenhouse have a direct impact on the solar heat gain and thereby affect the heating and cooling requirements of the greenhouse. Therefore, selecting the shape and orientation of the greenhouse is critical in order to have a high energy performance. Kendirli (2006) reported that in Marmara/Turkey, 85% of greenhouses are placed in the east–west direction, while 15% in the north–south direction, as placing the greenhouse in the east–west direction improves the solar energy efficiency. Dragicevic (2011) compared between orienting an uneven-span single shape greenhouse in the east-west and in the north-south directions. He found that at 44°N and 54°N, the solar heat gain in the east-west greenhouse was higher in winter and less in summer compared to the north-south greenhouse. Therefore, east-west orientation is preferable. The same conclusion was observed by Stanciu et al. (2016) for an even-span shaped greenhouse located at 44.25°N.

According to Sethi (2009), five types of single span greenhouses have been frequently used globally, and they are even-span, uneven-span, vinery, modified arch and Quonset, either oriented in the east-west or north-south directions. Singh and Tiwari, (2010) estimated the energy conservation in five shapes of greenhouses (standard peak even-span, standard peak uneven-span, vinery, arch and quonset) for winter conditions in Delhi, India. They found that the available solar energy inside the standard peak uneven-span shape was higher than the other shapes; because of the larger receiving area of that shape. Also, they evaluated the total energy (solar energy available and additional energy) required to maintain the greenhouse at 25 °C in all shapes. They concluded that the standard peak uneven-span shape had the lowest additional energy requirement due to the larger receiving area.

Sethi (2009) compared the most commonly used single span shapes of greenhouses (even-span, uneven-span, vinery, modified arch and quonset) as shown in Figure 4. The five shapes had the same dimensions and a mathematical model was developed and used to calculate the hourly transmitted total solar radiation. The results showed that at all latitudes, uneven-span shape had the highest gain of solar radiation during each month compared to other shapes, while the quonset shape gained the lowest solar radiation. Moreover, at 31 °N latitude, the greenhouse air temperature difference between uneven-span and quonset shapes was 4.6°C (maximum) and 3.5°C (daily average).

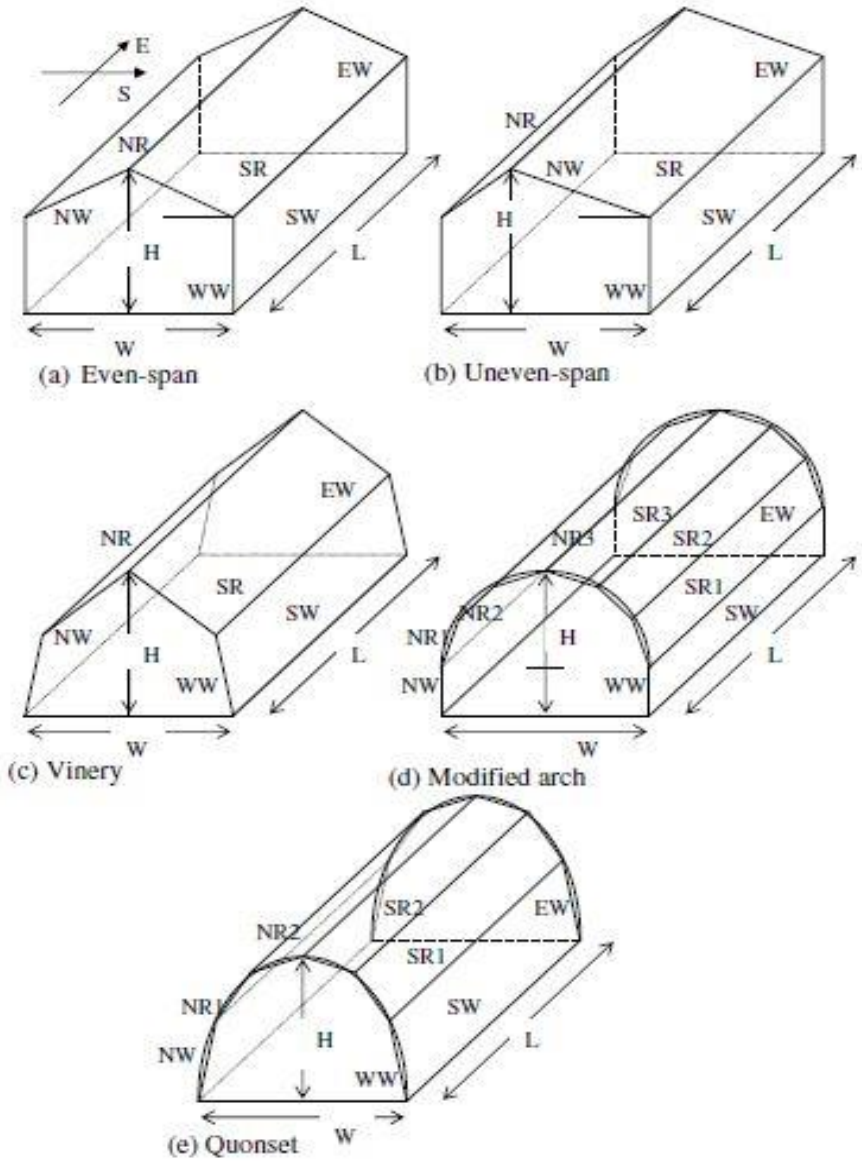

Figure 4. Most commonly used single span shapes of greenhouses. (Sethi, 2009)

2.2.2 Covering materials of greenhouses

A wide range of cover materials have been used in greenhouses. The cover material of the greenhouse should have high thermal resistance (R-value) and high light transmissivity. According to Sanford (2009), the most common cover materials used in

greenhouses are:

- Glass,
- Acrylic,
- Polycarbonate,
- Polyethylene (Poly film),
- Fiberglass.

Usually, double layers are used. However, these types can be used as single, double, or triple layers. Among these types, glass was the most used cover material in the past. However, most current greenhouses use poly films (Sanford, 2009). In Canada, 55% of the total greenhouses area is covered by poly films while 44% is covered by glass in 2016, as shown in Figure 5.

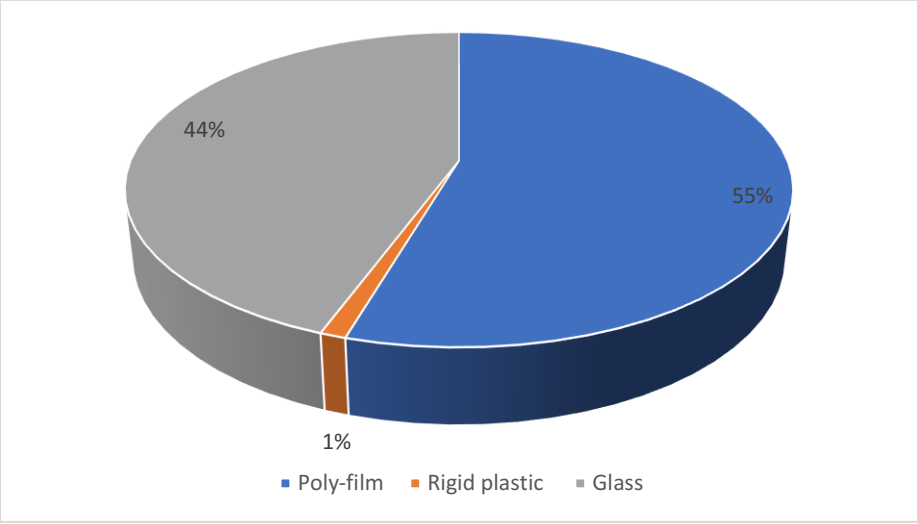

Figure 5. Cover materials percentage in Canadian greenhouses in 2016 (Statistics Canada. CANSIM Table 001-0047)

Each type of the cover material has specific properties as well as advantages and disadvantages. Some of the cover materials properties are given in Table 2.2. As shown in

Table 2.2, the transmissivity of single-layer glass is the highest compared to other materials. However, it has a low thermal resistance, which increases the heat loss of the greenhouse. According to Sanford (2009), triple polycarbonate is advised for walls, but not for roofs because it has about 4-5 % less transmissivity compared to other double layer materials. Table 2.3 shows a comparison of the main cover materials.

Table 2.2 Cover material properties.

Material	U-value (W/m^2K)	Short-wave transmissivity (%)	Long-wave transmissivity (%)	Life (Years)
Glass (Sanford, 2009), (Bastien, 2015)				
Single- Typical clear	5.9	88 - 93	3	25 +
Double Typical	2.73	75 - 80	< 3	25 +
Double-typical clear/ Typical low-e - Argon	1.65	63	-	-
Polyethylene (Poly film) (Eugene A. Scales and Associates, 2003), (Sanford, 2009)				
Single	6.2	87	50	4
Double	4	78	50	4
Double with an IR radiation additive	2.8	78	< 20	3 - 4
Polycarbonate (Sanford, 2009)				
Single	6.3	90	< 3	10 - 15
Double (6-10 mm	3 - 3.6	78 - 82	< 3	10 - 20
Triple (8-16 mm	2.4 - 3	74 - 76	< 3	10 - 20
Acrylic (Sanford, 2009)				
Single	6.4	90	< 5	30 +
Double	2.8 – 3.2	84	< 3	30 +
Fiberglass (Vadiee, 2013)	5.68	80 - 88	3	10 - 15

Table 2.3 Cover material characteristics (Sharon M. Rudnitski, 1987)

Material	Advantages	Disadvantages
Glass	• Outstanding transparency and appearance • Low thermal expansion and contraction • Easily available • Non-flammable • low long-wave transmittance	• Low thermal resistance • Physical damage creates safety hazard • Heavy weight • Hard to work with
Polycarbonate	• high thermal resistance • Outstanding transparency and appearance • lightweight • low long-wave transmittance	• High thermal expansion and contraction • Affected by UV radiation • Need protection for strengthening
Acrylic	• High transparency and good appearance • high thermal resistance • lightweight • Easy to work with • low long-wave transmittance	• high thermal expansion and contraction • Prone to abrasion • softens under moderate heat • Expensive
Polyethylene (Poly film)	• Easy to work with and cut • Very light weight • Permeable to $C0_2$	• High cost • Very short life-time • Low thermal resistance • Susceptible to melt under moderate heat and wind damage • Possible fire hazard • Poor visual appearance • Easy to get damaged • Low long-wave transmittance
Fiber glass reinforced polyester (FRP)	• High transparency • Very lightweight • Moderate impact resistance • Easy to work with • Easily available	• Prone to abrasion • Requires maintenance • High thermal expansion and contraction • Difficult to eliminate waviness from sheets

Low emissivity (low-e) double glazing can be used in greenhouses to reduce the heat loss, and thus, the heating requirement of greenhouses (Verre Plat, 2000). Hemming et al., (2007) studied the effect of cover materials on the performance of a traditional greenhouse in the Netherlands. He found that using double anti-reflection low-e glass reduced the energy requirement of the greenhouse by 33% compared to that of single glass. Cemek et al, (2006) investigated the performance of a greenhouse located in Turkey, with UV stabilized polyethylene, IR absorber polyethylene, double layers of polyethylene (D-Poly) and single layer of polyethylene (PE) as cover materials. They noticed a higher performance of the greenhouse with the double layers of polyethylene in terms of productivity and energy requirement compared to others.

Gupta and Chandra (2002) conducted a study to evaluate the effect of using air-inflated double-glazing instead of single transparent glazing in a greenhouse located in the north of India. The results showed a 23.4% reduction in the daily heating load with double-glazing. Papadopoulos and Hao (1997) found that replacing the single-layered glass cover of a greenhouse by double inflated polyethylene film (D-poly) or rigid-twin wall acrylic panels (acrylic) saved 30% of the heating requirement.

2.3 Thermal energy storage systems in greenhouses

Greenhouses are designed to maximize solar heat gain. A thermal energy storage system (TESS) can be integrated within the greenhouse to reduce the heating requirement. Thermal energy storage systems take advantage of the surplus heat inside the greenhouse, where this heat is stored in the TESs and released whenever it is needed. Santamouris et al., (1994b) classified agriculture greenhouses into two types: passive and

active solar greenhouses based on the use of solar energy for heating. Passive solar greenhouses do not utilize any outside energy while operating and the heat storage system is merged within the greenhouse cell. However, heat storage systems in active solar greenhouses are separated from greenhouses and fans or pumps are used to move the heat to the greenhouse.

The cost of active solar systems is considered to be high based on the cost of the collectors, occupied land, backup system, and the heat storage. However, they can significantly reduce the heating requirement of greenhouses (Santamouris, 1993). Sethi and Sharma (2008) conducted a comprehensive study on the heating technologies used in greenhouses including water storage, phase change materials storage, earth-to-air heat exchanger, and rock-bed storage systems. Table 2.4 shows the density and volumetric heat capacity of some of the common materials used for heat storage.

Table 2.4 Heat capacity of materials used for heat storage (Sharon M. Rudnitski, 1987)

Material	Density (kg/m^3)	Volumetric Heat Capacity ($MJ/m^3\ ^oC$)
Water	1000	4.19
Rock	2200	1.60
Clay brick	2000	1.65
Concrete	2200	1.60
Soil (medium moisture)	1600	1.80
Mud (saturated soil)	1900	3.00
Glauber's salt solution	1460	374

2.3.1 Water storage in greenhouses

The main advantage of water as a storage medium is the high heat storage capacity. Water storage systems can be used inside the greenhouse in water containers or outside

the greenhouse. During the day, the surplus heat is transferred to the thermal storage through a heat transfer fluid and returned during the night when the greenhouse temperature is below the desired temperature. If the heat storage is installed inside the greenhouse then the charging and discharging of the thermal storage are done by natural convection and radiation.

Kyritsis and Mavrogianopoulos (1987, (as cited in Sethi and Sharma, 2008)) used a water storage system in a tomato cropped greenhouse located in Greece. The water was filled in polyethylene bags and located on the ground floor. The water storage system was able to keep the temperature of the greenhouse 2-4°C higher than the ambient temperature. Nash and Williamson (1978) used water containers to reduce the heating requirement of a polyethylene greenhouse located in Nashville, USA. The greenhouse north wall was insulated to reduce the heat loss and the water containers were black painted to maximize the heat absorption. The greenhouse temperature was kept up 2-3°C higher than the outside temperature in January.

Santamouris et al., (1994b) stored water in black steel barrels at the north wall of a greenhouse located in Flagstaff, USA. The cover material of the greenhouse was made from reinforced polyester. The greenhouse temperature was 13–22°C higher than the minimum outside temperature in January. Fourcy (1982) used a water heat storage system in a glasshouse located in France. The north side of the greenhouse was a part of a hill, which reduced the heat losses. The water storage system reduced the greenhouse heating load by 70%.

Grafiadellis (1987) used a combination of underground heat storage and an air–water heat exchanger in a greenhouse located in Greece. Water was stored in underground containers. The storage system kept the temperature inside the greenhouse 5-6°C higher than the ambient temperature. Carnegie et al., (1984) used a single glazed shallow solar pond (SSP) water heater in a double-glazed greenhouse. The results showed that the shallow solar pond water heater covered 77% of the annual energy demand of the greenhouse.

2.3.2 Latent heat storage in greenhouses

Latent heat storage using phase change materials (PCMs) has gained much attention and considered a very promising technology due to the high storage density and small temperature swing (Tyagi et al., 2016). Phase change materials absorb and desorb heat, when there is a change in their phases, this change might be due to melting or solidification processes. As the material temperature increases, the material phase changes from solid to liquid in a melting process, thus, it absorbs heat. On the other hand, when the material temperature decreases, the material phase changes from liquid to solid in a solidification process, thus, it radiates heat. (Kuznik et al., 2011)

The heat storage capacity of phase change materials per unit volume is 5-14 times higher than those of sensible storage materials (e.g., water, masonry, or rocks) (Sharma et al., 2009). Ozturk (2005) studied the effect of using seasonal latent heat storage with paraffin wax PCM in a 180 m^2 greenhouse located in Turkey. 11.6 m^3 tank made of steel was filled with 6,000 kg of paraffin. The evaluation of the storage system efficiency was based on the energy and exergy analyses. The results showed that the average net energy

efficiency, which is the ratio of the heat stored in the storage system to the heat released from the storage system taking into consideration the power consumed by the fan was 40.4%. Benli (2011) evaluated the energy performance of a latent heat thermal storage tank connected to a ground-source heat pump heating system in a 30 m^2 greenhouse located in Turkey. The phase change material used in this experiment was calcium chloride hexahydrate. The results showed that the coefficient of performance of the overall heating system, which is the ratio of the condenser load to total work consumed by the pump, compressor, and condenser fan-coil unit, was found to be between 2 to 3.5. A 42% net energy efficiency of a paraffin latent heat storage was met during heating a 180 m^2 plastic greenhouse in Turkey. (Bascetincelik et al. 1999)

Baille and Boulard (1987) carried out a study on using a latent heat storage system in a 176 m^2 greenhouse located in France. The greenhouse cover material was double polycarbonate and the greenhouse was mechanically ventilated. 990 containers were filled with a 2,970 kg of $CaCl_2$. $6H_2O$. The results during February and March showed that the storage system covered 30 % of the greenhouse energy requirement. Benli et al. (2009) investigated the energy performance of a phase change thermal storage in a greenhouse located in Turkey. A 300 kg of $CaCl_2 6H_2O$ as a PCM was used in this experiment and filled in a tank inside the greenhouse. The melting temperature of the phase change material was 29°C. The storage system provided the greenhouse with 18–23% of the daily heating requirement.

2.3.3 Earth-to-air heat exchanger systems (EAHESS) in greenhouses

EAHESS can be used for heating or cooling in greenhouses. EAHESS consist of underground buried pipes and a mechanical airflow system to move the air through the pipes. During the cooling process, the greenhouse hot air is drawn through plastic or aluminum pipes, loses heat to soil, and returns to the greenhouse. The same process happens during heating, as the cold air extract heat from the soil and return to heat the greenhouse (Sethi et al., 2008). Gauthier, Lacroix, and Bernier (1997) conducted a study to evaluate the thermal performance of a soil heat exchanger-storage systems (SHESSs) in reducing the heating requirements in greenhouses. A numerical model was developed to predict the performance of the soil heat exchanger-storage system (SHESS). They found that the energy recovery ratio, which is the ratio of the heat stored to heat recovered, improved from 67% to 73% by insulating the SHESS perimeter. Moreover, increasing the depth of underground buried pipes increased the stored energy; however, it decreased the amount of energy recovered during the night and, as a result, the energy recovery ratio decreased.

Ghosal, Tiwari, and Srivastava (2004) carried out a study on evaluating the performance of an earth air heat exchanger connected to a greenhouse located in India. The performance of the system was evaluated in the summer and winter of 2002. The results showed that the greenhouse temperature was 6–7°C higher in winter and 3–4°C lower in summer compared to the greenhouse temperatures without using the heat exchanger. Santamouris et al., (1994) investigated using an earth-to-air heat exchanger and a mass storage wall of 30-cm thickness in a 1,000 m^2 greenhouse in Greece (latitude

= 38.5 N). 5 cm of polyurethane was used to insulate the external side of the thermal wall to reduce the heat losses and the inner side of the wall was painted black to increase solar absorption. The two years of operation results showed that the overall system (earth-to-air heat exchanger and the mass storage wall) covered 35% of the greenhouse heating requirements.

Ozgener and Ozgener (2011) investigated using an earth to air heat exchanger for heating a greenhouse located in Izmir, Turkey. The analysis results showed that the coefficient of performance, which is the ratio of the heat extracted from the system to work consumed by the blower, was 10.5. Santamouris et al., (1996) investigated using buried pipes in a 1,000 m^2 glass-covered greenhouse in Athens. During the daytime, hot air is circulated from the greenhouse through the buried pipes and heat is transferred to soil for the night use. The simulation results showed that as the pipe diameter and air velocity inside the pipes decrease the greenhouse air temperature increases during winter. Also, as the length of the pipe and the depth (up to 4 m) increase the greenhouse air temperature increases too. Overall, a good agreement was found between the measured and calculated values.

Mongkon et al., (2013) investigated the performance of a horizontal earth tube system in cooling a 30 m^2 greenhouse located in the north of Thailand. The highest COP value, which is the ratio of the heat extracted from the system for cooling to work consumed by the blower, for a typical summer day was 3.56, while it was 2 for a typical winter day. Moreover, they compared the experimental COP value to an average COP of a one ton of refrigeration of air conditioning in summer and the results showed that the

cooling system covered up to 75%. Yildiz, Ozgener, and Ozgener (2011) conducted a study on using an earth-to-air heat exchanger assisted by solar photovoltaic system (PV) to cool a greenhouse located in Turkey. The analysis was performed in the summer of 2010. The results showed that the average exergetic efficiencies of the PV and the heat exchanger were 4.94% and 56.3%, respectively. The PV system covered 31% of energy requirement during summer, while the exergetic efficiency of the overall system was 23.6%.

2.3.4 Rock-bed thermal storage in greenhouses

Rock-bed (pebble, gravel and bricks) heat storage material is very attractive in greenhouses due to the low cost of the system. Usually, the rock-bed is installed beneath the greenhouse in an insulated enclosure and the fluid used in this storage system is air (Hughes, Klein, & Close, 1976). During the discharging process, the greenhouse warm air is drawn by fans or blowers through the rock-bed, losses heat to rocks and return from the bottom as colder air. During the charging process, the greenhouse cold air is drawn through the rock-bed, extract heat from the rocks and return to the greenhouse as warmer air.

Kürklü and Bilgin (2004) conducted an experimental study on using a rock-bed system for cooling a 15 m^2 ground area of a plastic-tunnel-greenhouse. Two (3x 1.25x0.75) m^3 rock-bed canals were mined, insulated, and filled with rocks under the soil of the experimental greenhouse. A centrifugal fan with 1,100 m^3/h flow rate used to move the air through the rock bed. The experimental greenhouse was compared to an identical greenhouse (control greenhouse) without rock bed. The results showed that during a sunny day, the inside air temperature of the experimental greenhouse was 14°C lower

than control one, and close to the outside air temperature. Moreover, as the solar radiation and/or the ambient temperature increased, the temperature difference between the experimental greenhouse and the control one increased during the day. The coefficient of performance (COP) of the system was higher than 3. Also, the COP of the system can be improved by decreasing the difference between maximum and minimum set point temperatures of the controlled fan.

Öztürk and Başçetinçelik (2003) used energy and exergy analyses to evaluate the performance of a packed-bed heat storage for heating a 120 m^2 plastic tunnel greenhouse in the Cukurova region of Turkey. A volcanic material was selected as the heat storage material in the packed-bed heat storage system. A (6x2x0.6) m^3 packed-bed heat storage unit was built under the soil of the greenhouse and filled with 6,480 kg of volcanic material. A 27 m^2 of south-facing solar air heater was used as an external heat collection unit. The results showed that the average daily rates of thermal energy and exergy stored in the packed-bed heat storage during the charging periods were 1,242 W and 36 W, respectively. During the discharging period, the average daily rates of the thermal energy and exergy recovered from the packed-bed heat storage were 601 W and 20 W, respectively. Moreover, the net energy efficiency was 39.7 and the packed-bed heat storage system covered 18.9% of the greenhouse total heating requirements.

Chen and Liu (2004) studied the performance of a greenhouse with a passive solar heating room and rock bed heat storage as shown in Figure 6. The effect of the size, void fraction and the material type of the rock-bed were evaluated too. Their research aimed to find techniques to save more energy at lower cost and to provide thermal comfort

inside buildings in cold climates. The designed system comprised of a heating room and a greenhouse separated by a partition wall with a top and a bottom vent. The partition wall acted as a solar absorber from the greenhouse side and as an insulator from the heating room side. The numerical and experimental results showed that with a certain range of porosity, the thermal storage capability and the heating effects increased as the rock's size increased. Moreover, as the porosity of the thermal storage materials increased, the bed's temperature increased. Also, they found that both the specific heat capacity and thermal conductivity of the storage material had a significant impact on the average temperature of the rock-bed.

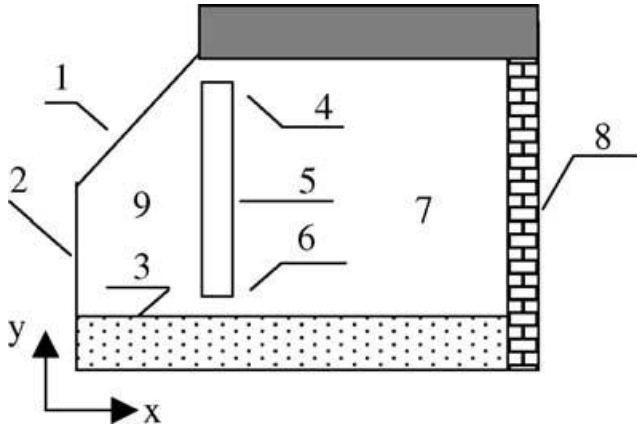

Figure 6. Schematic of a passive solar heating system with a greenhouse and a heat storage layer. 1–greenhouse roof; 2–glass wall of greenhouse; 3–heat storage layer; 4–top vent; 5–partition wall; 6–bottom vent; 7–heating room; 8–north wall; 9–greenhouse (Chen and Liu, 2004)

Gupta and Chandra (2002) conducted a study to reduce the need of conventional fuels in greenhouses. They investigated the effect of using a 350 m^3 rock-bed storage system in an east–west oriented greenhouse located in India. The gravel equivalent diameter was 5 cm, and a blower was used to move the air through the system. The rock-bed storage system kept the greenhouse temperature at 15°C during the night and 25°C during the

day. The rock-bed heat storage provided the greenhouse with all the heating requirement compared to a north–south oriented greenhouse with no rock-bed heat storage.

Kürklü, Bilgin, and Özkan (2003) used an underground rock-bed to heat a 15 m^2 polyethylene tunnel greenhouse located in Turkey. Two thermostats controlled a centrifugal fan with 1100 m^3/h flow rate used to move the air through the rock-bed. The results of the rock-bed greenhouse were compared to an identical greenhouse (a control greenhouse) without rock-bed heat storage. The effect of the rock-bed was noticed, as the temperature of the experimental greenhouse was 10°C higher than the controlled greenhouse temperature at night. Moreover, they calculated the daily discharging efficiency by taking the ratio of the heat stored during the day to the heat relased during the night, and the value was higher than 80%. The daily charging efficiency (solar energy collection) was calculated by taking the ratio of the heat stored during the day to the solar energy available inside the greenhouse, and the value was 34%.They concluded that the rock-bed heat storage system is more economical than traditional fuel based heating systems which used in Turkish greenhouses.

Willits, Chandra, and Peet (1985) conducted a study on evaluating the performance of a (3.0x10.0x1.8) m^3 rock-bed heat storage to heat and cool a (6.7x12.2) m^3 greenhouse. They studied the effects of infiltration, outside convection coefficients of the cover material, and the rate of moisture added from the plants on the overall system. The rock-bed heat storage was connected to the greenhouse by insulated ducts. Two existing models with some adjustments were used in this study. A good agreement was shown between the collected and predicted data (greenhouse temperature, greenhouse relative

humidity, and rock-bed temperature) of three non-sequential days. A significant effect from the rock-bed evaporation rate on the greenhouse relative humidity was noticed. Moreover, the mentioned factors did not have a significant effect on the greenhouse temperature. The moisture added from the plants had a slight effect on the total energy stored in the rock-bed, however, a significant effect by the moisture added from the plants was noticed on the fossil fuel consumption.

Bouhdjar et al., (1996) conducted a study to investigate using a rock-bed thermal storage in a 240 m^2 polyethylene greenhouse. Charging and discharging of the rock-bed thermal storage were applied in one-direction. Two blowers with total 1000 m^3/h mass flow rate were used to circulate the air through the storage. The results showed that the rock-bed thermal storage maintained the greenhouse temperature 7°C higher than the ambient temperature. Jain (2005) investigated using a packed-bed thermal storage, for crop drying purpose, in a greenhouse located in India. The results showed that the packed-bed thermal storage reduced the greenhouse temperature vacillation during the drying. Bricault (1982) investigated using a rock-bed thermal storage in a 2850 m^2 greenhouse located in Montreal. The greenhouse cover material was single polyethylene. The results showed that the rock-bed thermal storage covered 40% of the heating requiremnt of the greenhouse.

Fotiades (1987b) carried out a study on using a rock-bed thermal storage in a greenhouse located in Cyprus. The greenhouse cover material was double inflated polyethylene and a 1.7 kW fan was used to move the air through the system. the results showed that the rock-bed thermal storage covered 76% of the greenhouse heating

requiremnts. Brendenbeck (1987) investigated using a rock-bed thermal storage to heat a 1700 m^2 greenhouse located in Denmark. The greenhouse cover material was a triple polycarbonate with a thermal screen near the top. Twelve fans with 60,000 m^3/h total flow rate used to move the air through concrete pipes in the rock-bed thermal storage. The rock-bed thermal storage provided 30% of the heating requirements of the greenhouse. Table 2.5 shows a comparison between sensible (water, rocks) and latent heat storage systems. Sethi and Sharma (2008) carried out a survey on the application of rock-bed thermal storage systems in agricultural greenhouses and the summary of their survey is shown in Table 2.6.

Table 2.5 Storage mediums characteristics (Sharon M. Rudnitski, 1987), (O. Ercan Ataer, 2006)

Medium	Advantages	Disadvantages
Water	• Low cost of the storage system • High heat storage capacity • Water practically is free • widely available • Non-toxic	• Containers prone to leak • Water can be easily frozen • Water is highly corrosive
Rock-bed	• No freeze problems • Rocks can be an element of the greenhouse structure, while acting as a thermal storage mass • Low cost of rocks (higher than water) • Easy to work with and maintain • Long life • Rapid heat transfer between air and the rock-bed	• Low heat storage capacity compared to water and PCM • Low thermal conductivity
PCM	• High heat storage capacity • Required Low space for the storage	• Expensive • Short life • Some PCMs are corrosive and require special containers

Table 2.6 Summery of the performance of several agricultural greenhouses using rock-bed heat storage systems (Sethi and Sharma, 2008).

Location	Area(m^2)	Cover Material	Type and mass of rock used (kg)	Heat capacity of rocks/m^2	Performance	Reference
Nicosia, Cyprus	300	Polyethylene	Gravel, 74,000	177.6	Covered 76% of the heating requirements	Fotiades (1987b)
Prague, CZ	432	Glass	Gravel, 43,000	71.67	4–6 °C higher than the ambient Temperature	Jelinkova (1987)
Hannover, Denmark	1700	Polycarbonate	Gravel, not known	-	Covered 30% of the heating requirements	Brendenbeck (1987)
Montreal, Canada	2850	Polyethylene	Gravel, 202,000	51.03	Covered 40% of the heating requirements	Bricault (1982)
Budapest, Hungary	100	Polyethylene	Bricks, 48,000	489.6	Covered 53.4% of the heating requirements	Kavin and Kurtan (1987)
Oregon, USA	19	Glass	Gravel, 13,000	492.63	10–20 °C higher than the ambient Temperature	Santamouris et al. (1994b)
Baraki, Alzeria	240	Polyethylene	Gravel, 20,000	60.17	4–6 °C higher than the ambient Temperature	Bouhdgar and Boulbing (1990)
Tascend, USSR	40	Double polyethylene	Gravel, 5700	102.6	13°C higher than the ambient Temperature	Arizov and Niyazov (1980)
Bonn, Germany	161	Double glass	Gravel, 14,000	62.16	Covered 20% of the heating requirements	Santamouris et al. (1994b)
North Carolina, USA	176	Glass	Gravel, 15,700	64.22	5°C higher than the ambient Temperature	Huang et al. (1981)
Adana, Turkey	120	-	Volcanic, 6480	-	Covered 18.9% of the heating requirements	Ozturk and Bascetincelik (2003a, b)

Chapter 3

The attached solar greenhouse structure and modeling

3.1 Greenhouse structure

The attached solar greenhouse has a floor area of 28 m^2 and is located in Joliette/Quebec at 46°N, 73°W. A rock-bed thermal storage is located beneath the greenhouse to provide cooling during the day and heating during the night. The mechanical ventilation fan was not activated during this study .The dimensions of the overall system are shown in Figure. 7.

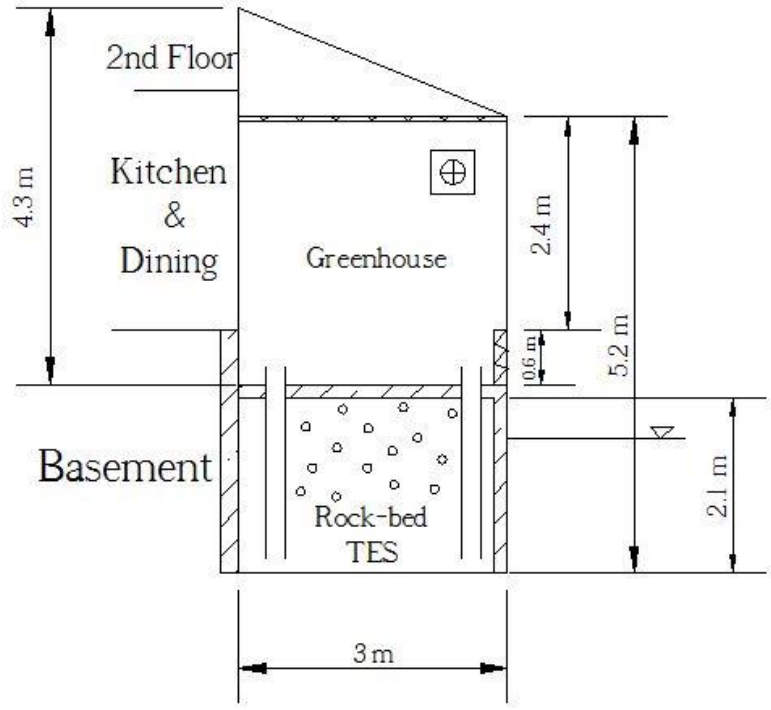

Figure 7. East-view of the Overall system (greenhouse and rock-bed thermal storage)

The rock-bed thermal storage is filled with 100 tons of limestone rocks with an average diameter of 15 cm. The side walls of the rock-bed thermal storage are well

insulated to reduce the environmental heat loss. A fan with 216 L/s (458 CFM) flow rate is located at the center of the greenhouse floor to circulate the air in the axial direction through the rock-bed thermal storage. During the day, the hot air of the greenhouse is drawn by the fan through the rock-bed thermal storage. The hot air loses its heat to the rocks and returns from the bottom through four openings to the greenhouse as colder air in a charging process. During the night, the cold air of the greenhouse is drawn through the rock-bed thermal storage and extracts heat from rocks, then returns from the bottom through four openings as warmer air to the greenhouse in a discharging process. Figure 8 shows a schematic of the greenhouse energy fluxes and air circulation through the rock-bed thermal storage.

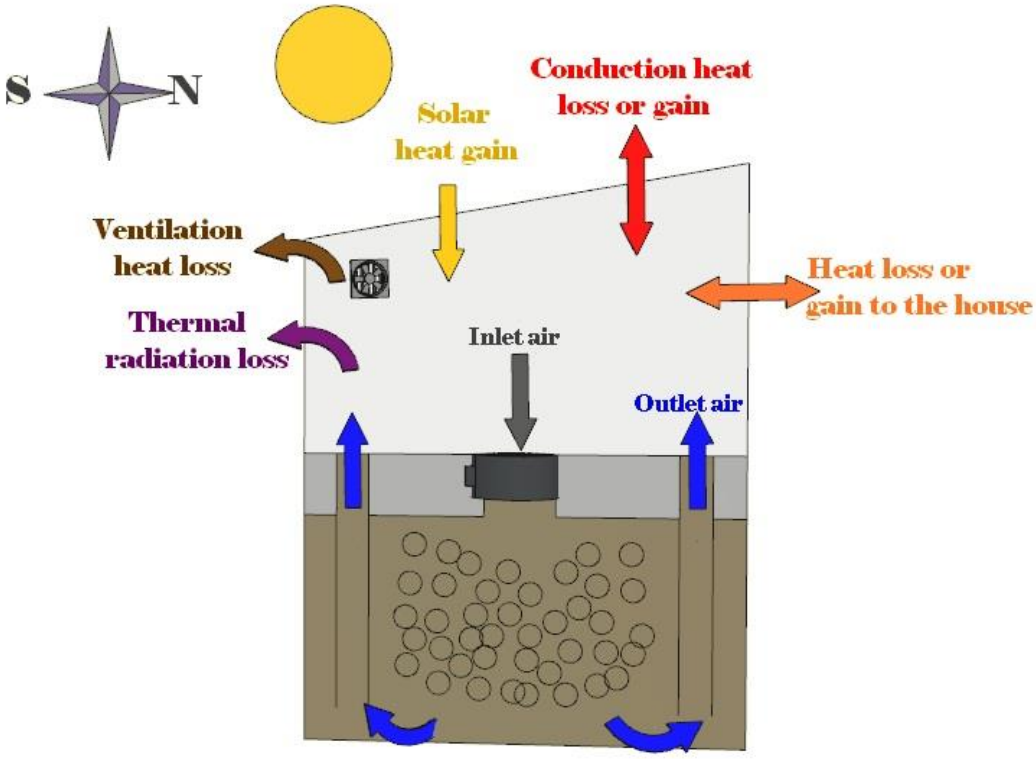

Figure 8. Air circulation and energy fluxes of the overall system

3.2 Greenhouse Modeling

The system modeling is done using TRNSYS 17 (TRaNsient SYstem Simulation) (TRNSYS, 2012). TRNSYS software has been applied by many researchers to simulate greenhouses thermal behavior in order to find the optimal design or to predict the greenhouse performance (Vadiee, 2011; Paula A. Claudino, 2016; Asdrubali et al., 2012; Aghbashlo et al., 2015). TRNSYS models consist of elements, known as types. Each type is defined by a specific number and expressed by a mathematical model. These types are connected to each other by a set of inputs and outputs. (TRNSYS, 2012). Figure 9 shows the overall system model in TRNSYS 17. The main types used in the greenhouse modeling are:

- Type 56 (Multi-zone building)
- Type 15 (Weather data)
- Type 10 (Rock-bed storage)
- Type 2 (Differential Controller)
- Type 3 (Fan)
- Others (Soil temperature, equations, online plotter)

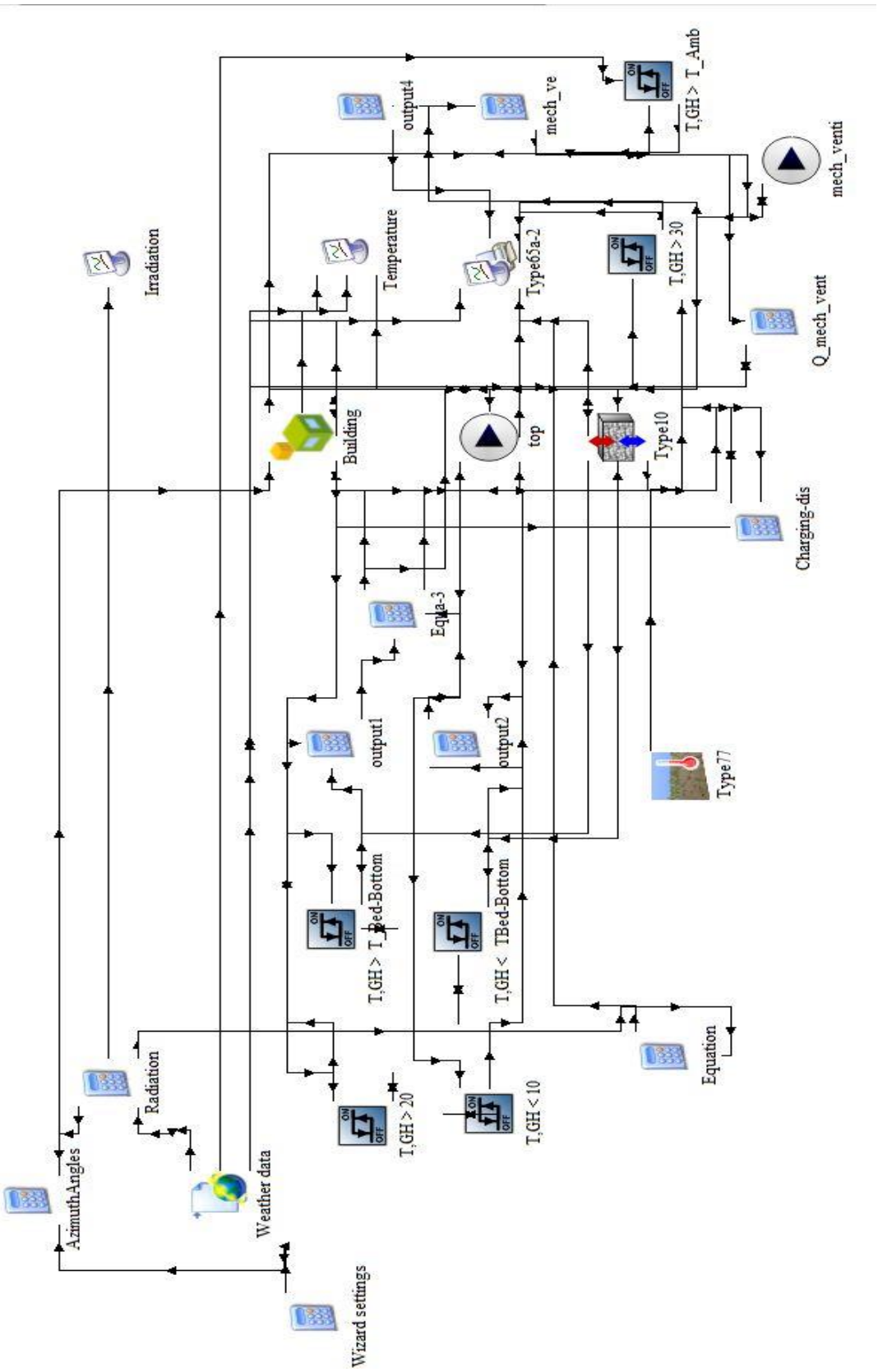

Figure 9. The overall system model in TRNSYS

3.2.1 Multi-zone building (Type 56)

This type expresses the thermal behavior of multi-zone buildings. Multi-zone building characteristics (e.g., walls, windows, working schedules) are defined through an additional tool called TRNBUILD (TRNSYS, 2012). Type 56 in the current design consists of two zones; the first zone represents the attached solar greenhouse and the second zone represents the residential house. The multi-zone building was designed in SketchUp software (Sketchup/3D modeling, n.d.), and imported into TRNSYS through TRNSYS plugin for SketchUp. The attached solar greenhouse design is shown in Figure 10.

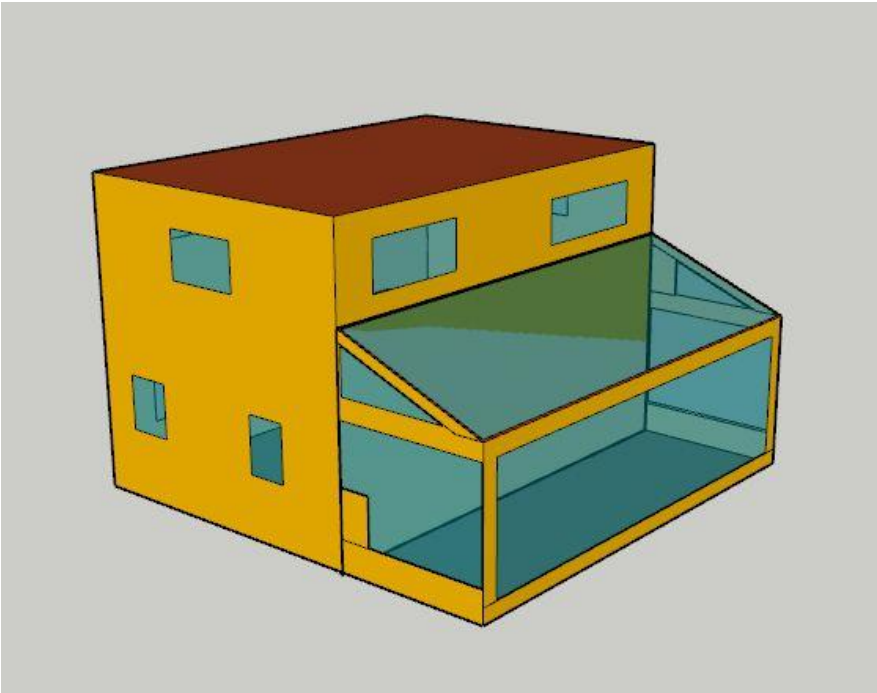

Figure 10. 3D-model of the attached solar greenhouse in SketchUp

The greenhouse roof cover material is triple polycarbonate. This type of glazing material does not exist in TRNSYS window library. Therefore, the triple polycarbonate cover material properties were developed and imported into the TRNSYS window library using another software package called WINDOW 6.3 (LBNL, 2013). Lawrence Berkeley

National Labs created WINDOW 6.3 to design and develop new glazing systems with any desired properties (i.e., frame, U-value, transmissivity) (LBNL, 2013). The greenhouse characteristics are shown in Table 3.1.

Table 3.1 The attached solar greenhouse characteristics

Location	Joliette/Quebec
Orientation	South
Weather data	Meteonorm (Type 15) /Montreal
Volume	101.96 m^3
Glazing	Roof: Triple Polycarbonate U-value= 2.57 W/m^2K, Transmissivity = 0.718 Other surfaces: Double low-E glass with argon U-value= 1.4 W/m^2K, Transmissivity = 0.622
Window frame	Wood frame for all windows, U-value= 2.27 W/m^2K, solar absorptance = 0.6, emissivity= 0.9
External roof (95% glass + frame)	U-value = 1.13 W/m^2K, emissivity= 0.9
External wall	U-value = 0.639 W/m^2K, emissivity= 0.9
Adjacent wall	U-value= 0.246 W/m^2K, emissivity= 0.9
Bottom wall 1	U-value= 0.241 W/m^2K, emissivity= 0.9
Bottom wall 2	U-value= 0.294 W/m^2K, emissivity= 0.9
Ground floor	U-value = 3.209 W/m^2K, emissivity= 0.8
Roof tilt angle	20°

* Adjacent wall: the wall that separates the solar greenhouse from the residential house.
* Bottom walls: the small walls between windows.

Each wall of the greenhouse consists of single or multiple layers. Layers in TRNSYS have specific properties defined within the software, such as thickness and specific heat capacity. TRNSYS allows the user to control a set of parameters of the wall surfaces (back and front), like the convective heat transfer coefficient and solar absorptance. The terms 'back' and 'front' refer to the external and internal surfaces of the walls, respectively. The structure of the greenhouse and the overall UA-values of the walls are shown in Table 3.2.

Table 3.2 UA-values of the walls

Wall type	U-value (W/m^{2}K)	Area (m^2)	UA-value (W/K)
South wall			
External wall	0.64	4.82	3.1
Double low-E glass	1.4	20.26	28.4
WTYPE1	0.24	2.79	0.67
Total			**32**
West wall			
External wall	0.64	1.51	1
Double low-E glass	1.4	6.62	9.27
WTYPE1	0.24	2.47	0.6
WTYPE12	0.29	0.56	0.17
Total			**11**
East wall			
External wall	0.64	1.56	1
Double low-E glass	1.4	6.59	9.23
WTYPE1	0.24	2.47	0.6
WTYPE12	0.29	0.54	0.16
Total			**11**
Adjacent wall	0.25	39.02	**9.6**
Ground floor	3.21	27.87	**89.4**
Roof			
External roof	1.13	1.25	1.42
Triple	2.57	28.77	74
Total			**75.4**

The longwave emission coefficient and the convective heat transfer coefficient values were kept as generated by TRNSYS. For the convective heat transfer coefficient values of the inside and outside surfaces TRNSYS uses by 11 kJ/h.m^2.K and 64 kJ/h.m^2.K, respectively. These values are in agreement with ASHRAE specified values (Judkoff et al., 2011). For the outside surface of the greenhouse floor, the convective heat transfer coefficient value was set to 33 kJ/h.m^2.K (Howell, Sauer, and Coad, 2005). The default value of 0.9 for the inside and outside longwave emission coefficients for walls were assigned. Table 3.3 shows the characteristics of the greenhouse walls and layers.

Table 3.3 The attached solar greenhouse envelope characteristics

material	Thickness (cm)	Conductivity (kJ/h·m·K)	Heat Capacity (kJ/kg·K)	Density (kg/m^3)	Wall Solar Absorptance		Convective Heat Transfer Coefficient (kJ/h·m^2·K)	
					Front	Back	Front	Back
External walls					0.6	0.6	11	64
Wood-siding	2.5	0.504	0.9	530	-		-	
Prestwood	1.2	0.2	1	300	-		-	
Wood-siding	14	0.504	0.9	530	-		-	
Roof					0.6	0.6	11	64
Wood-siding	2.5	0.504	0.9	530	-		-	
Prestwood	1.2	0.2	1	300	-		-	
Wood-siding	14	0.504	0.9	530	-		-	
Adjacent wall					0.6	0.6	11	11
Gyps-board	1.3	1.04	1	600	-		-	
Fiberglass	14	0.144	0.84	12	-		-	
Wood-siding	3.8	0.504	0.9	530	-		-	
Wall- board	2.5	1.04	1	800	-		-	
Ground floor					0.6	0.6	11	33
Concrete	10	4.068	1	1400	-		-	
WTYPE1					0.6	0.6	11	64
Wood-siding	2.5	0.504	0.9	530	-		-	
Prestwood	1.2	0.2	1	300	-		-	
Fiberglass	14	0.144	0.84	12	-		-	
Wall- board	2.5	1.04	1	800	-		-	
WTYPE12					0.6	0.6	11	64
Wood-siding	2.5	0.504	0.9	530	-		-	
Prestwood	1.2	0.2	1	300	-		-	
Fiberglass	11	0.144	0.84	12	-		-	
Wall- board	2.5	1.04	1	800	-		-	

3.2.1.1 The attached greenhouse mathematical model

The greenhouse performance is affected by factors such as: sensible energy, latent energy (Moisture levels), and heat supplied/removed by the thermal storage. Therefore, it is necessary to define the energy balance equations through the greenhouse to evaluate the performance of the overall system.

The following assumptions and conditions were made to facilitate the dynamic model:

- The effect of plants is not taken into consideration (non-cropped greenhouse).
- The greenhouse is perfectly sealed (no infiltration).
- The greenhouse air temperature is uniform (well mixed air).
- The thermal storage is the only heating system in the greenhouse (no supplemental heating systems).

By considering the mentioned assumptions and conditions, the sensible energy balance for a thermal zone in TRNSYS is described as follow:

$$\dot{Q}_i = \dot{Q}_{surf,i} + \dot{Q}_{vent,i} + \dot{Q}_{cplg,i} + \dot{Q}_{solair,i} + \dot{Q}_{rock-bed} \quad (1)$$

Where $\dot{Q}_i$ is the total heat gain; $\dot{Q}_{surf,i}$ is the convective heat gain from each surface; $\dot{Q}_{vent,i}$ is the ventilation heat gain; $\dot{Q}_{cplg,i}$ is the heat gain from due to an air flow from node I or boundary conditions; $\dot{Q}_{solair,i}$ is the solar radiation entering the zone from the windows; $\dot{Q}_{rock-bed}$ is the heat gains from the rock-bed thermal storage.

3.2.2 Rock-bed thermal storage (Type 10)

As mentioned before, the actual rock-bed thermal storage has four outlets. However, the rock-bed type 10 used in TRNSYS 17 has only one outlet. Therefore, for the comparison between the simulation results and the actual data, the average temperature of the four outlets of the rock-bed was taken. The rock-bed outlet temperature is calculated by dividing the rock-bed storage into (N) number of segments as shown in Figure 11. The recommended number of segments by TRNSYS is 5. The mathematical model of the rock-

bed thermal storage used in TRNSYS is shown in equations 2 and 3 and the rock-bed thermal storage (type 10) parameters are shown in Table 3.4.

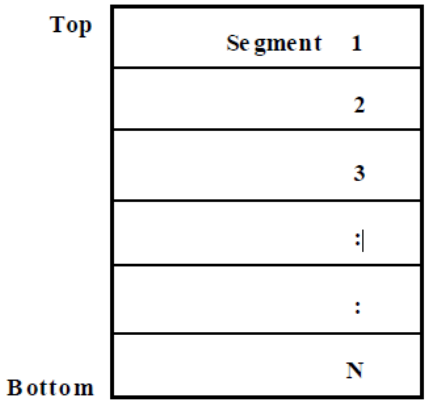

Figure 11. Rock-bed segmentation (Trnsys 17, *4*)

- For downwards air flow, the equation at segment 1 can be written as (Trnsys 17,*4*):

$$\frac{V}{N} * \rho_r * c_r \frac{\partial T1}{\partial t} = \dot{m} * C_p(T_{in} - T_1) - \frac{\text{UPL}}{N}(T_1 - T_{env}) - \frac{\text{K*A}}{L/N}(T_1 - T_2) \quad (2)$$

For segment N:

$$\frac{V}{N} * \rho_r * c_r \frac{\partial T_N}{\partial t} = \dot{m} * C_p(\text{T}_{\text{N-1}} - \text{T}_{\text{N}}) - \frac{\text{UPL}}{N}(T_N - T_{env}) - \frac{\text{K*A}}{L/N}(\text{T}_{\text{N-1}} - \text{T}_{\text{N}}) \quad (3)$$

Table 3.4 Rock-bed parameters

Parameter	Value	Reference
Specific heat of air	1.0035 kJ/kg.K	
Length of rock bed	2.13 m	
Cross-sectional area	27.9 m^2	
Perimeter	22.5 m	
Specific heat of rock	0.68 kJ/kg.K	(Waples & Waples, 2004)
Apparent rock bed density	1548 kg/m^3	
Loss coefficient	12.26 $kJ/hr.m^2.K$	
Effective thermal conductivity	12.4 kJ/hr.m.K	(Sharma, 2002)

3.2.3 Weather data

Type 15 component is used to read and interpolate data from imported weather data files at different time steps for specific locations, to be used by other TRNSYS components. The external weather data file used in this study is type TMY2, which includes the data files for a typical meteorological year (TMY) derived from the 1961-1990 National Solar Radiation Data Base (NSRDB) (TRNSYS, 2012). TMY2 data files are generated by the National Renewable Energy Laboratory's (NREL's) and the purpose of these files is to be used for simulating solar energy conversion systems and building systems. The location of the greenhouse is in Joliette/Quebec. However, the weather data for Joliette is not available in TRNSYS 17 weather data library. Therefore, the weather data file of Montreal was used and modified by Meteotest AG. The modification of Montreal weather data consisted of replacing the ambient temperature and horizontal solar radiation data of Montreal by the actual measured data of Joliette/Quebec for the periods used in the validation of simulation results with data obtained from the greenhouse monitoring system.

3.3 Data acquisition and control system

All sensors are connected to a Web Energy Logger (WEL) (Malone, 2011), from Thermo Dynamics Ltd and this system (shown in figure 12) was used to collect the measured data. This low-cost equipment (WEL) allows the viewing of the measured data online as graphs on a private website, and its logs can be downloaded and viewed through Excel. Also, it can be connected to a large number and different types of sensors. The main components connected to WEL are the power supply, one-wire Digital Thermometers, humidity

sensors, pyranometer, 8 local contact closures, two 0-10V Analog inputs and on/off controllers. The temperature, relative humidity, and solar radiation were measured in several locations as shown in Table 3.5.

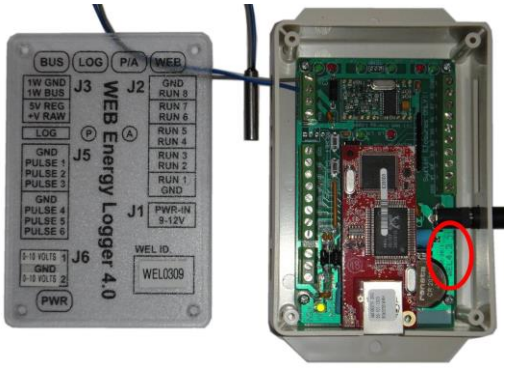

Figure 12. The Web Energy Logger (WEL) without the connections (Malone, 2011)

Table 3.5 location of sensors

Measured data and location	Type of sensors	Quantity
Temperature		
Inside greenhouse, basement, and ambient	one-wire digital thermometer	3
Rock-bed inlet air, and outlet air at the bottom	one-wire digital thermometer	5
Top temperature of the rocks	one-wire digital thermometer	1
Humidity		
Inside greenhouse, basement, and ambient	HIH-4000 series humidity sensors	3
Rock-bed inlet air and outlet air at the bottom	HIH-4000 series humidity sensors	5
Solar radiation		
Outside	pyranometer (photo-diode and battery sensing chip, DS2438)	1
South vertical window	pyranometer (photo-diode and battery sensing chip, DS2438)	1
Inside surface of the roof	pyranometer (photo-diode and battery sensing chip, DS2438)	1
Horizontal surface of the ground floor	pyranometer (photo-diode and battery sensing chip, DS2438)	1

3.3.1 Temperature sensors

The temperature is measured via digital thermometers type DS18B20 (Maxim Integrated Products, 2015a), which provide 9-bit to 12-bit Celsius temperature readings with measuring range from -55°C to +125°C with ±0.5°C accuracy over the range of -10°C to +85°C (Maxim Integrated Products, 2015a). This sensor is called 1-Wire sensor because it communicates with a central microprocessor through 1-Wire bus, therefore, it requires only two lines (data and ground lines). Moreover, the DS18B20 does not require an external power supply since the power can be derived from the data line (Maxim Integrated Products, 2015a). The central microprocessor can control many DS18B20 units since each DS18B20 has a special 64-bit serial code. Therefore, many DS18B20 units can be connected on the same 1-wire bus. This characteristic makes using this type of thermometer very practical especially in HVAC environmental controls, temperature monitoring systems inside buildings, and control systems (Maxim Integrated Products, 2015a). The pin diagram of the DS18B20 is shown in Figure 13.

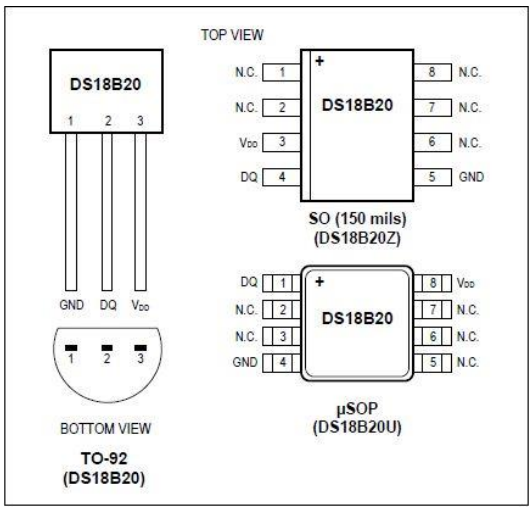

Figure 13. The DS18B20 digital thermometer Pin Configuration (Maxim Integrated Products, 2015a)

3.3.2 Relative Humidity sensors

The relative humidity is measured via HIH-4000 series humidity sensor (Honeywell, n.d.), which can be connected to controllers or other devices (e.g., WEL). The low current draw of the HIH-4000 series makes it suitable for battery operated systems. The HIH-4000 series sensor is designed to resist most application hazards like dust, dirt, or environmental chemicals. The most important features of this type of sensor are: low power design, high accuracy about ± 3.5 %, fast response time, and chemically resistant. The HIH-4000 Series can be used in HVAC (Heating, Ventilation and Air Conditioning) equipment, medical equipment, or battery-powered systems. The humidity sensor image is shown in Figure 14.

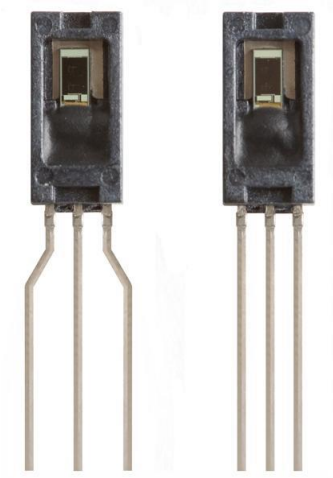

Figure 14. HIH-4000 Series Humidity Sensor (Honeywell, n.d.)

3.3.3 Solar radiation sensor (Pyranometer)

Four pyranometers were used to measure the solar radiation inside and outside the greenhouse. They consist of photo-diodes type SFH203P and battery sensing chips type DS2438 (OSRAM Opto Semiconductors GmbH, 2015). Each photo-diode has a wavelength

range from 400-1100 nm and can be used for control and drive circuits or in Industrial electronics (OSRAM Opto Semiconductors GmbH, 2015).

The most important functions which the DS2438 provides are: A/D converter to measure the current and voltage, an integrated current accumulator to integrate the ingoing and outgoing currents, and 40 bytes of nonvolatile EEPROM memory. The DS2438 transfers the information through a 1-Wire interface connected to a central microprocessor. Moreover, each DS2438 has a special serial number, therefore, many DS2438 units can be connected to the same 1-Wire bus. Figure 15 shows the pin diagram of the battery sensing chip and the photo-diode. (Maxim Integrated Products, 2015b)

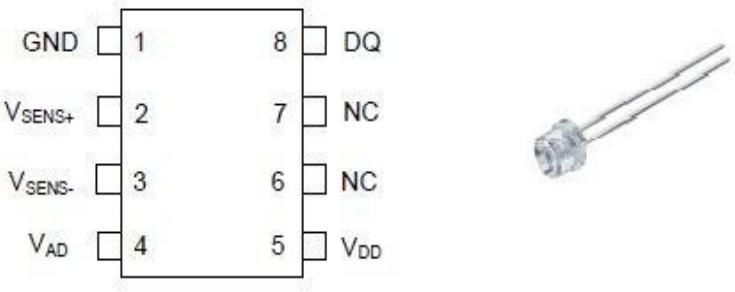

Figure 15. Pyranometer components (Maxim Integrated Products, 2015b), (OSRAM Opto Semiconductors GmbH, 2015)

3.4 Greenhouse temperature control

Temperature control is required to ensure effective operation of the rock-bed thermal storage and mechanical ventilation. Several studies have been carried out to provide environmental control systems in greenhouses to minimize the energy consumption

(Martinović and Simon 2014; Stanghellini And Meurs, 1992; Aaslyng et al., 2005; Chen et al., 2015).

In this study, the temperature was controlled via differential controllers with a dead band ± 1°C to prevent rapid ON/OFF cycles. The controlling strategy is based on five possible scenarios as shown below:

First scenario:

If $T_{GH} > T_{cooling\text{-}set\text{-}point}$ and $T_{GH} > T_{Bed\text{-}Bottom}$, then the greenhouse air is drawn through the rock-bed and charges the rock-bed thermal storage. Then, the colder air at the bottom of the rock-bed will return to the greenhouse to modulate the greenhouse temperature.

Second scenario:

If $T_{Bed\text{-}Bottom}$ is not enough to cool the greenhouse to the acceptable temperature range in the first scenario. Then, the mechanical ventilation will run to modulate the greenhouse temperature until T_{GH} falls within the acceptable temperature range.

Third scenario:

If the greenhouse temperature is within the acceptable temperature range ($T_{heating\text{-}set\text{-}point} \leq T_{GH} \leq T_{cooling\text{-}set\text{-}point}$), both fans (ventilation and rock-bed fan) will be turned off.

Fourth scenario:

If $T_{GH} < T_{heating\text{-}set\text{-}point}$ and $T_{GH} < T_{Bed\text{-}Bottom}$, then the greenhouse air will be drawn through the rock-bed to discharge the rock-bed thermal storage, while the $T_{Bed\text{-}Bottom}$ will return to the greenhouse to heat the greenhouse.

Fifth scenario:

If $T_{Bed\text{-}Bottom}$ is not enough to heat the greenhouse to the acceptable temperature range in the fourth scenario, then, an auxiliary heating device is needed to heat the greenhouse.

3.5 Model Validation

Many statistical methods such as, Total Sum of Squared Error (TSSE), Root Mean Squared Error (RMSE), or Model Efficiency (EF) have been used to measure the accuracy of model predictions. In this study, the methods used to evaluate the agreement between the measured and predicted values are the sample correlation coefficient (r), the Pearson coefficient of determination (r^2) and Mean Absolute Error (MAE). MAE is one of the most widely used methods in indicating the accuracy of a prediction (Chai and Draxler, 2014). A low value of the MAE indicates a high accuracy of the prediction and vice versa, MAE is defined in Equation 4.

$$MAE = \frac{1}{n}\sum_{i=1}^{n}|Actual - Forecast| \quad (4)$$

where,

n: is the sample size

$Actual$: Actual data

$Forecast$: Simulated data

The correlation coefficient is defined by Rodgers et al. (1988) as shown in equation 5. The r value also indicates how accurate the prediction is and it ranges from -1 to 1, where 1 indicates perfect positive relationship, -1 indicates a perfect negative relationship, and 0 indicates no linear relationship exists between the predicted and the actual data.

Moreover, the r^2 value vary from 0 to 1, and the higher the value the more accurate the prediction.

$$r = \frac{\sum_{i=1}^{n}(x_i-\bar{x})(y_i-\bar{y})}{\sqrt{\sum_{i=1}^{n}(x_i-\bar{x})^2}\sqrt{\sum_{i=1}^{n}(y_i-\bar{y})^2}} \quad (5)$$

where,

n: is the sample size

x_i, y_i : are single samples

$\bar{x}$, $\bar{y}$: are the sample mean

The results of TRNSYS simulation and the actual greenhouse data for several periods of the year will be introduced and compared in the next chapter.

Chapter 4

Results and discussion

The indoor environment of greenhouses is affected by several factors such as the greenhouse construction characteristics, outside temperature and relative humidity. The plant growth inside a greenhouse is highly dependent on the inside air temperature, which is influenced by many factors such as cover materials, weather conditions and greenhouse design. The rock-bed thermal storage performance is affected by operational parameters like heating and cooling set-point temperatures, and design parameters like rock-bed size and air flow rate used in the rock-bed thermal storage. In this chapter, the capability of TRNSYS 17 in predicting the indoor temperature of the attached greenhouse will be discussed. Also, the energetic performance of the rock-bed thermal storage will be analyzed based on the measured data. Finally, the effect of the rock-bed size, air flow rate, cover material, and heating/cooling set-point temperatures will be studied using TRNSYS simulation results in order to improve the overall design.

To validate the predictions of the TRNSYS model developed, the measured greenhouse and rock-bed average outlet temperatures are compared to TRNSYS simulation results. The measured and predicted data are compared for three periods (February, March, and April) to ensure an accurate validation of the model. As mentioned before, the evaluation of the comparison will be based on r, r^2, and MAE criteria. The relative humidity (RH) validation is not included in this study and left for future work. As mentioned in section 3.2.3, the weather data used in this study was modified by Meteotest AG. The modification of Montreal weather data consisted of replacing the

ambient temperature and horizontal solar radiation data of Montreal by the actual measured data of Joliette/Quebec for the periods used in the validation of simulation results with data obtained from the greenhouse monitoring system. Several greenhouse cooling (rock-bed charging) set-point temperatures that vary between 12-22°C, as shown in Table 4.1, were used during the validation periods. The cooling set-point temperature was changed in a way to be 3-4°C higher than rock-bed outlet temperature. 8°C and 10°C greenhouse heating (rock-bed discharging) set-point temperatures were used during the validation periods as shown in Table 4.1.

Table 4.1 Charging and discharging set-point temperatures during the validation periods

Days	Heating set-point temperature (°C) (Discharging)	Cooling set-point temperature (°C) (Charging)
Feb 6-28	8	12
Mar 1-2	10	12
Mar 3-5	10	14
Mar 6-19	10	16
Mar 20-26	10	18
Mar 27-31	10	20
April 1-26	10	20
April 27-30	10	22

4.1 TRNSYS model validation

The Model was run for a full year (0-8760 hours) to guarantee equilibrium conditions were reached in each zone. The measured ambient temperature values for the validation periods (February 6-28, March 1-31 and April 1-30) are shown in Figure 16 (a)-(c), and the

measured horizontal solar radiation values for the validation periods are shown in Figure 17 (a)-(c).

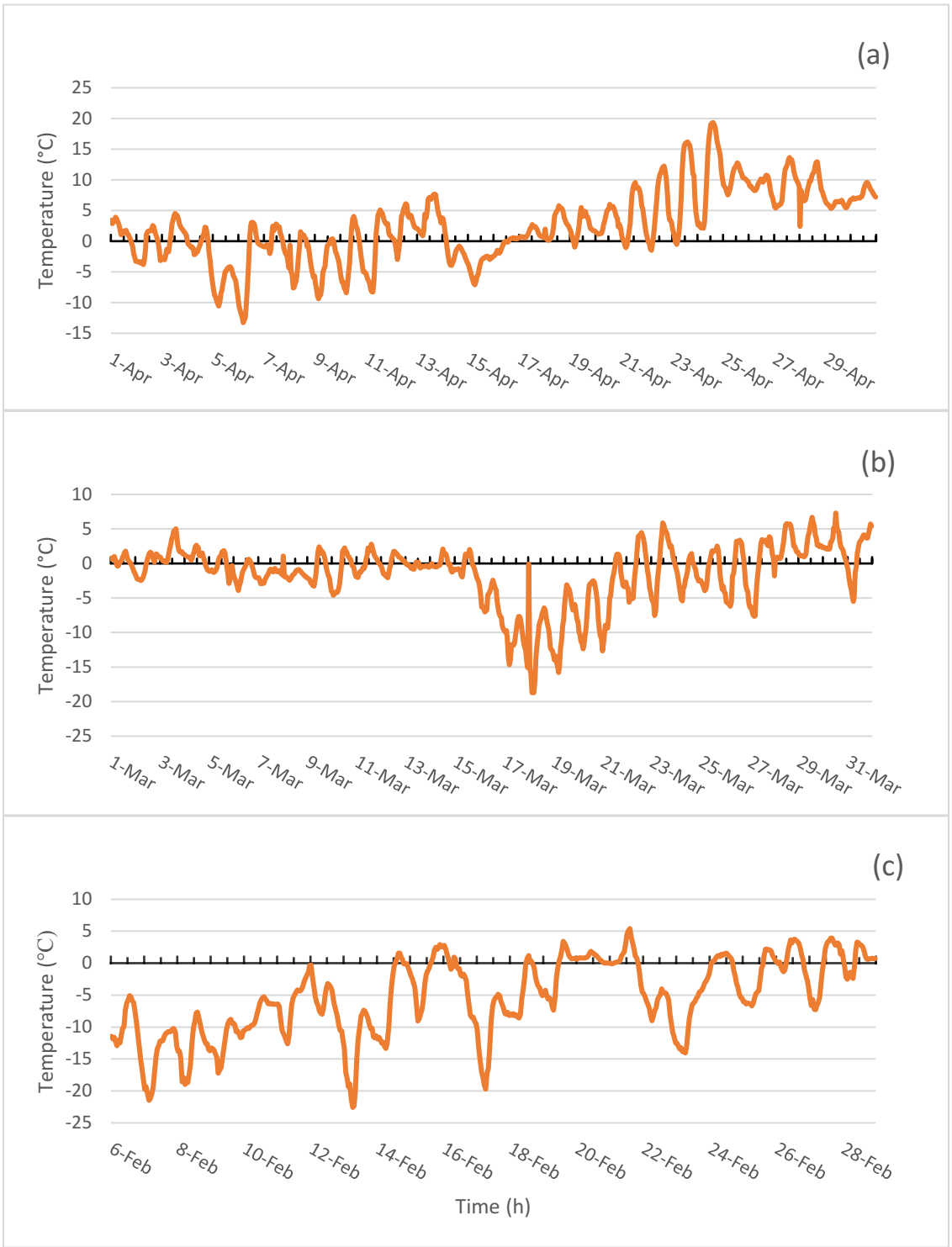

Figure 16 (a)-(c). Ambient temperatures during the validation periods

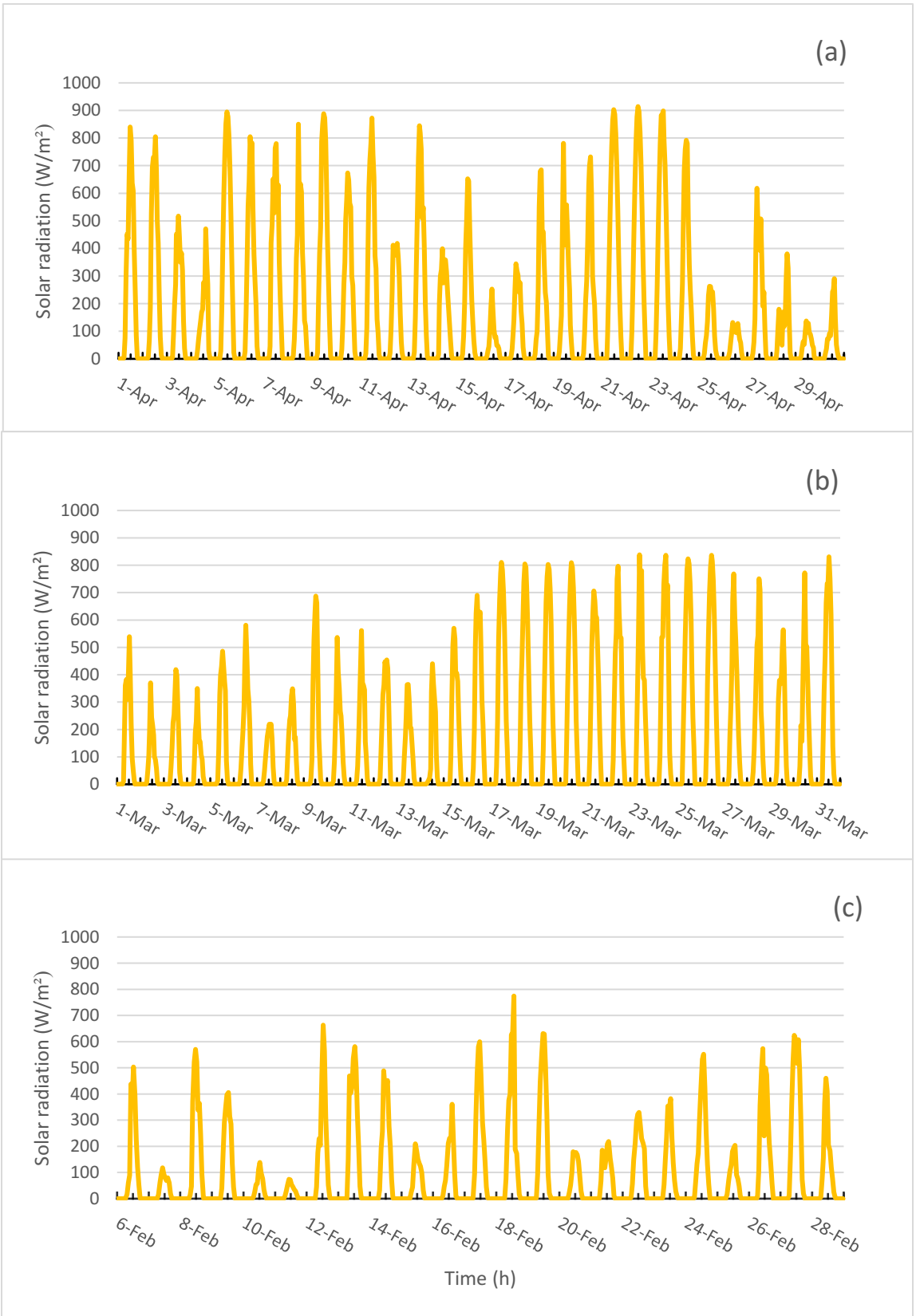

Figure 17 (a)-(c). Measured horizontal solar radiation during the validation periods

4.1.1 Comparison between measured and predicted greenhouse indoor temperatures

Figure 18 (a)-(c) shows the comparison between measured and predicted greenhouse indoor temperatures for the three validation periods. The heating and cooling set-point temperatures are shown in Table 4.1. The good agreement between the measured and predicted temperatures can be visually seen in Figure 18 (a)-(c). In February, the maximum difference between the measured and predicted temperatures during the day is 4°C, while during the night it is 3°C. The model slightly underpredicts the greenhouse indoor temperature during the day, which is likely due to the passive heat gain from the thermal storage whenever the fan turns off.

In March, most of the differences are happening during the night, where the measured greenhouse temperatures are higher than the predicted. This is due to the passive heat gain from the rock-bed thermal storage which happens during the night by natural convection. In the TRNSYS model, if the rock-bed fan is off, there is no air movement from the rock-bed outlet to the greenhouse; while in reality even though the fan is off, the rock-bed outlets are still open and there is an air movement from the rock-bed to the greenhouse. As a result, it causes a passive heat gain in the greenhouse.

In April, the measured greenhouse indoor temperature does not exceed 40°C, and it is above 10°C most of the days, thus, the rock-bed thermal storage only charges for most of the month as it will be shown in section 4.2, where the rock-bed energetic performance is discussed.

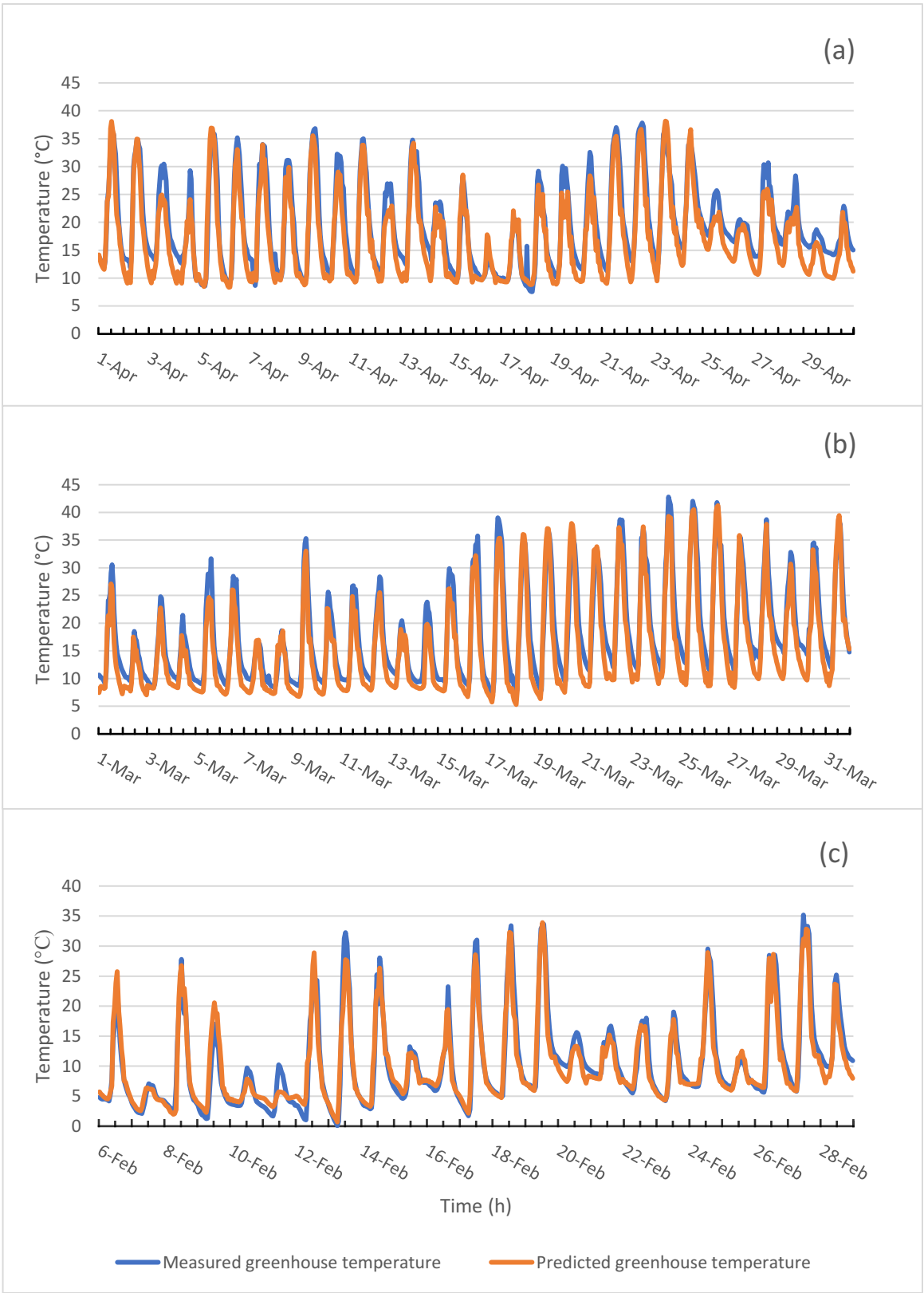

Figure 18 (a)-(c). Comparison between measured data and predicted greenhouse indoor temperatures during the validation periods

Table 4.2 shows the statistical criteria which evaluate the accuracy of the predictions for all three periods. For all periods, r and r^2 values are around 0.97 and 0.93, which are very close to 1. This indicates that there is a strong positive linear relationship between the greenhouse measured and predicted temperatures, and the model predictions are highly accurate. The Mean Absolute Error (MAE) values are 1.4°C, 2.7°C and 2.4°C in February, March, and April, respectively, confirming the accuracy of the predictions as shown in Table 4.2.

Table 4.2 Measured versus predicted greenhouse temperature statistical criteria.

Period	Criteria		
	r	r^2	MAE (°C)
February 6^{th} – 28^{th}	0.97	0.93	1.4
March	0.97	0.93	2.7
April	0.96	0.92	2.4

In addition to statistical criteria, the scatter plot is used to evaluate the accuracy of TRNSYS model in predicting greenhouse indoor temperatures for the validation periods as shown in Figure 19 (a)-(c). The slope points out the linear relationship between the measured and predicted data, and the y-intercept points out any bias in the comparison. A slope of 1 and a y-intercept of 0 mean a perfect match exists between the measured and predicted data. The scatter plot for the validation periods shown in Figure 19 (a)-(c) indicates that the slope and y-intercept values are all very close to perfect values, which further confirms the good agreement between the measured and predicted greenhouse indoor temperatures during the validated periods.

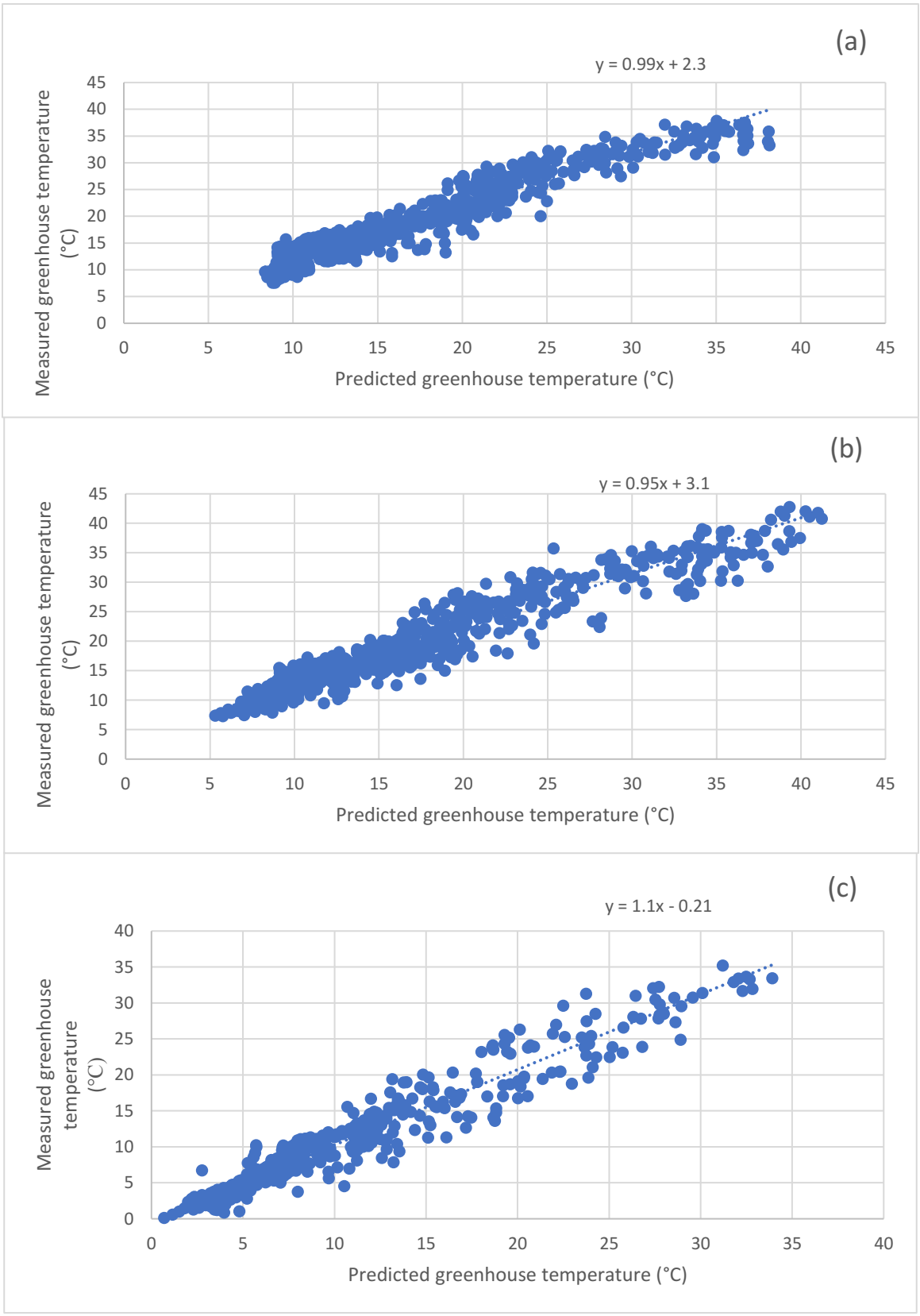

Figure 19 (a)-(c). Scatter plots of measured versus predicted greenhouse temperatures

4.1.2 Comparison between measured and predicted rock-bed outlet temperatures

For the TRNSYS model validation, the average temperature of the four outlets of the rock-bed was taken to be compared to the predicted rock-bed outlet temperature. The comparison between measured and predicted rock-bed outlet temperatures for the three periods is shown in Figure 20 (a)-(c). Both temperatures follow the same pattern in the three validation periods, with the difference between them varying between 0-4°C.

The oscillation in the measured rock-bed outlet average temperature is due to the flow reversal during the night whenever the rock-bed inlet fan is off. The oscillation in the measured rock-bed outlet average temperature is more apparent in the comparisons of March and April. Also, Figure 20 (a)-(c) show that the rock-bed outlet temperatures slightly increase with time; this is because the rock-bed is being charged more than being discharged during all the validation periods as it will be shown in section 4.2, where the rock-bed energetic performance is discussed. The rock-bed outlet average temperature in April is the highest compared to March and February, which shows the effect of the rock-bed thermal storage as a seasonal thermal storage.

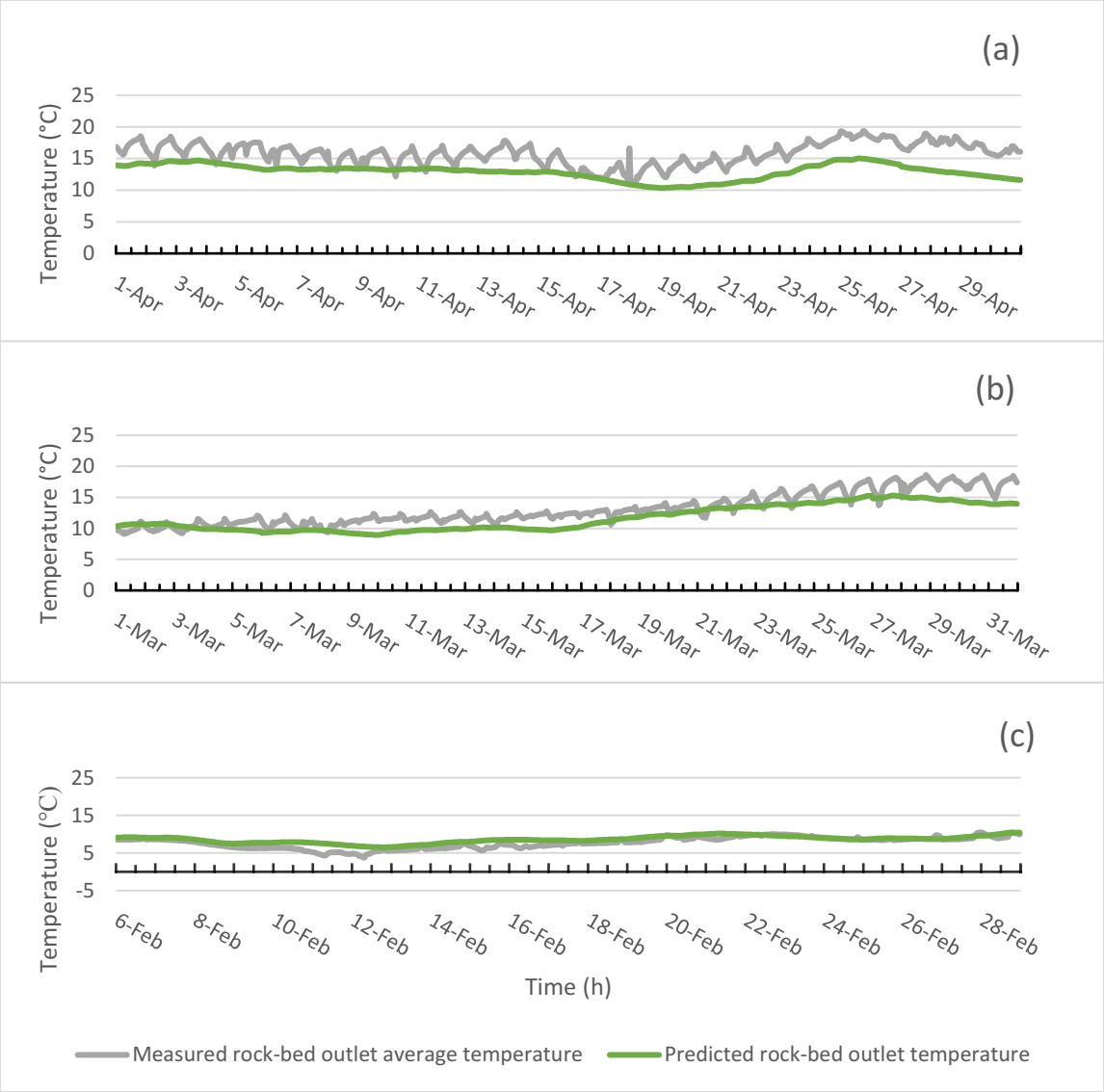

Figure 20 (a)-(c). Comparison between measured and predicted rock-bed outlet temperatures

4.2 Energetic analysis of the rock-bed thermal storage

Daily charging and discharging processes of the rock-bed were evaluated based on the actual measured data for each outlet from February 6th to June/2018, using Equation 6. The rock-bed inlet and outlet temperatures used in equation 6 are shown in Figure 21. The rock-bed inlet temperature is measured after the rock-bed fan to account for the heat added from the rock-bed fan in the energetic analysis.

$$Q = \rho * \dot{V} * C_p * (T_{in} - T_o) \quad (6)$$

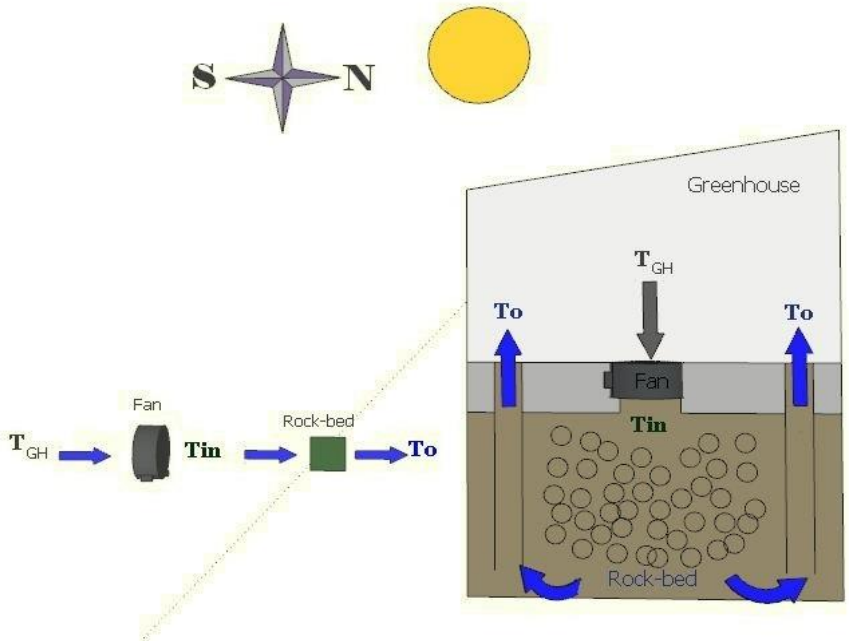

Figure 21. Inlet and outlet temperatures of the rock-bed

Figure 22 shows the monthly heat charged and discharged from February 6th to June/2018. As mentioned above, the amount of heat charged (stored) in the rock-bed thermal storage in this period is much higher than the heat discharged from the rock-bed thermal storage as shown in Figure 22. The amount of heat discharged from the rock-bed is almost half of the amount of heat charged in the rock-bed in February. In March, the amount of heat discharged drops to 185 MJ while the amount of heat charged in the rock-bed thermal storage is around 2,540 MJ. The amount of heat charged and discharged in April is 135 MJ and 1,875 MJ, respectively. During May and June, the amount of heat discharged is negligible, while the amount of heat charged is around 2,000 MJ and 1,200 MJ, respectively.

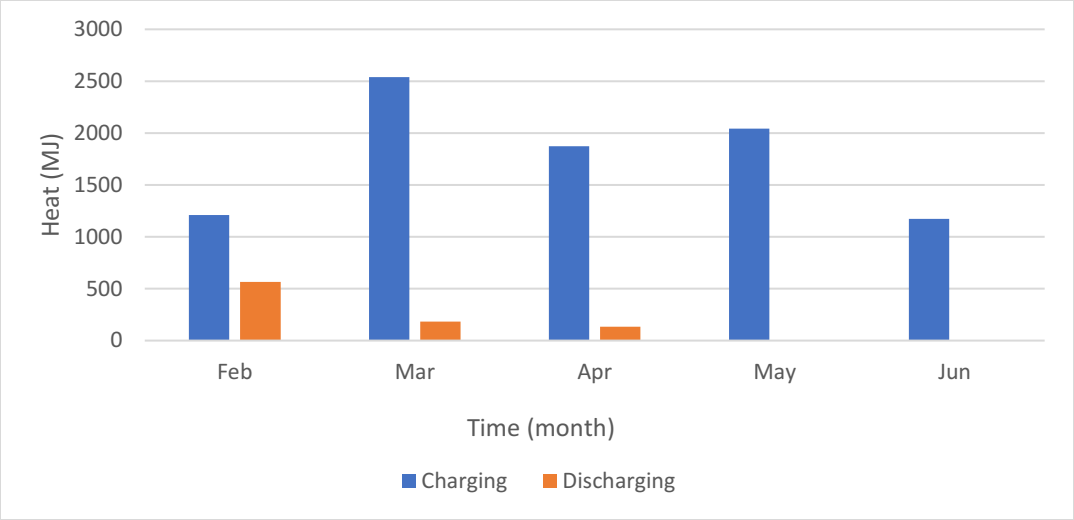

Figure 22. Rock-bed monthly heat charged and discharged

Figure 23 shows the monthly heat charged, discharged, and monthly rock-bed outlet average temperatures. The increase in the average temperature of air from the rock-bed outlets during summer is visible clearly in Figure 23. The average temperature of the rock-bed outlets increased from 8°C in February to 16°C in April then to 23°C in June. The rock-bed thermal storage acts as a seasonal thermal storage, as the rock-bed outlet temperatures keep increasing since more heat is being charged than discharged in summer.

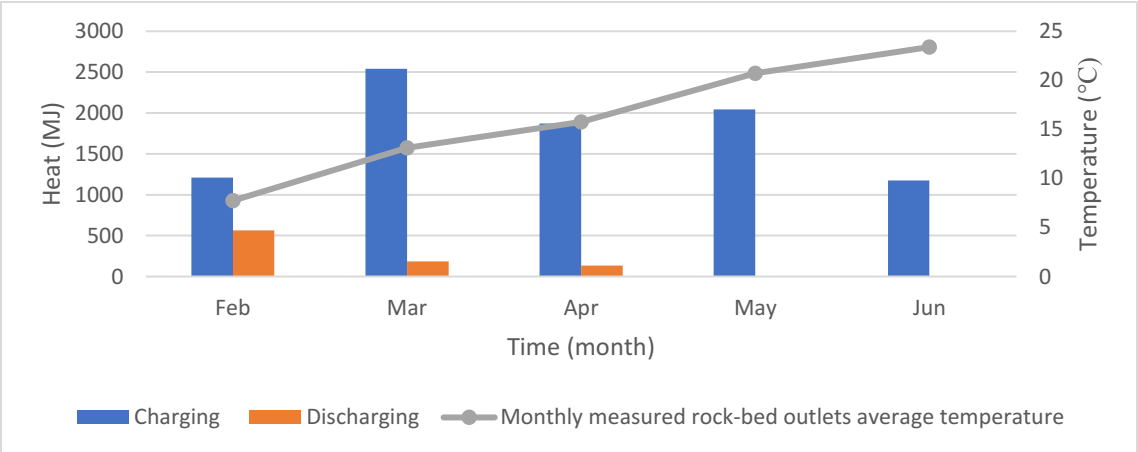

Figure 23. Rock-bed monthly heat charged, discharged and average rock-bed outlet temperature

4.3 The greenhouse performance with and without the rock-bed thermal storage

After validating the TRNSYS model, the attached greenhouse was simulated in TRNSYS 17 without the rock-bed thermal storage to observe the effect of the rock-bed thermal storage on the greenhouse indoor temperature. The attached greenhouse floor was located on soil instead of rock-bed thermal storage. Figure 24 shows the comparison between greenhouse indoor temperatures with and without the rock-bed thermal storage. The effect of the rock-bed thermal storage on the greenhouse indoor temperature is visually seen in Figure 24. In winter nights[1], the greenhouse indoor temperatures of TRNSYS model with rock-bed thermal storage are 5-10°C higher than that of TRNSYS model without rock-bed thermal storage. While in the daytime in winter, the greenhouse indoor temperatures of TRNSYS model with rock-bed thermal storage are less than that of TRNSYS model without rock-bed thermal storage since the heat is being charged into the rock-bed thermal storage. The effect of the rock-bed thermal storage in summer days is more significant than summer nights. The greenhouse indoor temperatures of TRNSYS model with rock-bed thermal storage are 15-20°C less than that TRNSYS model without rock-bed thermal storage. In summer nights, the greenhouse indoor temperatures of TRNSYS model with rock-bed thermal storage are higher than the heating set-point temperature (10°C) or between the heating and cooling set-point temperatures. Therefore, the fan is off most of the time in summer nights, which explains the closeness between the greenhouse indoor temperatures of both models.

[1] The upper half of the temperature plot in Figure 23 is from the daytime and the lower half is from the night time.

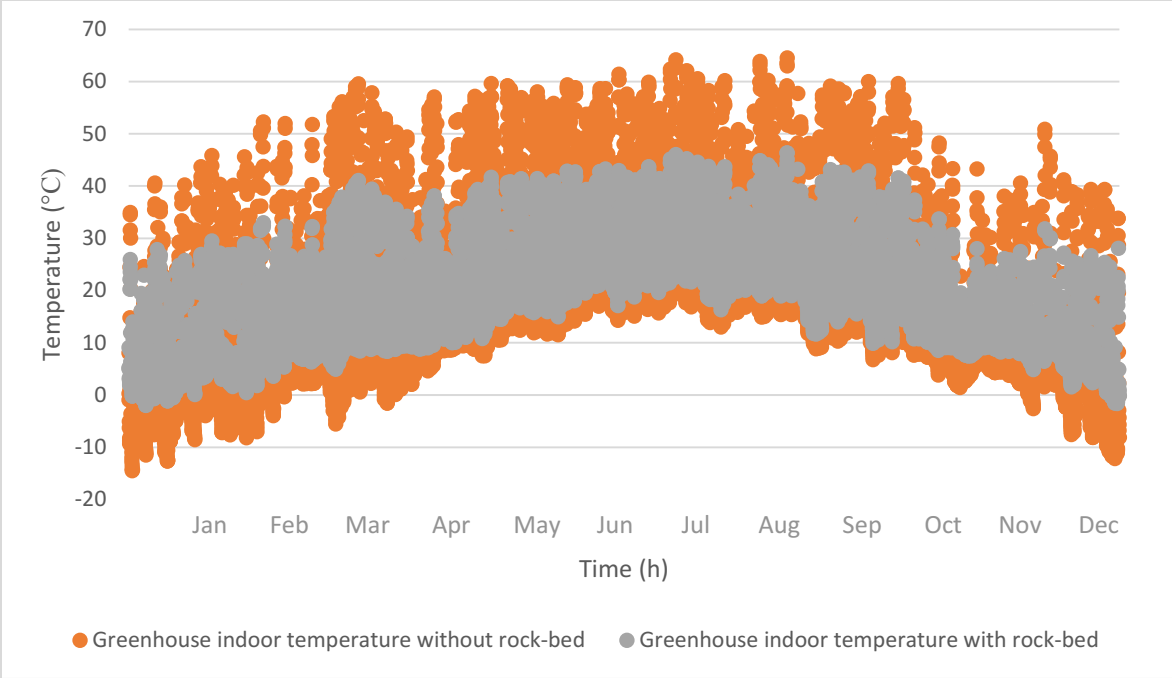

Figure 24. Comparison between greenhouse indoor temperatures with and without the thermal storage.

4.4 Factors affect the energy performance of the attached greenhouse

In order to determine whether it is possible to improve the overall design to achieve better thermal performance, factors that affect the energy performance of the greenhouse should be studied. Several studies have been carried out to study the parameters that affect the performance of greenhouses or rock-beds (Vadiee, 2013; Willits et. al., 1985; Chauhan, 1995; Hänchen, Brückner, and Steinfeld, 2011). Based on the experience gained from previous studies as well as practicality considerations, the following factors are considered in this chapter:

- Heating and cooling set point temperatures,
- Rock-bed air flow rate,
- Cover materials,
- Rock-bed thermal storage size

To avoid overheating the greenhouse, a fan with 1420 L/s (3000 CFM) flow rate was added to the TRNSYS model to provide mechanical outside air ventilation to the greenhouse. The mechanical outside air ventilation is controlled by two differential controllers and the controlling strategy works in a way such that:

- If $T_{GH} > 30°C$ and $T_{GH} > T_{ambient}$, then the mechanical ventilation fan will run to cool the greenhouse.
- Otherwise, the mechanical ventilation will not be activated.

The mechanical outside air ventilation will reduce the amount of heat available inside the greenhouse, and as a result, reduce the amount of heat charged into the rock-bed thermal storage. However, it will eliminate or minimize the undesirable high indoor temperatures, especially in summer.

4.4.1 Effect of heating and cooling set-point temperatures

Temperature control is essential to ensure higher productivity in greenhouses. The ideal temperature in the greenhouse depends on the type of plants grown (Paula A. Claudino, 2016). For example, the best temperature range for cool-season crops, such as onions, cabbage or broccoli, is from 5°C to 16°C, while for warm-season crops, such as tomatoes, cucumbers or eggplants, the best growth temperature is from 16°C to 27°C (MacCullagh, 1978). In this work, several heating and cooling set-point temperatures have been used for greenhouse operation. To study the effect of changing heating/cooling set-point temperatures, six TRNSYS scenarios with different heating/cooling set point

temperatures were developed and run for the whole year (8760 hours). Heating and cooling set-point temperatures used in each scenario are shown in Table 4.3.

Table 4.3 Heating and cooling set-point temperatures

Scenario	Heating set-point temperature (°C) (Discharging)	Cooling set-point temperature (°C) (Charging)
1	10	12
2	10	14
3	10	16
4	10	18
5	10	20
6	10	22

The comparison between the scenarios result is based on the greenhouse indoor temperatures, amount of heat charged into and discharged from the rock-bed thermal storage. Figure 25 shows the greenhouse indoor temperatures for all scenarios. The greenhouse indoor temperatures are very close to each other in all scenarios. In all scenarios, the lowest greenhouse indoor temperature throughout the whole year is -2°C which is in January. while the highest temperature is in July and it is around 34°C when the operation of the ventilation fan is not sufficient to keep the greenhouse temperature below 30°C due to the high outside temperature.

Figure 26 shows the rock-bed outlet temperatures for all scenarios. Since greenhouse indoor temperatures are close to each other, the rock-bed outlet temperatures are similar as well. The lowest rock-bed outlet temperature throughout the year in all scenarios is around 5°C, which is in January, while the highest temperature is 20°C in July.

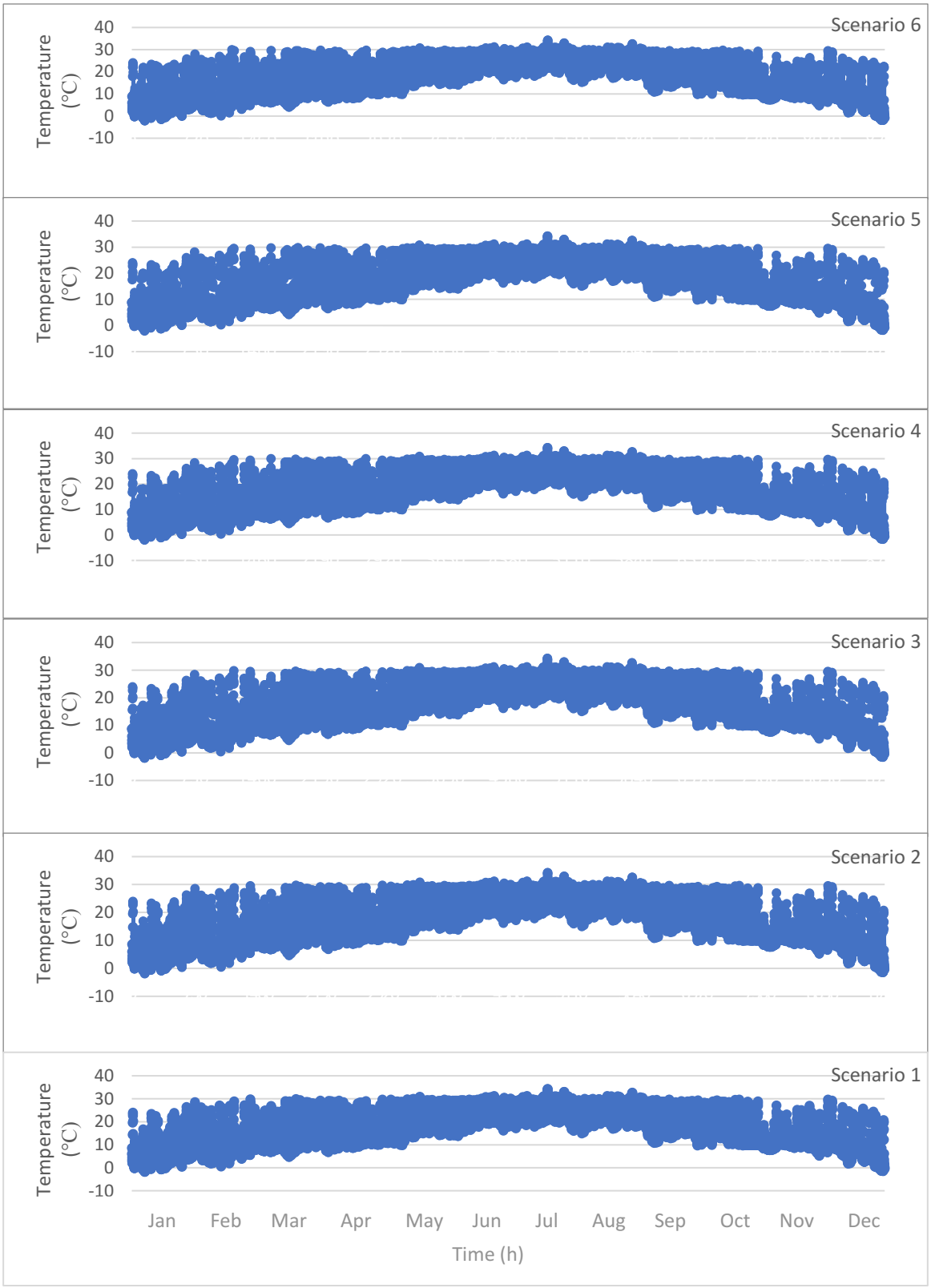

Figure 25. Greenhouse indoor temperatures; effect of heating and cooling set-point temperature

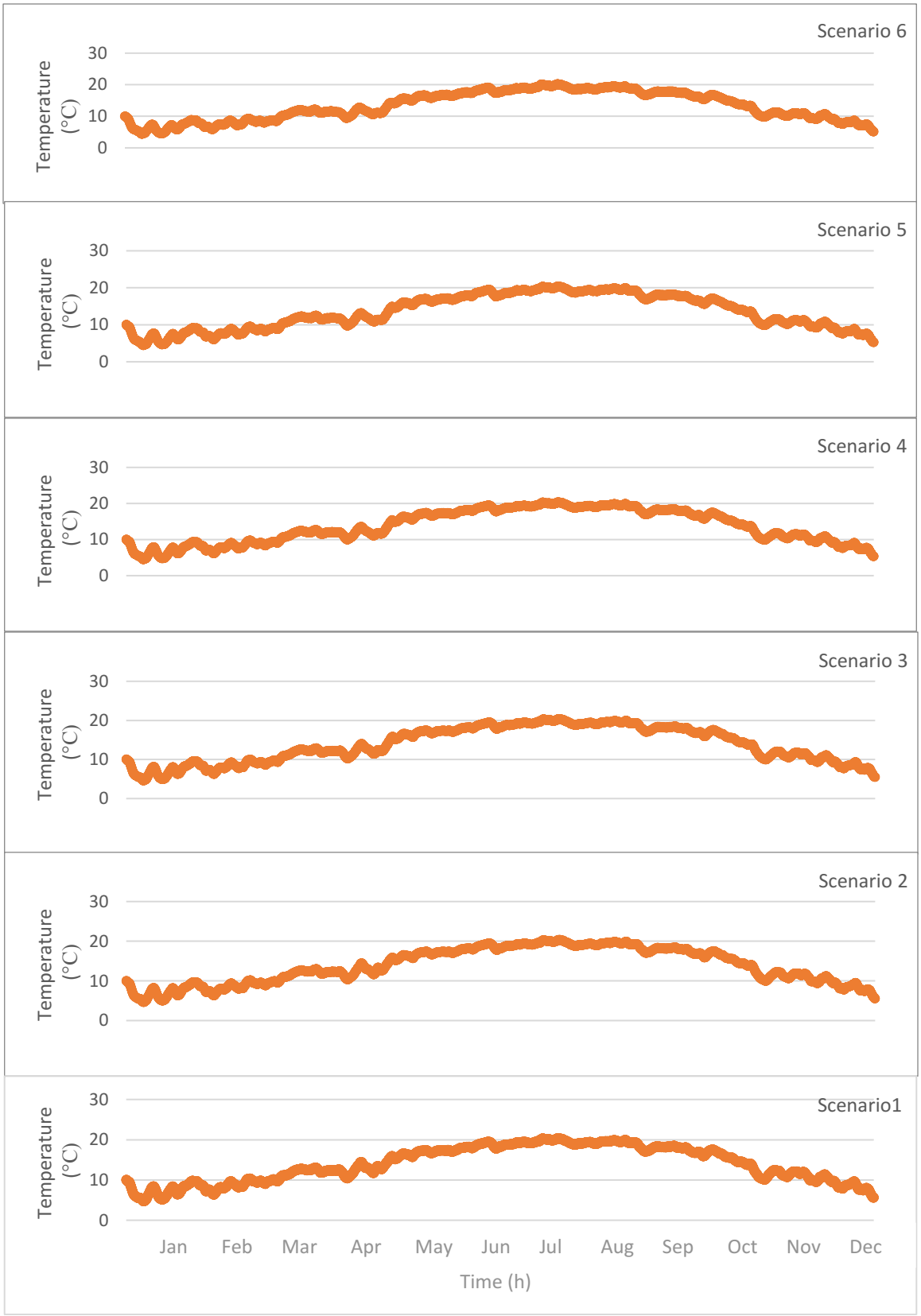

Figure 26. Rock-bed outlet temperatures; effect of heating and cooling set-point temperatures

The amounts of heat charged into the rock-bed thermal storage by all scenarios are shown in Figure 27. As the temperature difference between the heating and cooling set-point temperatures decreases, the fan operates longer. As the fan operates longer the amount of heat charged into the rock-bed thermal storage increases in winter months (January -April and November-December) as shown in Figure 27. The amount of heat charged into the rock-bed in Scenario 1 is higher than other scenarios, because Scenario 1 has the lowest temperature difference between the heating and cooling set-point temperatures.

All scenarios predict correctly that in summer months (May to October) the greenhouse indoor temperatures rarely fall below the heating set-point temperature. The fan operation periods are almost the same in all scenarios throughout the summer due to the mechanical outside air ventilation. As a result, the amount of heat charged into the rock-bed thermal storage during summer months is almost the same for all scenarios.

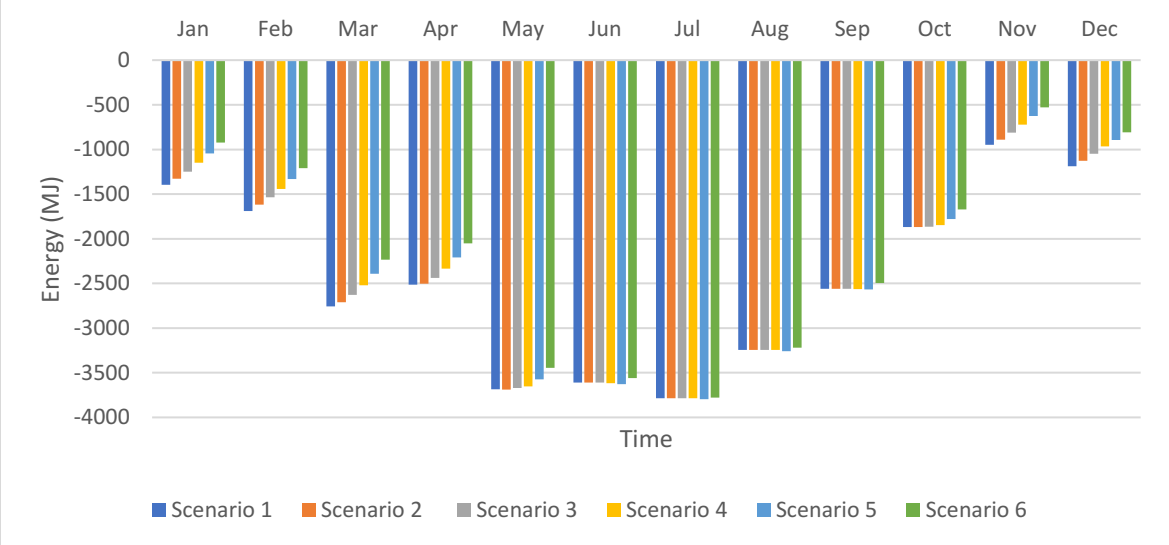

Figure 27. Rock-bed Charging process; effect of heating and cooling set-point temperatures

Figure 28 shows the amount of heat discharged from the rock-bed thermal storage by all scenarios. As the temperature difference between the heating and cooling set-point temperatures decreases, the fan operates longer and, therefore, the amount of heat discharged from the rock-bed thermal storage increases. The amount of heat discharged from the rock-bed by Scenario 1 is slightly higher than other scenarios as shown in Figure 28. In January, the highest amount of heat discharged from the rock-bed thermal storage is 1870 MJ by Scenario 1, while the lowest amount of heat discharged is 1790 MJ by Scenario 6.

In summer, all scenarios predict that the greenhouse indoor temperatures are higher than the heating set-point temperature most of the time, therefore, the amount of heat discharged from the rock-bed thermal storage in summer is negligible for all scenarios as shown in Table 4.4.

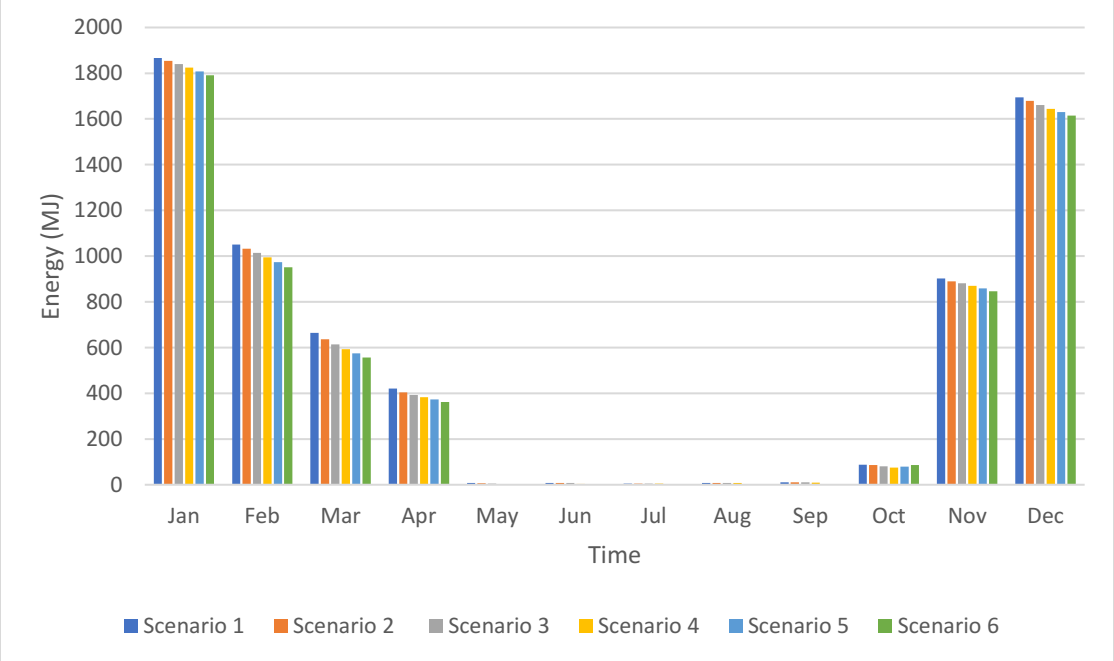

Figure 28. Rock-bed discharging process; effect of heating and cooling set-point temperatures

Table 4.4 shows the total amount of heat charged and discharged from the rock-bed thermal storage and heat added by the rock-bed fan in winter (January-April and November-December) and summer (May-October). As the temperature difference between the heating and cooling set-point temperatures decreases, the fan operates longer and, therefore, the amounts of heat added by the rock-bed fan increases. Scenario 1 has the lowest temperature difference between the heating and cooling set-point temperatures, and therefore, it has the highest amount of heat added by the rock-bed fan compared to other scenarios in winter, while Scenario 6 has the lowest. In summer, the amounts of heat charged into the rock-bed thermal storage by all scenarios are close to each other. Therefore, the amounts of heat added by the rock-bed fan by all scenarios are close to each other as well.

Table 4.4 Heat charged, discharged and heat added from the rock-bed fan, effect of heating and cooling set-point temperature

Scenario	Heating-Cooling set-point temperature-s (°C)	Heat charged in winter (GJ)	Heat charged in summer (GJ)	Heat discharged in winter (GJ)	Heat discharged in summer (GJ)	Heat added by rock-bed fan in winter (GJ)	Heat added by rock-bed fan in summer (GJ)
1	10-12	10.5	18.8	6.6	0.13	0.27	0.28
2	10-14	10.2	18.8	6.5	0.12	0.25	0.28
3	10-16	9.71	18.7	6.4	0.11	0.23	0.27
4	10-18	9.13	18.7	6.3	0.10	0.21	0.26
5	10-20	8.89	18.6	6.2	0.08	0.20	0.25
6	10-22	7.76	18.2	6.1	0.08	0.20	0.22

4.4.2 Effect of Air Flow Rate

The rock-bed fan operation depends on the greenhouse and rock-bed outlet temperatures. The control strategy works in a way that prevents over-heating or over-cooling as explained in Chapter 3. Heating and cooling set-point temperatures used in this section are 10°C and 20°C, respectively. The rock-bed air flow rate used in the TRNSYS model validation was 220 L/s (460 CFM) and is referred to as the original scenario. Table 4.5 shows the air flow rate of each scenario in kg/h, as used in TRNSYS and the equivalent values in CFM and L/s[2].

Table 4.5 Air flow rates

Scenario	Air flow rate (kg/h)	Air flow rate (CFM)	Air flow rate (L/s)
Original	955	460	220
1	1910	920	430
2	3090	1500	710
3	4115	2000	945
4	6175	3000	1420

TRNSYS model calculates the power consumption of the fan by taking into consideration the fan speed, pressure drop and rock-bed size. Based on the motor and the fan efficiencies, it was assumed that 50% of the rock-bed fan power consumption was converted to thermal energy into the rock-bed thermal storage.

[2] All volumetric values citied in this work are based on ASHRAE standard air conditions (68 °F and 14.7 psia)

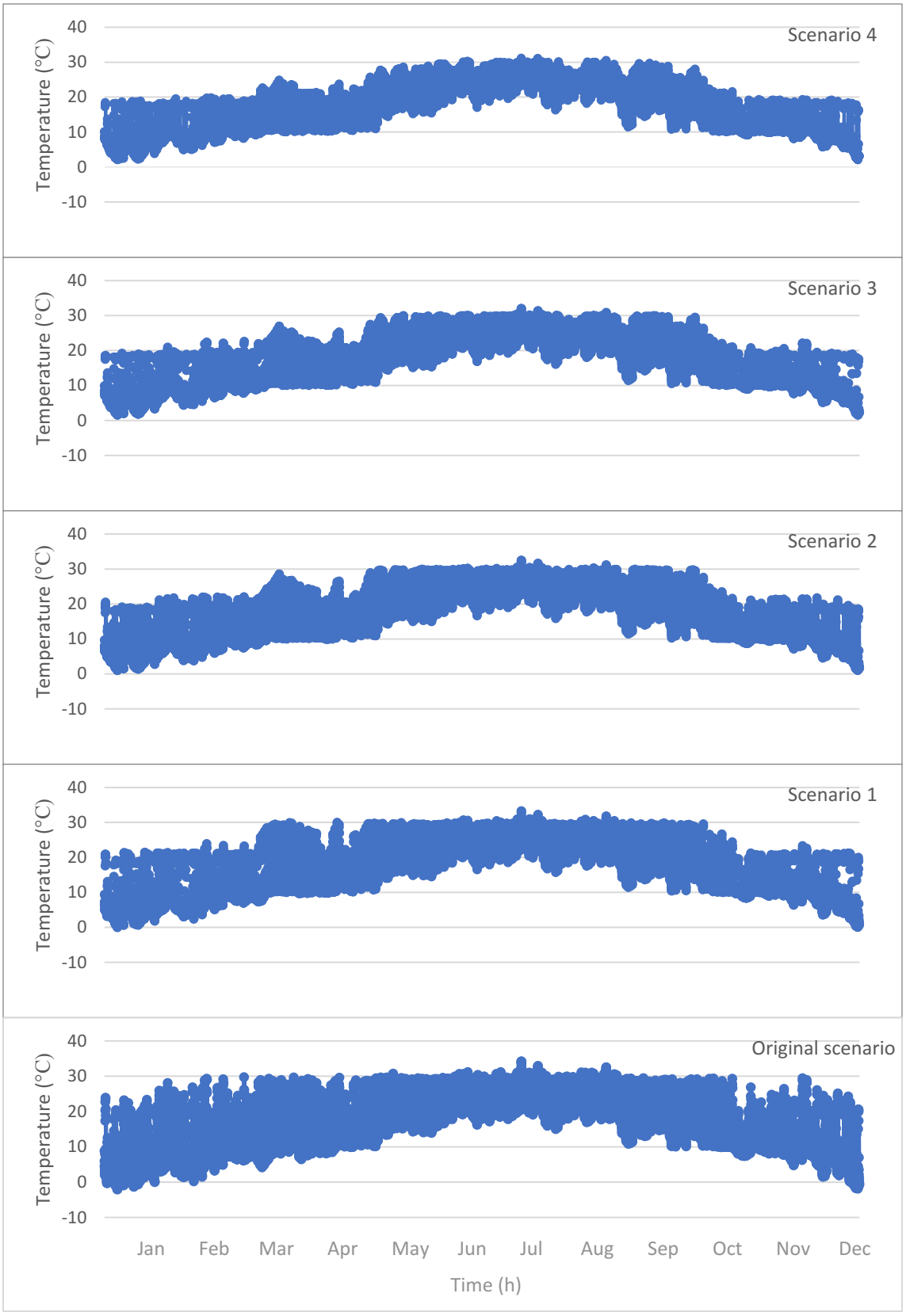

Figure 29. Greenhouse indoor temperatures; effect of air flow rate

Figure 29 shows the greenhouse indoor temperatures for all scenarios. The air flow rate has a significant impact on the greenhouse indoor temperatures as shown in Figure 29. As the air flow rate increases, the amount of heat discharged from the rock-bed thermal storage increases and, therefore, the greenhouse indoor temperatures increase during the discharging process in winter, which is mostly during the night as shown in Figure 29[3]. This is also illustrated in Figure 30, which shows the rock-bed outlet temperatures for all scenarios. As the air flow rate increases the greenhouse indoor temperatures increase and, therefore, the rock-bed outlet temperatures increase. The highest greenhouse indoor temperature during winter nights is 3°C by Scenario 4, while the lowest is -2°C by the Original scenario.

During the day, when the charging process mostly happens, the greenhouse indoor temperatures decrease as the air flow rate increases as shown in Figure 29[3]. This is because more heat is being charged into the rock-bed thermal storage with the higher air flow rate. This is clearly shown in winter days more than summer days since the mechanical outside air ventilation is used more in summer to ventilate the greenhouse whenever the temperature exceeds 30°C. Figure 30 further confirms that the rock-bed outlet temperatures increase as the flow rate increases, which is due to the increase in the amount of heat charged into the rock-bed thermal storage. During summer days, the greenhouse indoor temperatures are very close to each other due to the mechanical

[3] The upper half of the temperature plot in Figure 29 is from the daytime and the lower half is from the night time.

outside air ventilation. In summer nights, all scenarios predict that the greenhouse indoor temperatures are higher than the heating set-point temperature (10°C) most of the time. Therefore, the greenhouse indoor temperatures are close to each other in all scenarios.

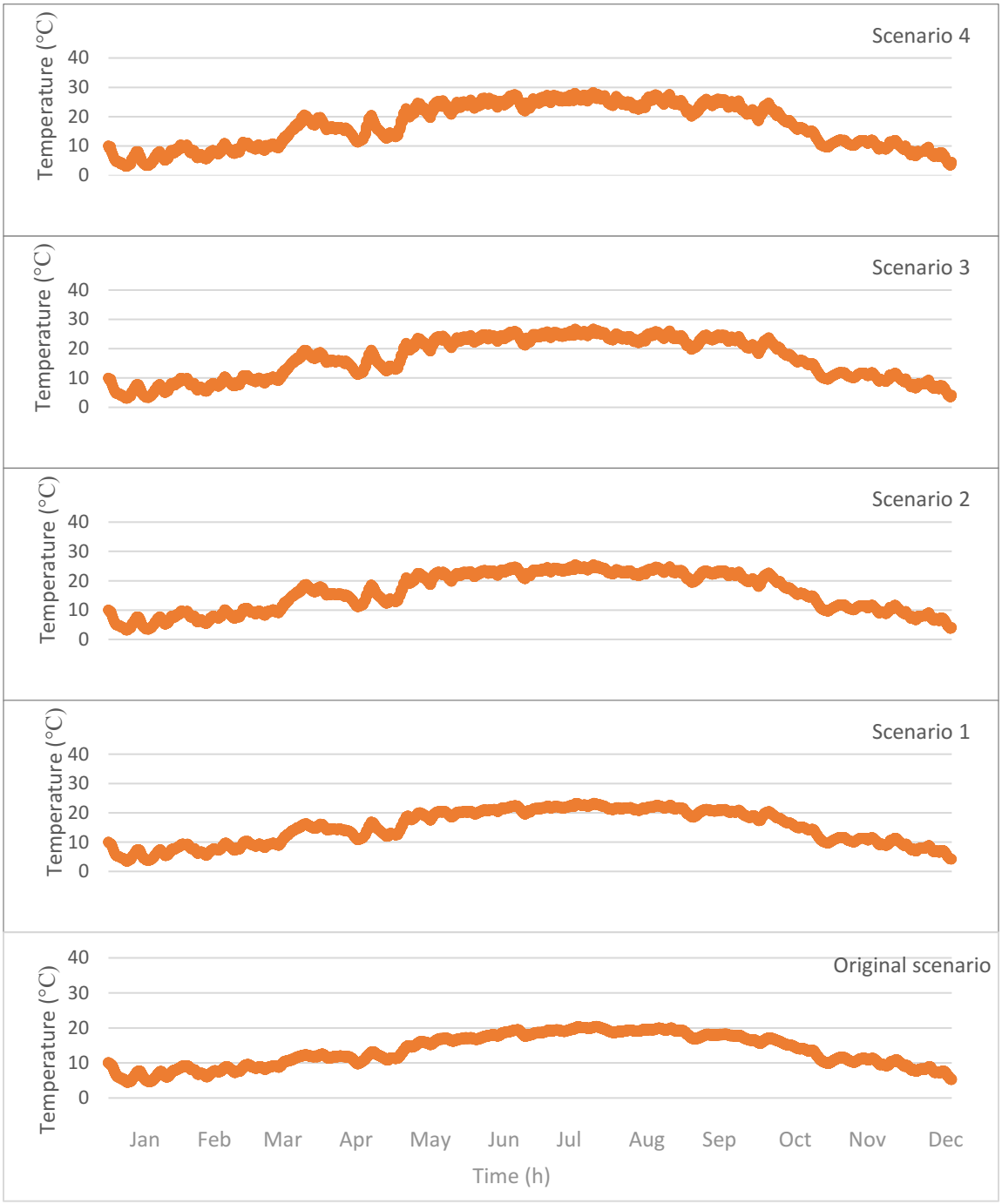

Figure 30. Rock-bed outlet temperatures; effect of air flow rate

Figure 31 shows the amount of heat charged into the rock-bed thermal storage by each scenario. The amount of heat charged into the rock-bed thermal storage increases with the air flow rate as shown in Equation (6). Therefore, as the air flow rate increases the amount of heat charged into the rock-bed thermal storage increases as well. As a result, the greenhouse indoor temperatures decrease during the charging process, which is mostly during the day, since more heat is being charged into the rock-bed with higher flow rates. As to be expected, more heat is charged in summer months.

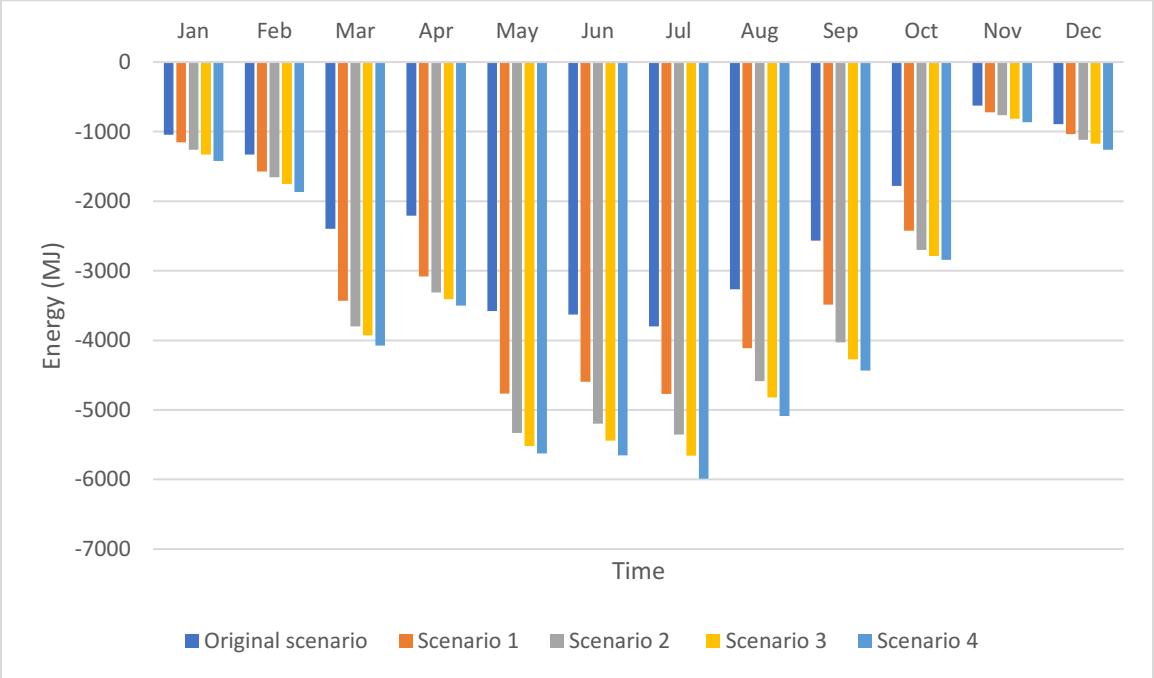

Figure 31. Rock-bed charging process; effect of air flow rate

Figure 32 shows the amount of heat discharged from the rock-bed thermal storage by each scenario. The amount of heat discharged from the rock-bed thermal storage increases with the air flow rate as shown in Equation (6). Therefore, as the air flow rate increases, the amount of heat discharged from the rock-bed thermal storage increases as shown in Figure 31. This explains the increase in the greenhouse indoor temperatures

during winter nights, as more heat is being discharged with higher flow rates. As mentioned before, all scenarios predict that the greenhouse indoor temperatures are higher than the heating set-point temperature (10°C) most of the time in summer. Therefore, the amount of heat discharged from the rock-bed thermal storage in summer by all scenarios is negligible.

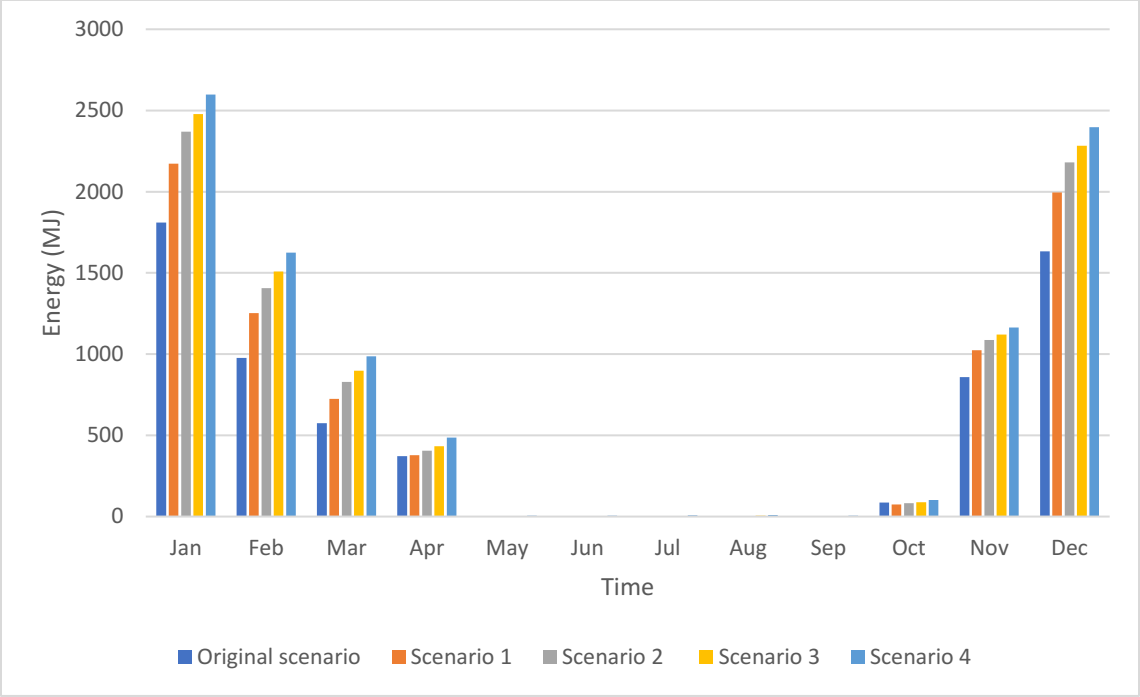

Figure 32. Rock-bed discharging process; effect of air flow rate

The amounts of heat charged and discharged from the rock-bed thermal storage and heat added by the rock-bed fan in winter (January-April and November-December) and summer (May-October) are shown in Table 4.6. As the air flow rate of the rock-bed fan increases, the power consumption of the rock-bed fan increases, as a result, the amount of heat added by the rock-bed fan increases as well. The rock-bed fan in Scenario 4 has the highest air flow rate compared to other scenarios, therefore, the amount of heat

added by the rock-bed fan in Scenario 4 is the highest in winter and summer. While the Original scenario has the lowest air flow rate compared to other scenarios, and therefore, the amount of heat added by the rock-bed fan in the Original scenario is the lowest.

Table 4.6 Heat charged, discharged and heat added by the rock-bed fan, effect of air flow rate

Scenario	Air flow rate (L/s)	Heat charged in winter (GJ)	Heat charged in summer (GJ)	Heat discharged in winter (GJ)	Heat discharged in summer (GJ)	Heat added by rock-bed fan in winter (GJ)	Heat added by rock-bed fan in summer (GJ)
Original	220	8.9	18.6	6.2	0.08	0.21	0.25
1	430	11	24.1	7.5	0.08	0.41	0.5
2	710	11.9	27.2	8.3	0.09	0.61	0.78
3	945	12.4	28.5	8.7	0.1	0.85	1.1
4	1420	13	29.6	9.3	0.13	1.3	1.8

4.4.3 Effect of greenhouse cover materials

Traditionally, the cover material used in greenhouses was glass, but double layer of poly film glazings are used in most new greenhouses (Sanford, 2009). The covering materials used in the test greenhouse are triple polycarbonate in the roof and double low-E glass with argon in the side walls. Light transmissivity and heat transfer coefficient (U-value) are the most important characteristics that should be considered when selecting the greenhouse cover material. These parameters affect the greenhouse indoor temperature and, therefore, the greenhouse production.

Double polycarbonate transmits 4-5% more light than triple polycarbonate, and it is preferred to be used in roofs (Sanford, 2009). Therefore, the double polycarbonate cover material properties were developed in WINDOW 6.3 software and imported into the TRNSYS window library to be used for the roof as shown in Scenarios 1, 3 and 5. The cover materials used in this section are triple polycarbonate, double low-E glass with argon, double polycarbonate, and single glass. The properties of these cover materials are shown in Table 2.2 in Chapter 2.

Table 4.7 Greenhouse cover materials

Scenario	Cover materials	U-value (W/m^2K)
Original	Side walls: double low-E glass with argon Roof: triple Polycarbonate	1.4 2.57
1	Side walls: double low-E glass with argon Roof: double Polycarbonate	1.4 3.43
2	Side walls: triple Polycarbonate Roof: triple Polycarbonate	2.57 2.57
3	Side walls: triple Polycarbonate Roof: double Polycarbonate	2.57 3.43
4	Side walls: single glass Roof: double Polycarbonate	5.68 3.43

Table 4.7 shows the cover materials for each scenario including the test greenhouse, which is referred to as the Original scenario. Heating and cooling set-point temperatures used in this section are 10°C and 20°C, respectively. The order of scenarios in Table 4.7 is based on the overall U-value, where the overall U-value increases with the order from Original scenario to Scenario 4.

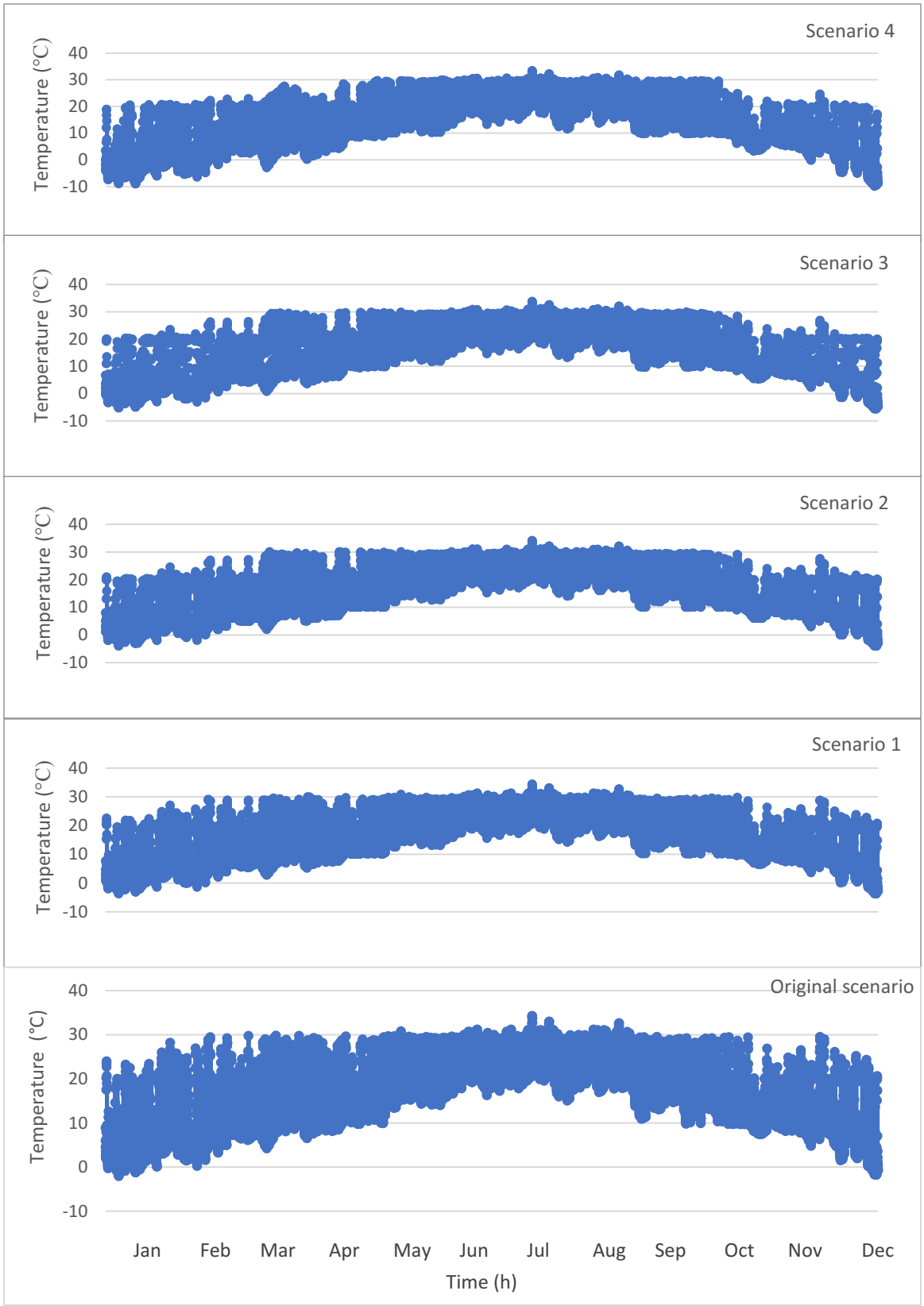

Figure 33. Greenhouse indoor temperatures; effect of greenhouse cover materials

Figure 33 shows the greenhouse indoor temperatures for all scenarios. As the overall U-value increases the amount of heat loss increases as well, and as a result, the greenhouse indoor temperatures decrease. The Original scenario has the lowest heat loss compared to other scenarios since its cover material has the lowest U-value. Therefore, it has the highest greenhouse indoor temperatures throughout the year compared to other scenarios, as the lowest greenhouse indoor temperature in the Original scenario simulation results is -2°C, as shown in Figure 33.

Scenario 4 has the highest U-value compared to other cover materials, therefore, Scenario 4 has the lowest greenhouse indoor temperatures. The lowest greenhouse indoor temperature in Scenario 4 simulation results is -10°C. With the order of scenarios in Table 4.7, the simulation results of all scenarios fall in a reasonable pattern. In summer days, the greenhouse indoor temperatures of all scenarios are very close to each other due to the mechanical outside air ventilation.

Figure 34 shows the rock-bed outlet temperatures of each scenario. As the greenhouse indoor temperature increases, the rock-bed outlet temperature increases as well. Therefore, the Original scenario has the highest rock-bed outlet temperatures compared to other scenarios, while Scenario 4 has the lowest rock-bed outlet temperatures.

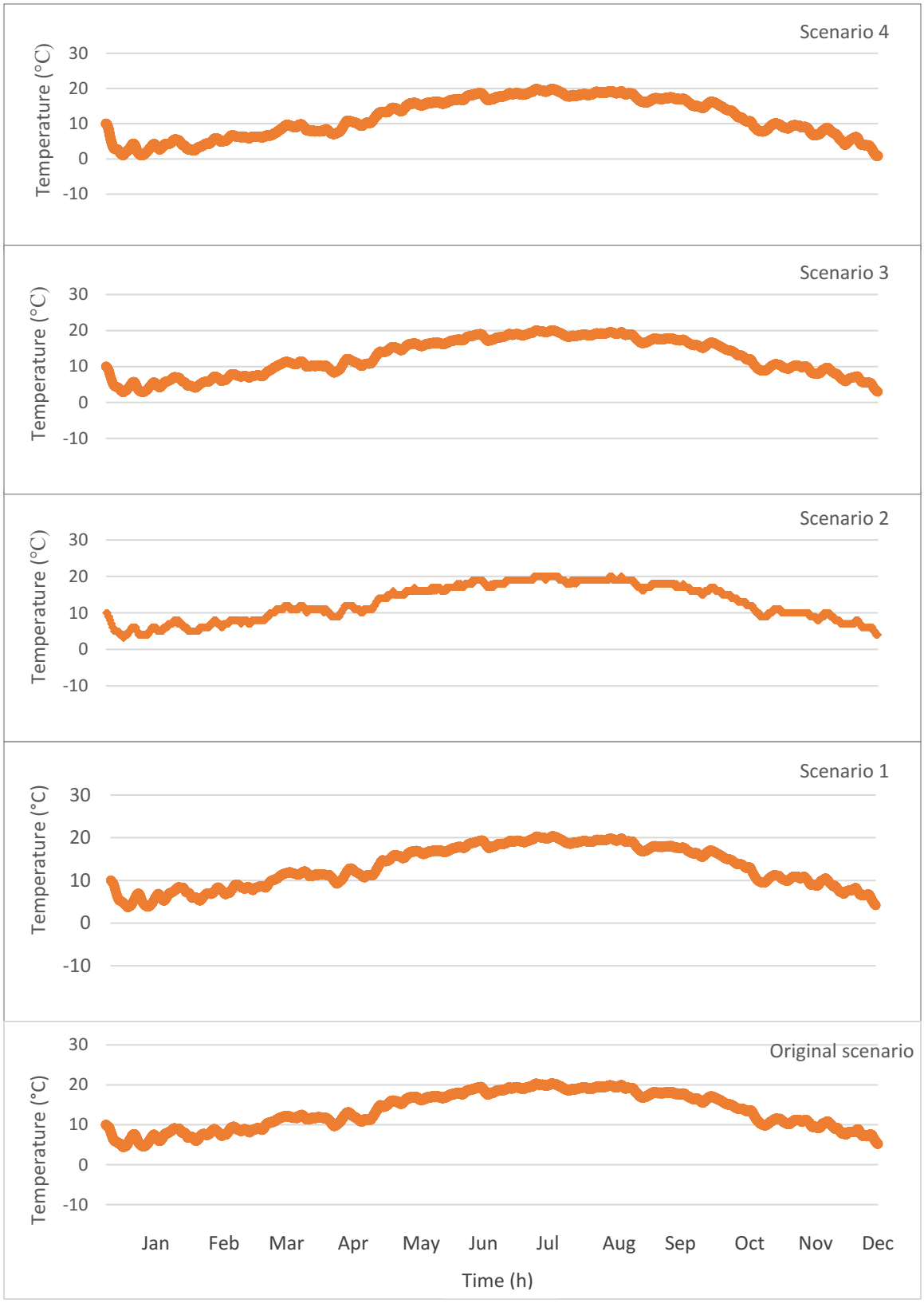

Figure 34. Rock-bed outlet temperatures; effect of greenhouse cover materials

Figure 35 shows the amount of heat charged into the rock-bed thermal storage by all scenarios. As the greenhouse indoor temperature and rock-bed outlet temperature increase, the amount of heat charged into the rock-bed thermal storage increases. The Original scenario has the highest greenhouse indoor temperatures and rock-bed outlet temperatures, therefore, the amount of heat charged into the rock-bed thermal storage by the Original scenario is the highest compared to other scenarios. Since Scenario 4 has the lowest greenhouse indoor temperatures and rock-bed outlet temperatures, the amount of heat charged into the rock-bed thermal storage by Scenario 4 is the lowest compared to other scenarios. With the order of scenarios in Table 4.7, the simulation results of all scenarios fall in a reasonable pattern. In summer days, the greenhouse indoor temperatures and rock-bed outlet temperatures of all scenarios are very close to each other due to the mechanical outside air ventilation. Therefore, the amounts of heat charged into the rock-bed thermal storage by all scenarios in summer are close to each other.

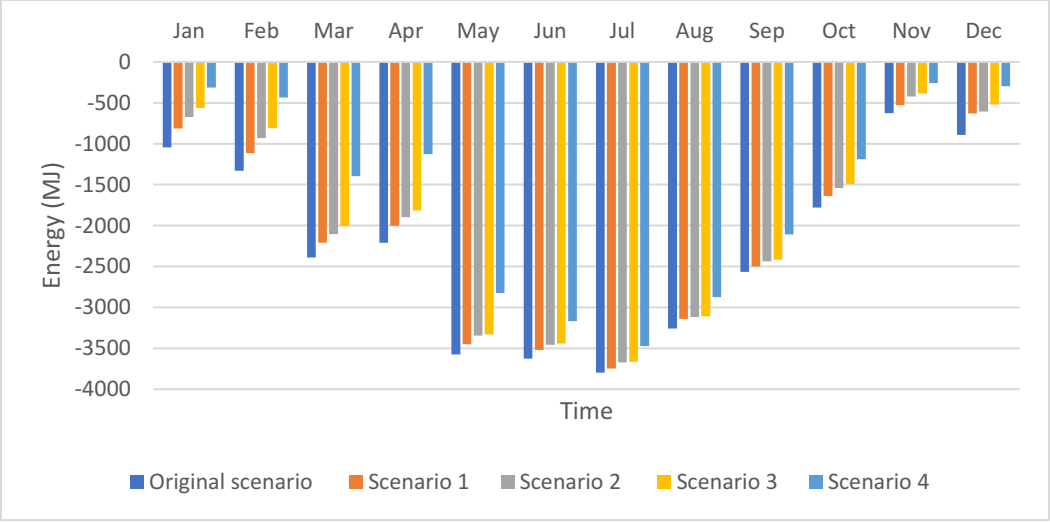

Figure 35. Rock-bed charging process; effect of greenhouse cover materials

Figure 36 shows the amount of heat discharged from the rock-bed thermal storage by all scenarios. The greenhouse indoor temperatures of all scenarios are higher than the heating set-point temperature (10°C) most of the time in summer. Therefore, the amounts of heat discharged from the rock-bed thermal storage by all scenarios are negligible in summer as shown in Figure 36 and Table 4.8. As the greenhouse indoor temperature decreases, the amount of heat discharged from the rock-bed thermal storage increases. Scenario 4 has the lowest greenhouse temperatures compared to other scenarios. Therefore, the amount of heat discharged from the rock-bed thermal storage by Scenario 4 is the highest compared to other scenarios. The highest monthly amount of heat discharged from the rock-bed thermal storage by Scenario 4 is around 3000 MJ in January. While the Original scenario has the highest greenhouse indoor temperatures compared to other scenarios. Therefore, the Original scenario has the lowest amount of heat discharged from the rock-bed thermal storage as shown in Figure 36. The highest monthly amount of heat discharged from the rock-bed thermal storage by the Original scenario is 1800 MJ in January.

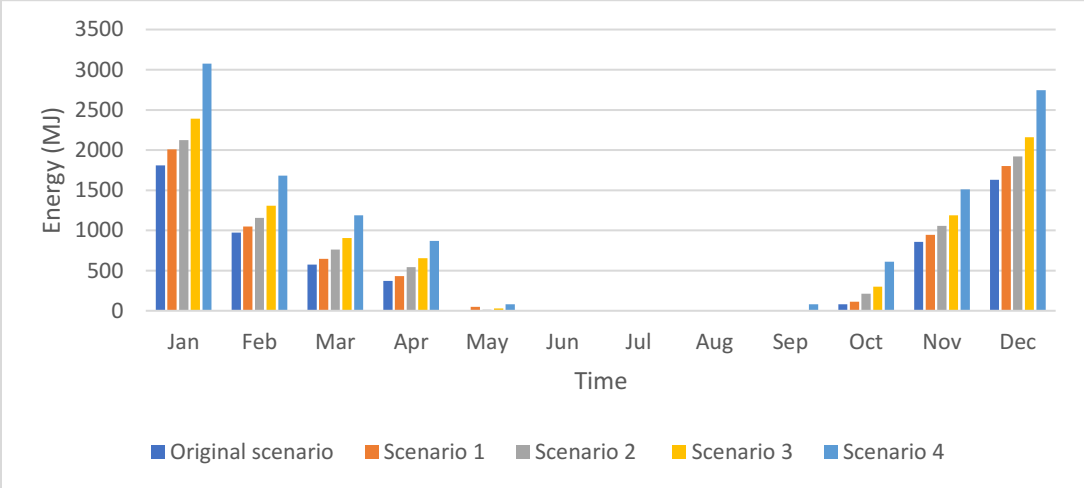

Figure 36. Rock-bed discharging process; effect of greenhouse cover materials

In winter (January- April and November-December), Scenario 4 has the lowest greenhouse indoor temperatures, and therefore, the highest amount of heat discharged from the rock-bed thermal storage. As a result, the amount of heat added by the rock-bed fan in Scenario 4 is the highest in winter compared to other scenarios. While in summer (May-October), the greenhouse indoor temperatures of the Original scenario are the highest compared to other scenarios, and therefore, the amount of heat charged into the rock-bed thermal storage by the Original scenario is the highest in summer. As a result, the amount of heat added by the rock-bed fan in the Original scenario is the highest in summer compared to other scenarios as shown in Table 4.8.

Table 4.8 Heat charged, discharged and heat added from the rock-bed fan, effect of greenhouse cover materials

scenario	U-value (W/m^2K)	Heat charged in winter (GJ)	Heat charged in summer (GJ)	Heat discharged in winter (GJ)	Heat discharged in summer (GJ)	Heat added by rock-bed fan in winter (GJ)	Heat added by rock-bed fan in summer (GJ)
Original	Walls: 1.4 Roof: 2.57	8.9	18.6	6.2	0.08	0.21	0.25
1	Walls: 1.4 Roof: 3.43	7.3	17.9	6.9	0.16	0.22	0.24
2	Walls: 2.57 Roof: 2.57	6.6	17.6	7.6	0.2	0.22	0.23
3	Walls: 2.57 Roof: 3.43	6.1	17.5	8.6	0.3	0.23	0.22
4	Walls: 5.68 Roof: 3.43	3.8	15.6	11	0.8	0.24	0.18

4.4.4 Effect of the rock-bed size

The rock-bed size has a direct impact on how much heat can be charged and discharged in the rock-bed thermal storage. Several studies have been carried out to study the effect of the rock-bed size on the amount of heat charged and discharged from the rock-bed thermal storage (Chauhan, 1995; Hänchen, Brückner, and Steinfeld, 2011). The test rock-bed dimensions used in the TRNSYS model validation are (9x3x2)m^3 and referred to as the Original scenario. Five scenarios including the original one, were developed in TRNSYS to study the effect of the rock-bed size on the overall system as shown in Table 4.9. Heating and cooling set-point temperatures used in this section are 10°C and 20°C, respectively.

Table 4.9 Rock-bed dimensions

Scenario	Rock-bed size (LxWxH) (ft, ft^3)	Rock-bed size (LxWxH) (m, m^3)
Original	30x10x7=2100	9x3x2=57
1	20x10x7=1400	6 x3x2=37
2	20x5x5=500	6x1.5x1.5=14
3	15x5x5=375	4.6x1.5x1.5=10
4	10x5x5=250	3x1.5x1.5=7

Figure 37 shows the greenhouse indoor temperatures for all scenarios. As the rock-bed size increases, the amount of heat discharged from the rock-bed thermal storage increases. Therefore, the greenhouse indoor temperatures increase during winter nights, as shown in Figure 37. The highest greenhouse indoor temperature during winter nights is -2°C by the Original scenario, while the lowest is -9°C by Scenario 4.

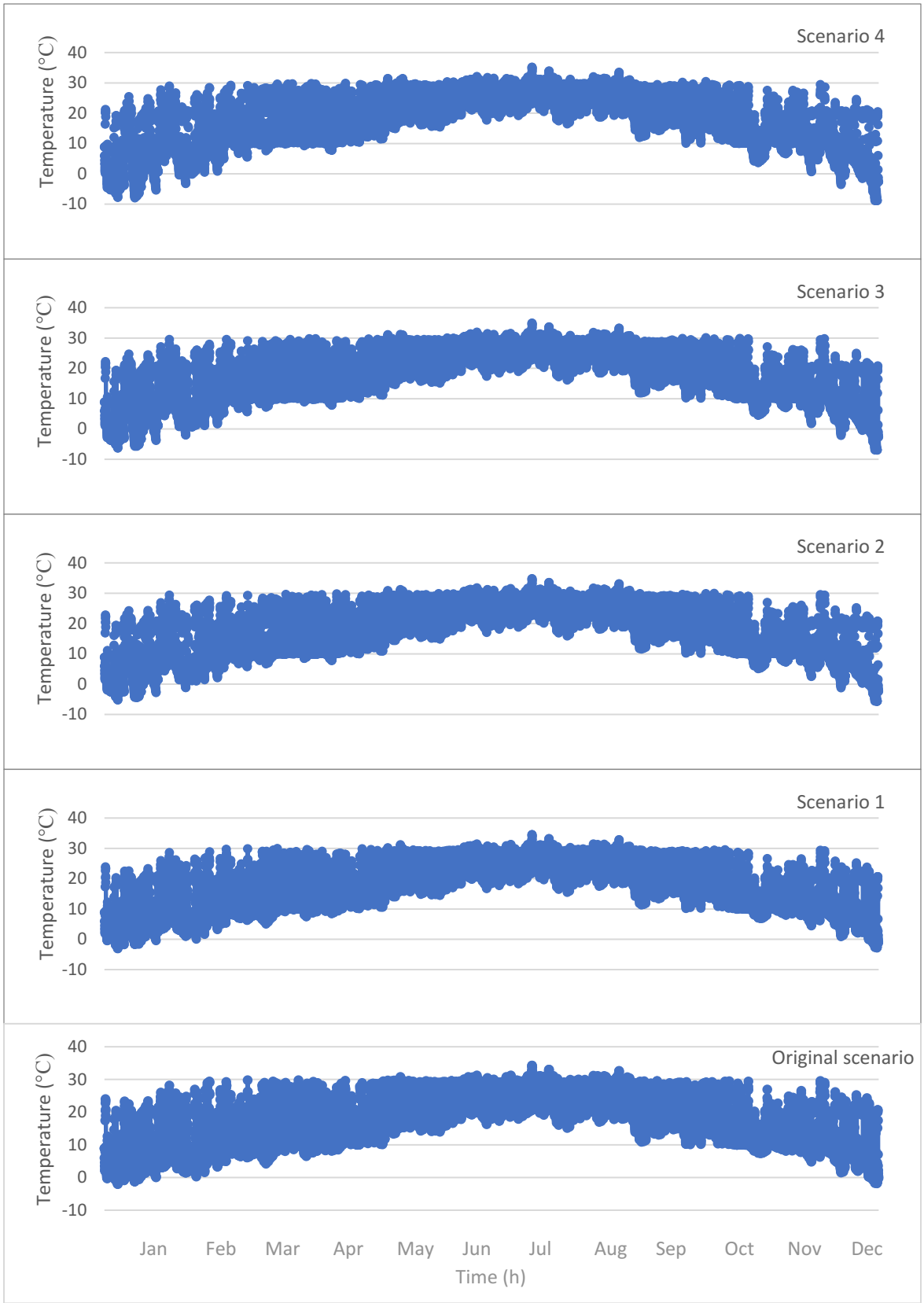

Figure 37. Greenhouse indoor temperatures, effect of the rock-bed size

During the day, when the charging process mostly happens, as the rock-bed size increases the amount of heat charged into the rock-bed thermal storage increases. Therefore, the greenhouse indoor temperatures decrease as shown in Figure 37. This is clearly shown in winter days more than summer days since the mechanical outside air ventilation is used more in summer to ventilate the greenhouse whenever the temperature exceeds 30°C. During summer days, the greenhouse indoor temperatures of all scenarios are very close to each other due to the mechanical outside air ventilation. In summer nights, all scenarios predict that the greenhouse indoor temperatures are higher than the heating set-point temperature (10°C) most of the time. Therefore, the greenhouse indoor temperatures are close to each other in all scenarios.

Figure 38 shows the rock-bed outlet temperatures of each scenario. During the discharging process in winter nights, as the rock-bed size increases the greenhouse indoor temperatures increase. Therefore, the rock-bed outlet temperature increases as shown in Figure 38. The Original scenario has the highest rock-bed outlet temperature during winter nights compared to other scenarios, as the minimum reaches 4°C. The rock-bed outlet temperature keeps decreasing during winter nights as the rock-bed size decreases until it reaches the minimum in Scenario 4, which is -1°C. During the charging process, the rock-bed outlet temperatures decrease as the rock-bed size increases, which is due to the increase in the amount of heat charged into the rock-bed thermal storage as shown in Figure 38. The Original scenario has the lowest rock-bed outlet temperature in summer compared to other scenarios, as it reaches 20°C July, while Scenario 4 has the highest as it reaches 38°C in July.

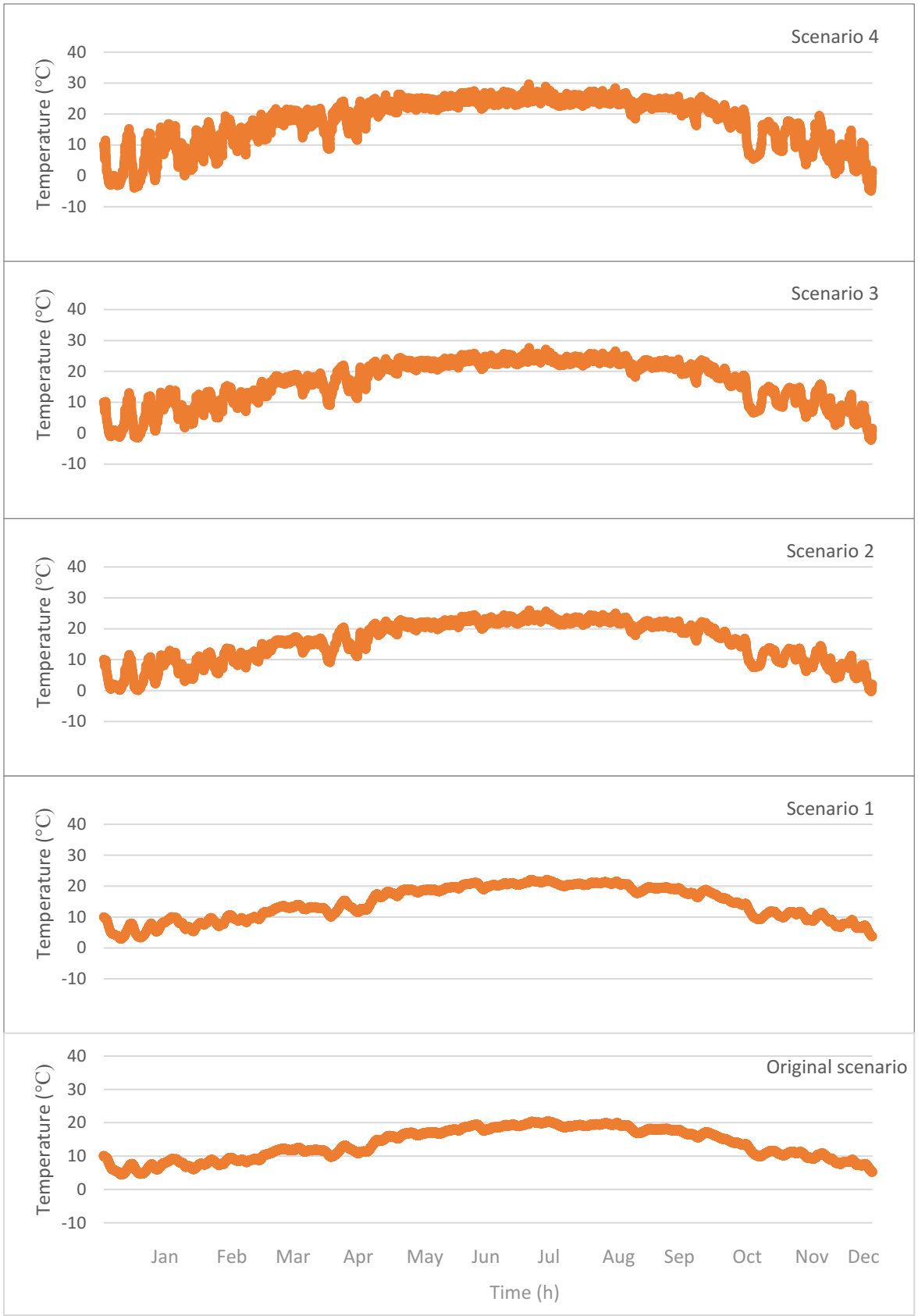

Figure 38. Rock-bed outlet temperatures, effect of the rock-bed size

Figure 39 shows the amount of heat charged into the rock-bed thermal storage by each scenario. The amount of heat charged into the rock-bed thermal storage increases as the rock-bed size increases. The Original scenario has the highest amount of heat charged into the rock-bed thermal storage, as it reaches 3,800 MJ in July. While Scenario 4 has the lowest amount of heat charged into the rock-bed thermal storage, as it reaches 1,700 MJ in July. The greenhouse indoor temperatures of all scenarios are very close to each other during the charging process in winter days, therefore, the amounts of heat charged into the rock-bed thermal storage by all scenarios during winter are close as well.

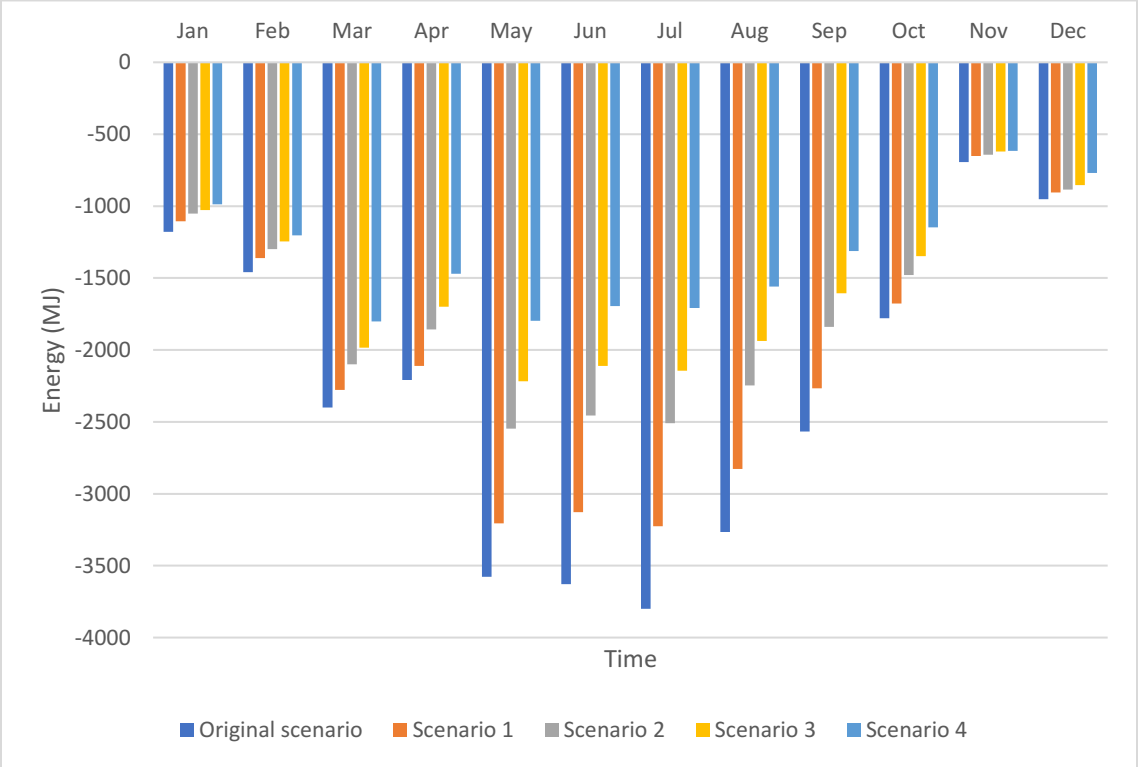

Figure 39. Rock-bed charging process, effect of the rock-bed size

The amount of heat discharged from the rock-bed thermal storage by each scenario is shown in Figure 40. In summer, all scenarios predict that the greenhouse indoor temperatures are higher than the heating set-point temperature (10°C) most of the time. Therefore, the amounts of heat discharged from the rock-bed thermal storage by all scenarios are negligible in summer. During the discharging process, as the rock-bed outlet and greenhouse indoor temperatures decrease at the same time, the amount of heat discharged from the rock-bed thermal storage decreases. Therefore, Scenario 4 has the lowest amount of heat discharged from the rock-bed thermal storage compared to other scenarios. While the Original scenario has the highest amount of heat discharged from the rock-bed thermal storage as shown in Figure 40.

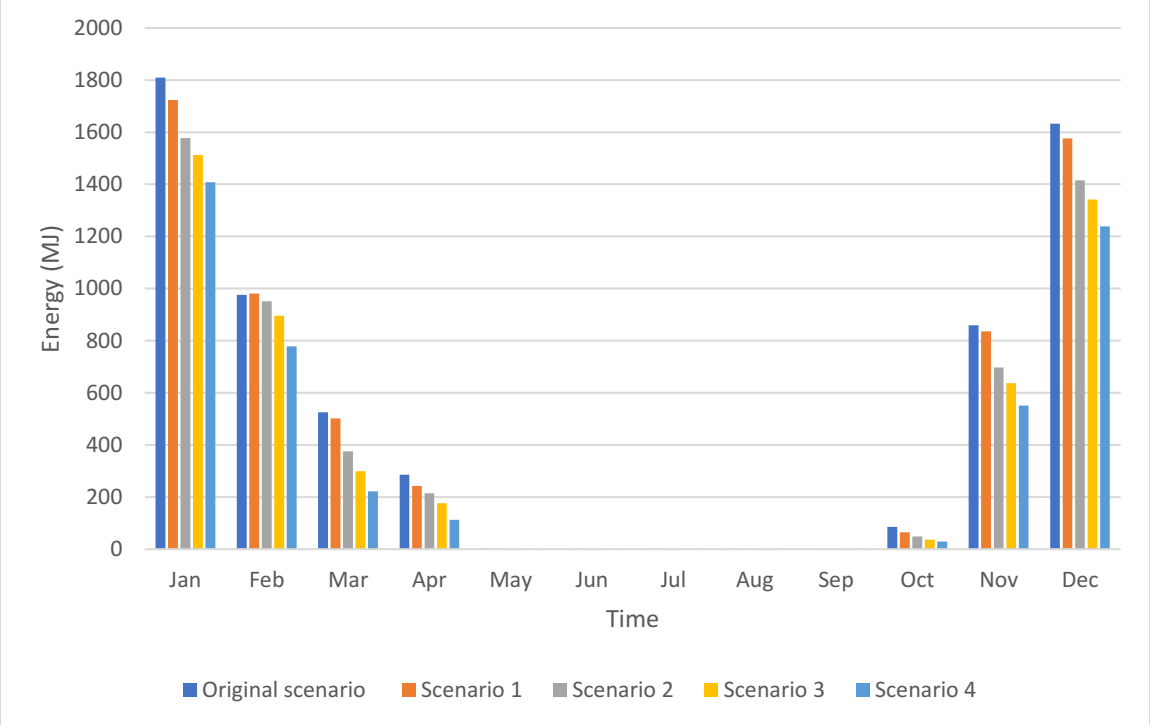

Figure 40. Rock-bed discharging process, effect of the rock-bed size

The amounts of heat charged and discharged from the rock-bed thermal storage and heat added by the rock-bed fan in winter (January-April and November-December) and summer (May-October) are shown in Table 4.10. As the rock-bed size increases, the amounts of heat charged into and discharged from the rock-bed thermal storage increase. As a result, the amount of heat added by the rock-bed fan increases as well. The Original scenario has the highest amount of heat charged and discharged from the rock-bed thermal storage in winter and summer compared to other scenarios. Therefore, it has the highest amount of heat added by the rock-bed fan as shown in Table 4.10. While Scenario 4 has the lowest amount of heat charged and discharged from the rock-bed thermal storage in winter and summer compared to other scenarios. As a result, it has the lowest amount of heat added by the rock-bed fan.

Table 4.10 Heat charged, discharged and heat added by the rock-bed fan, effect of rock-bed size

Scenario	Rock-bed volume (m^3)	Heat charged in winter (GJ)	Heat charged in summer (GJ)	Heat discharged in winter (GJ)	Heat discharged in summer (GJ)	Heat added by rock-bed fan in winter (GJ)	Heat added by rock-bed fan in summer (GJ)
Original	57	8.9	18.6	6.2	0.08	0.22	0.25
1	37	8.4	16.3	5.8	0.06	0.21	0.24
2	14	7.8	13	5.2	0.05	0.2	0.23
3	10	7.4	11.3	4.8	0.04	0.19	0.2
4	7	6.8	9.2	4.3	0.03	0.18	0.17

Chapter 5 Conclusion and Future work

5.1 Conclusion

Solar greenhouses are designed to maximize the heat gain and get the advantage of the excess heat inside the greenhouse in order to reduce the heating requirement of the greenhouse. The excess heat can be stored for short-term or long-term (seasonal) in the greenhouse structure or in a thermal energy storage system. The optimal temperature inside the greenhouse varies based on the type of plant grown inside the greenhouse. Therefore, temperature control is necessary to ensure an optimal growing environment inside the greenhouse. In this study, an attached solar greenhouse connected to a rock-bed thermal storage was instrumented and monitored to study its thermal behavior. The rock-bed thermal storage was designed to store the excess heat during the day and release it whenever the greenhouse indoor temperature falls below the heating set-point temperature. The energetic performance of the rock-bed thermal storage was analyzed based on the amount of heat charged and discharged from the rock-bed during the months of operation. A TRNSYS model was developed in order to predict the indoor temperatures of the attached solar greenhouse and the rock-bed outlet temperatures. Moreover, a parametric study was conducted based on TRNSYS simulation results to study the effect of the heating and cooling set point temperatures, rock-bed air flow rate, cover materials and rock-bed thermal storage size on the greenhouse and rock-bed performance.

TRNSYS model simulation results were validated by comparing the measured greenhouse indoor temperatures and rock-bed outlet temperatures to the predicted

ones for three periods (February, March and April). The validation process of the three periods showed that there is a good agreement between the measured and predicted data with r and r^2 values around 0.97 and 0.93, respectively. The Mean Absolute Error (MAE) values of February, March and April were 1.4°C, 2.7°C and 2.4°C, respectively.

The predicted indoor temperatures of the attached greenhouse with rock-bed were compared to the ones of the same attached greenhouse without rock-bed thermal storage to study the effect of the rock-bed thermal storage on the greenhouse indoor temperatures. The simulation results showed that on summer days the rock-bed thermal storage was capable of reducing the greenhouse indoor temperatures 15-20°C below those without rock-bed thermal storage. On winter nights, the indoor temperatures of the greenhouse with rock-bed thermal storage were 5-10°C higher than those without rock-bed thermal storage. The energetic analysis of the rock-bed thermal storage was based on the measured greenhouse and rock-bed outlet average temperatures from February to June. The measured greenhouse indoor temperatures were higher than the heating set-point temperature (10°C) most of the time during this period. Therefore, the rock-bed thermal storage was charged more than being discharged, and as a result, the rock-bed average outlet temperature kept increasing with time.

The main findings of the parametric study were:

- Changing the cooling (rock-bed charging) set-point temperature from 12°C-22°C while keeping the heating (rock-bed discharging) set-point temperature fixed at 10°C did not have a significant effect on the greenhouse indoor temperature as

shown Table 5.1. However, as the cooling (rock-bed charging) set-point temperature decreased from 22°C to 12°C while keeping the heating (rock-bed discharging) set-point temperature fixed at 10°C, the fan operated longer. As a result, the amounts of heat charged and discharged from the rock-bed thermal storage and the amount of heat added by the rock-bed fan increased as shown in Table 5.1. Scenario 1 has the highest amount of heat charged and discharged from the rock-bed thermal storage and Scenario 6 has the lowest values. As the temperature difference between the heating and cooling set-point temperatures decreased, the amount of heat charged into the rock-bed thermal storage increased in winter. Therefore, the ratio of heat discharged from the rock-bed to heat charged decreased and the ratio of heat charged into the rock-bed to solar heat gain increased in winter as shown in Table 5.1. Scenario 6 has lowest amount of heat charged in winter, and therefore, it has the highest ratio of heat discharged from the rock-bed to heat charged, and lowest ratio of heat charged into the rock-bed to solar heat gain in winter. Scenario 1 has the highest amount of heat charged into the rock-bed thermal storage in winter, and as a result, it has the lowest ratio of heat discharged from the rock-bed to heat charged, and highest ratio of heat charged into the rock-bed to solar heat gain compared to other scenarios. The amounts of heat charged into the rock-bed thermal storage by all scenarios in summer are very close to each other. Therefore, the ratios of heat charged into the rock-bed to solar heat gain by all scenarios in summer are close as well.

Table 5.1 Yearly charged, discharged heat and minimum greenhouse indoor temperature of each scenario, effect of heating and cooling set-point temperature
(For all scenarios, solar heat gain into the greenhouse in winter and summer are 46 GJ and 64.5 GJ, respectively)

Scenario	Heating-Cooling set-point temperature-es (°C)	Charged Heat (GJ)		Discharged heat (GJ)		Discharged /Charged heat (winter)	Heat added from fan (GJ)		Energy charged/ solar heat gain		Heat stored in rock-bed and lost to ground (GJ)	Minimum greenhouse indoor temperatur e (°C)
		W	S	W	S		W	S	W	S		
1	10-12	10.5	18.8	6.6	0.13	0.63	0.27	0.28	0.23	0.29	22.5	-2
2	10-14	10.2	18.8	6.5	0.12	0.64	0.25	0.28	0.22	0.29	22.3	-2
3	10-16	9.71	18.7	6.4	0.11	0.66	0.23	0.27	0.21	0.29	21.9	-2
4	10-18	9.13	18.7	6.3	0.10	0.69	0.21	0.26	0.2	0.29	21.4	-2
5	10-20	8.9	18.6	6.2	0.08	0.7	0.21	0.25	0.19	0.29	21.2	-2
6	10-22	7.76	18.2	6.1	0.08	0.79	0.20	0.22	0.17	0.28	19.7	-2

W: Winter (January -April, November-December)

S: Summer (May-October)

Heat stored in rock-bed and lost to ground= (Heat charged (winter + summer) – Heat discharged (winter + summer))

- As the rock-bed air flow rate increased, the greenhouse indoor temperatures decreased during the day time due to the increases in the amount of heat charged into the rock-bed thermal storage in winter and summer as shown in Table 5.2. As a result, the ratio of heat charged into the rock-bed to solar heat gain increased. Also, as the rock-bed air flow rate increased, the greenhouse indoor temperatures increased at night due to the increase in the amount of heat discharged from the rock-bed thermal storage.

- Scenario 4 has the highest air flow rate compared to other scenarios, and therefore, it has the highest amounts of heat charged and discharged from the rock-bed thermal storage. As a result, it has the highest ratio of heat charged into the rock-bed to solar heat gain and the highest greenhouse indoor temperatures at night compared to other scenarios, as the minimum reached 3°C. The Original scenario has the lowest air flow rate , and therefore, it has the lowest amounts of heat charged and discharged from the rock-bed thermal storage. As a result, it has the lowest ratio of heat charged into the rock-bed to solar heat gain and the lowest greenhouse indoor temperatures at night, as the minimum reached -2°C.
- Moreover, as the rock-bed air flow rate increased, the rock-bed fan power consumption increased. As a result, the amount of heat added by the rock-bed fan increases in winter and summer as shown in Table 5.2. The ratios of heat discharged from the rock-bed to heat charged into the rock-bed by all scenarios are very close to each other. Among the five scenarios, Scenario 4 has the highest amount of heat charged and discharged from the rock-bed. However, the rock-

bed fan in Scenario 4 has the highest power consumption compared to other scenarios.

- If the purpose is to reduce the rock-bed fan power consumption and prevent the greenhouse from freezing at the same time, then the air flow rate of Scenario 2 is recommended. The simulation results of Scenario 2 showed that the amounts of heat charged and discharged from the rock-bed thermal storage were higher than those of the Original scenario and Scenario 1, and close to those of Scenarios 3 and 4. Although the rock-bed fan power consumption in Scenario 2 was higher than those of the Original scenario and Scenario 1, the rock-bed thermal storage in Scenario 2 prevented the greenhouse from freezing. Unlike those in the Original scenario and Scenario 1, as the greenhouse indoor temperatures in the Original scenario and Scenario 1 fell below 0°C.

Table 5.2 Yearly charged, discharged heat and minimum greenhouse indoor temperature of each scenario, effect of air flow rate

(For all scenarios, solar heat gain into the greenhouse in winter and summer are 46 GJ and 64.5 GJ, respectively)

Scenario	Air flow rate (L/s)	Charged Heat (GJ)		Discharged heat (GJ)		Discharged /Charged heat (winter)	Heat added from fan (GJ)		Energy charged/ solar heat gain		Heat stored in rock-bed and lost to ground (GJ)	Minimum greenhouse indoor temperature (°C)
		W	S	W	S		W	S	W	S		
Original	220	8.9	18.6	6.2	0.08	0.7	0.21	0.25	0.19	0.29	21.2	-2
1	430	11	24.1	7.5	0.08	0.68	0.41	0.5	0.24	0.37	27.5	-1
2	710	11.9	27.2	8.3	0.09	0.7	0.61	0.78	0.26	0.42	30.7	1
3	945	12.4	28.5	8.7	0.1	0.7	0.85	1.1	0.27	0.44	32.1	2
4	1420	13	29.6	9.3	0.13	0.71	1.3	1.8	0.28	0.46	33.3	3

W: Winter (January -April, November-December)

S: Summer (May-October)

Heat stored in rock-bed and lost to ground= (Heat charged (winter + summer) – Heat discharged (winter + summer))

- The U-value of the greenhouse cover material has a significant effect on the greenhouse indoor temperatures. Among triple polycarbonate, double low-E glass with argon, double polycarbonate, and single glass, the greenhouse with double low-E glass with argon and triple polycarbonate cover materials (Original scenario) had the lowest heat loss compared to others. Therefore, the indoor temperatures of the greenhouse in the Original scenario simulation results were the highest as shown in Table 5.3, as the minimum greenhouse indoor temperature in winter reached -2°C in the Original scenario simulation results. As a result, the amount of heat charged into the rock-bed thermal storage by the Original scenario was the highest and the amount of heat discharged from the rock-bed thermal storage by the Original scenario was the lowest compared to other scenarios. Scenario 4 has the highest overall U-value, and therefore, it has the highest heat loss compared to other scenarios. Although Scenario 4 has the highest amount of heat discharged from the rock-bed thermal storage compared to other scenarios, it has the lowest greenhouse indoor temperatures as the mimimum reached -10°C in winter, as shown in Table 5.3.
- In winter, Scenario 4 has the highest amount of heat discharged from the rock-bed thermal storage. As a result, the amount of heat added by the rock-bed fan in Scenario 4 was the highest in winter compared to other scenarios. While in summer, the Original scenario has the highest amount of heat charged into the rock-bed thermal storage. As a result, the amount of heat added by the rock-bed

fan in the Original scenario was the highest in summer compared to other scenarios as shown in Table 5.3.

- As the overall U-value of the greenhouse cover material decreased, the amount of heat charged into rock-bed thermal storage increased. As a result, the ratio of heat charged into the rock-bed to solar heat gain increased as shown in Table 5.3. With the order of scenarios in Table 5.3, the simulation results of all scenarios fall in a reasonable pattern.

- In winter days, the greenhouse indoor tempratures decreased as the overall U-value of the greenhouser cover material increased. This explains the decrease in the amount of heat charged into the rock-bed thermal storage. However, whenever the overall U-value of the greenhouser cover material was 2.57 W/m^2K or above (as in Scenarios 2, 3 and 4), the greenhouse indoor temperatures were lower than the cooling set-point temperature (20°C) most of the time in winter days. As a result, the amount of heat discharged from the rock-bed thermal storage in winter was higher than the amount of heat charged into the rock-bed thermal storage as shown in the ratio of heat discharged from the rock-bed to heat charged in Table 5.3. This shows the effect of the rock-bed thermal storage as it acts as a seasonal thermal storage.
- Overall, it is recommended to use the cover material of the the Original scenario since the simulation results showed that the greenhouse and rock-bed of the Original scenario showed a better performance than other scenarios.

Table 5.3 Yearly charged, discharged heat and minimum greenhouse indoor temperature of each scenario, effect of greenhouse cover materials

Scenario	U-value (W/m^2K)	Charged Heat (GJ)		Discharged heat (GJ)		Discharged /Charged heat (winter)	Heat added from fan (GJ)		Energy charged/ solar heat gain		Solar heat gain into the greenhou-se (GJ)		Heat stored in rock-bed and lost to ground (GJ)	Minimum greenhouse indoor temperatur e (°C)
		W	S	W	S		W	S	W	S	W	S		
Original	Walls: 1.4 Roof: 2.57	8.9	18.6	6.2	0.08	0.7	0.21	0.25	0.19	0.29	45.9	64.5	21.2	-2
1	Walls:1.4 Roof: 3.43	7.3	17.9	6.9	0.16	0.9	0.22	0.24	0.15	0.28	46.1	64.7	18.1	-3
2	Walls:2.57 Roof: 2.57	6.6	17.6	7.6	0.2	1.1	0.22	0.23	0.14	0.27	46.2	64.8	16.4	-4
3	Walls:2.57 Roof: 3.43	6.1	17.5	8.6	0.3	1.4	0.23	0.22	0.13	0.26	46.7	65.3	14.6	-6
4	Walls:5.68 Roof: 3.43	3.8	15.6	11	0.8	2.9	0.24	0.18	0.08	0.22	50	68.3	7.6	-10

W: Winter (January -April, November-December)

S: Summer (May-October)

Heat stored in rock-bed and lost to ground= (Heat charged (winter + summer) – Heat discharged (winter + summer))

- As the rock-bed size increased , the greenhouse indoor temperatures decreased during the day time due to the increase in the amount of heat charged into the rock-bed thermal storage as shown in the amount of heat charged into the rock-bed thermal storage in winter and summer in Table 5.4. Also, as the rock-bed size increased, the amount of heat discharged from the rock-bed thermal storage increased. As a result, the greenhouse indoor temperatures increased in winter nights. Therefore, the amount of heat added by the rock-bed fan increased as the rock-bed size increased due to the increase in the amount of heat charged into and discharged from the rock-bed thermal storage.
- The rock-bed size of the Original scenario is the biggest compared to other scenarios, and therefore, the Original scenario has the highest amounts of heat charged and discharged from the rock-bed thermal storage in winter and summer compared to other scenarios. As a result, it has the highest greenhouse indoor temperatures in winter nights and the highest amount of heat added by the rock-bed fan as shown in Table 5.4. The rock-bed size of Scenario 4 is the smallest compared to other scenarios, and therefore, it has the lowest amounts of heat charged and discharged from the rock-bed thermal storage. As a result, it has the lowest greenhouse indoor temperatures in winter nights and the lowest amount of heat added by the rock-bed fan.
- As the rock-bed size increased, the ratio of heat discharged from the rock-bed to heat charged increased. However, the ratio became constant whenever the rock-bed volume was 37 m^3 or above (as in the Original scenario and Scenario 1) as

shown in Table 5.4. Therefore, Among the five scenarios, the rock-bed size of Scenario 1 is recommended to be used, since the difference between the amount of heat discharged from the rock-bed thermal storage and the minimum greenhouse indoor temperatures in the Original scenario and Scenario 1 simulation results is not significant. Also, the rock-bed volume in Scenario 1 is almost half of that in the Original scenario, which shows that installation cost savings can be achieved by selecting the rock-bed size of Scenario 1 instead of that of the Original scenario.

- Finally, the mechanical outside air ventilation is necessary in the attached solar greenhouse to avoid the undesirable high indoor temperatures especially in summer.

Table 5.4 Yearly charged, discharged heat and minimum greenhouse indoor temperature of each scenario, effect of the rock-bed size

(For all scenarios, solar heat gain into the greenhouse in winter and summer are 46 GJ and 64.5 GJ, respectively)

Scenario	Rock-bed volume (m^3)	Charged Heat (GJ)		Discharged heat (GJ)		Discharged /Charged heat (winter)	Heat added from fan (GJ)		Energy charged/ solar heat gain		Heat stored in rock-bed and lost to ground (GJ)	Minimum greenhouse indoor temperature (°C)
		W	S	W	S		W	S	W	S		
Original	57	8.9	18.6	6.2	0.08	0.7	0.21	0.25	0.19	0.29	21.2	-2
1	37	8.4	16.3	5.8	0.06	0.7	0.21	0.24	0.18	0.25	18.8	-3
2	14	7.8	13	5.2	0.05	0.68	0.2	0.23	0.17	0.2	15.6	-6
3	10	7.4	11.3	4.8	0.04	0.65	0.19	0.2	0.16	0.17	13.9	-7
4	7	6.8	9.2	4.3	0.03	0.62	0.18	0.17	0.15	0.14	11.7	-9

W: Winter (January -April, November-December)

S: Summer (May-October)

Heat stored in rock-bed and lost to ground= (Heat charged (winter + summer) – Heat discharged (winter + summer))

5.2 Recommendations

Attached greenhouses can be built for different purposes such as an extra living space, as solar collectors to reduce the heating requirement of the attached buildings or for plant production. The purpose of the attached greenhouse decides the factors which the owner should focus on the most. This work shows that when designing an attached solar greenhouse for plant production, many factors should be taken into consideration. Based on the results of this work and some of the conducted studies from the literature, these steps are recommended while designing an attached solar greenhouse:

- The orientation of the greenhouse is critical because it affects the solar heat gain. In cold climates, south oriented greenhouses are recommended since it maximizes the solar heat gain, and therefore, it reduces the heating costs of the greenhouse.
- Thermal storage systems can be used in greenhouses to take advantage of the surplus heat inside the greenhouse. This study showed that the rock-bed thermal storage was able to reduce the attached greenhouse heating and cooling requirements throughout the year. However, the rock-bed thermal storage was not sufficient enough to prevent the greenhouse from freezing whenever the ambient temperature falls below -23°C and to keep the greenhouse indoor temperature above the heating set-point temperature (10°C) whenever the ambient temperature falls below -2°C. Also, the rock-bed thermal storage was not sufficient enough to keep the greenhouse indoor temperature below the cooling set-point temperature (20°C) on sunny days. Therefore, it is recommended to have a backup heating and ventilation systems in the greenhouse.

- The greenhouse high production quality can be achieved by maintaining the optimal growing conditions inside the greenhouse. However, every plant has special optimal growing conditions, and therefore, the growing conditions of the plants which are intended to be grown inside the greenhouse should be carefully studied in order to pick the appropriate plants.
- Increasing the rock-bed size does not necessarily means improving the rock-bed performance in terms of installation and energy costs. As the results of this study showed that with 220 L/s air flow rate, the yearly amount of heat discharged from a rock-bed size of 37 m^3 was close to that of 57 m^3. Also, the minimum greenhouse indoor temperatures of the both rock-bed sizes were close as well.
- Double low-E glass cover material is recommended to be used for the side walls in greenhouses in cold climates, because it has very attractive characteristics such as high thermal resistance, high solar transmittance, low infrared transmittance and durability. As the results of this study showed that the greenhouse with Double low-E glass cover material had higher greenhouse indoor temperatures than those with other cover amterials.

5.3 Recommendations for future work

In this study, the outside air ventilation was used to cool the attached greenhouse whenever the indoor temperature exceeds 30°C. As a result, a significant amount of heat can be wasted to the outside environment. Future work is highly recommended to study using the excess heat in the attached solar greenhouse to heat the residential house (attached house) to reduce the heating requirement of the residential house instead of dumping the excess heat to the environment.

This study focused on the temperature control of the attached solar greenhouse. However, humidity control is essential to obtain high productivity. Based on the literature, whenever RH is around 95% condensation occurs in the cooler spots inside the greenhouse such as on the leaves (Vadiee, 2013), While low RH values cause plant desiccation (MacCullagh, 1978). Therefore, it is recommended that the inside RH of the greenhouse should be between 75-85% (Nederhoff, 1998; Vadiee, 2013). Moreover, the effect of the moisture added from crops through evapotranspiration was not included in the TRNNSYS model since the attached solar greenhouse was empty during this study. Therefore, future work should be done to develop an evapotranspiration model to represent the plants inside the greenhouse and a humidity control model to prevent any crop damages due to condensation or fungal diseases.

The attached solar greenhouse is located in Joliette/Quebec and the average temperatures of Quebec range between 5°C to 25°C in summer and −10°C to −25°C, in winter (Wikipedia contributors, 2019). A future work should focus on using the current

TRNSYS model to evaluate the performance of attached greenhouses in other parts of Canada with different climatic conditions.

70-80% of the greenhouse heating happens at night (Sanford, 2011). Thermal screens or curtains can be added to the greenhouse to reduce the heat loss at night, and therefore, reduce the heating requirement. Based on the type of curtains used in the greenhouse, the amount of heat loss reduction possible to achieve using curtains at night ranges from 20-75% (Sanford, 2011). Moreover, curtains can be used during summer as a shading device to reduce the cooling load of the greenhouse. Using curtains in greenhouses in cold climates to reduce the heating requirement and cooling load should be investigated.

As mentioned before, the ideal temperature inside the attached solar greenhouse depends on the type of plant grown. However, the current design of the attached solar greenhouse cannot be maintained at suitable growth temperatures without the use of supplementary heating systems. Therefore, future work on integrating solar technologies such as photovoltaics or PCMs in the current greenhouse design is highly recommended.

The passive heat gain from the rock-bed whenever the fan was off was not included in the energetic analysis of the rock-bed thermal storage. Therefore, the amount of heat discharged from the rock-bed thermal storage would be more realistic if a future analysis that takes into consideration the passive heat gain. Finally, an economic analysis should be conducted to evaluate the energy cost savings and the payback period of the overall system.

References

Aaslyng, J. M., Ehler, N., & Jakobsen, L. (2005). Climate control software integration with a greenhouse environmental control computer. Environmental Modelling & Software, 20(5), 521-527.

A. Bascetincelik, H.H. Ozturk, H.O. Paksoy, Y. Demirel. Energetic and exergetic efficiency of latent heat storage system for greenhouse heating Renewable Energy, 16 (1999), pp. 691-694.

Aghbashlo, M., Müller, J., Mobli, H., Madadlou, A., & Rafiee, S. (2015). Modeling and Simulation of Deep-Bed Solar Greenhouse Drying of Chamomile Flowers. Drying Technology, 33(6), 684–695.

American Society of Agricultural and Biological Engineers. 2008. Heating, Ventilating and Cooling Greenhouses. ANSI/ASAE EP 406.4 Jan 2003 (R2008). St. Joseph, MI.

Arizov, A., Niyazov, S.K., 1980. Rock-bed as a heat storage material for greenhouse applications. Applied Solar Energy 16, 430–437.

Asdrubali, F., Cotana, F., & Messineo, A. (2012). On the evaluation of solar greenhouse efficiency in building simulation during the heating period. Energies, 5(6), 1864–1880.

Bakos, G. C., & Tsagas, N. F. (2000). Technology , thermal analysis and economic evaluation of a sunspace located in northern Greece.

Bastien, D. (2015). Methodology for Enhancing Solar Energy Utilization in Solaria and Greenhouses Presented in Partial Fulfillment of the Requirements For the Degree of Doctor of Philosophy (Building Engineering) at, (December).

Bataineh, K. M., & Fayez, N. (2011). Analysis of thermal performance of building attached sunspace. Energy & Buildings, 43(8), 1863–1868.

Beckman, W. A., Broman, L., Fiksel, A., Klein, S. A., Lindberg, E., Schuler, M., & Thornton,

J. (1994). TRNSYS the most complete solar energy system modeling and simulation software. Renewable Energy, 5(1-4), 486-488.

Benli H, Durmus A. Performance analysis of a latent heat storage system with phase change material for new designed solar collectors in greenhouse heating. Solar Energy. 2009;83:2109–19.

Benli, H. (2011). Energetic performance analysis of a ground-source heat pump system with latent heat storage for a greenhouse heating. Energy Conversion and Management, 52(1), 581-589.

Bot, G., Braak, N. Van De, Challa, H., Hemming, S., Rieswijk, T., & Straten, G. (2005). The Solar Greenhouse : State of the Art in Energy Saving and Sustainable Energy Supply, 501–508.

Bouhdjar, A., Belhamel, M., Belkhiri, F. E., & Boulbina, A. (1996). Performance of sensible heat storage in a rockbed used in a tunnel greenhouse. Renewable Energy, 9(1–4), 724–728.

Bouhdgar, A., Boulbing, A., 1990. Rockbed as a heat storage material for greenhouse heating. In: Sayigh Reading, A. (Ed.), Proceedings of Congress Energy and the Environment, UK, London, pp. 2325–2327.

Boulard, T., Fatnassi, H., Majdoubi, H., & Bouirden, L. (2008). Airflow and microclimate patterns in a one-hectare canary type greenhouse: An experimental and CFD assisted study. Acta Horticulturae, 801 PART 2, 837–845.

Boulard, T., Baille, J., 1987. Thermal performance and model of two types of greenhouses with solar energy storage. Acta Horticulture 263, 121–130.

Brendenbeck, H., 1987. Greenhouse heating using rockbed heat storage system. In: von Zabeltitz, C. (Ed.), Greenhouse Heating with Solar Energy. REU Technical Series 1. FAO, ENEA, Roma, pp. 89–95.

Bricault, M., 1982. Use of heat surplus from a greenhouse for soil heating. In: Proceedings of the International Conference on Energex 82, Regina, pp. 564–568.

Carnegie, E.J., Walter, V.R., Niles, P.W., 1984. Shallow solar pond to heat greenhouses. Acta Horticulturae 2 (184), 791–798.

Cemek, B., Demir, Y., Uzun, S., & Ceyhan, V. (2006). The effects of different greenhouse covering materials on energy requirement , growth and yield of aubergine, 31, 1780–1788.

Chai, T., & Draxler, R. R. (2014). Root mean square error (RMSE) or mean absolute error (MAE)? – Arguments against avoiding RMSE in the literature. Geoscientific Model Development, 7(3), 1247-1250

Chauhan, P. M. (1995). CONOMIC DESIGN OF A ROCK BED ST0 AGE DEVICE FOR STORING SOLAR THERMAL ENERGY e., 55, 29–37.

Chen J, Xu F, Tan D, Shen Z, Zhang L, Ai Q. A control method for agricultural greenhouses heating based on computational fluid dynamics and energy prediction model. Appl Energy 2015;141:106–18.

Chen, W., & Liu, W. (2004). Numerical and experimental analysis of convection heat transfer in passive solar heating room with greenhouse and heat storage. Solar Energy, 76(5), 623–633.

Costa, J.M., Heuvelink, E. and Botden, N. (eds.). 2004. Greenhouse Horticulture in China: Situation & Prospects. Horticultural Production Chains group. Wageningen University, The Netherlands, 140 p.

Critten, D. L., & Bailey, B. J. (2002). A review of greenhouse engineering developments during the 1990s. Agricultural and Forest Meteorology, 112(1), 1–22.

Duffie, J. A., & Beckman, W. A. (2013). Solar engineering of thermal processes. Hoboken: John Wiley.

Dragicevic, S. (2011). Determining the optimum orientation of a greenhouse on the basis of the total solar radiation availability. Thermal Science, 15(1), 215-221.

Eugene A. Scales and Associates. (2003). Energy Conservation Opportunities for Greenhouse Structures. Minnesota: Minnesota Department of Commerce Energy Office.

Fernandez, J. E., & Bailey, B. J. (1994). The Influence of Fans on Environmental Conditions in Greenhouses. Journal of Agricultural Engineering Research.

Flores-Velazquez, J., Montero, J. I., Baeza, E. J., Lopez, J. C., Pérez-Parra, J. J., & Bonachela, S. (2009). Analysis of Mechanical Ventilation in a Three-Span Greenhouse Using Computational Fluid Dynamics (Cfd), (April 2011).

Fourcy, A., 1982. Use of solar energy for heating of greenhouses in mild winter climates. In: Bilgen, E., Hollands, K.G.T. (Eds.), Proceedings of Conference on Solar Greenhouses, Perpignan, p. 133.

Fotiades, I., 1987b. Use of solar energy for heating of greenhouses. In: von Zabeltitz, C. (Ed.), Energy Conservation and Renewable Energies for Greenhouse Heating. REU Technical Series 3. FAO, ENEA, Roma, pp. 28–35.

Gauthier, C., Lacroix, M., & Bernier, H. (1997). Numerical simulation of soil heat exchanger-storage systems for greenhouses. Solar Energy, 60(6), 333–346.

Goldammer, T. (2017). Greenhouse Management, A Guide to Operations and Technology. 1st ed. Apex Publishers.

Grafiadellis, M., 1987. Recent experiences with passive system for heating greenhouses. In: von Zabeltitz, C. (Ed.), Greenhouse Heating with Solar Energy. REU Technical Series 1. FAO, ENEA, Roma, pp. 167–173.

Ghosal, M. K., Tiwari, G. N., & Srivastava, N. S. L. (2004). Thermal modeling of a greenhouse with an integrated earth to air heat exchanger : an experimental validation, 36, 219–227.

Gupta, M. J., & Chandra, P. (2002). Effect of greenhouse design parameters on conservation of energy for greenhouse environmental control. Energy, 27(8), 777–794.

Hänchen, M., Brückner, S., & Steinfeld, A. (2011). High-temperature thermal storage using a packed bed of rocks - Heat transfer analysis and experimental validation. Applied Thermal Engineering, 31(10), 1798–1806.

Hemming, S., Kempkes, F., & Mohammadkhani, V. (2007). New glass coatings for high insulating greenhouses without light losses – energy saving , crop production and economic potentials.

Honeywell. (n.d.). honeywell-sensing-hih4000 series-product-sheet-009017-5-EN. Retrieved from www.honeywell.com/sensing.

Howell, R. H., Sauer, H. J., & Coad, W. J. (2005). Principles of Heating, Ventilating and Air Conditioning.

Huang, B.K., Ozisik, M.N., Toksoy, M., 1981. Development of greenhouse solar drying for farm crops and processed products. AMA (Japan) 12 (1), 47–52.

Hughes, P.J., 1975. The design and predicted performance of Arlington House. MSc thesis, University of Wisconsin – Madison.

Hughes, P.M., Klein, S.A., and Close, D., "Packed Bed Thermal Storage Models for Solar Air Heating and Cooling Systems", Journal of Heat Transfer, May (1976).

Jain, D. (2005). Modeling the performance of greenhouse with packed bed thermal storage on crop drying application. Journal of Food Engineering, 71(2), 170–178.

Jeffreson, C. P., "Prediction of Breakthrough Curves in Packed Beds," AIChE Journal, Vol. 18, No. 2, Mar. 197.

Jelinkova, H., 1987. Utilization of solar energy in greenhouse. In: von Zabeltitz, C. (Ed.), Greenhouse Heating with Solar Energy. REU Technical Series 1. FAO, ENEA, Roma, pp. 86–93.

Judkoff, R. D., Mcdowell, T. P., Rees, S. J., Witte, M. J., Newman, H. M., Marriott, C. E., … Peterson, J. C. (2011). ASHRAE ADDENDA Standard Method of Test for the Evaluation of Building Energy Analysis Computer Programs, 8400.

Kavin, J., Kurtan, S., 1987. Utilization of solar energy in greenhouse. In: von Zabeltitz, C. (Ed.), Greenhouse Heating with Solar Energy. REU Technical Series 1. FAO, ENEA, Roma, pp. 178–185.

Kendirli B. Structural analysis of greenhouses: a case study in Turkey. Build Environ 2006;41:864–71.

Kittas, C., Karamanci, M. and Katsoulas, N. 2005. Air temperature in a forced ventilation greenhouse with rose crop. Energy and Building 37:807-812.

Kürklü, A., Bilgin, S., & Özkan, B. (2003). A study on the solar energy storing rock-bed to heat a polyethylene tunnel type greenhouse. Renewable Energy, 28(5), 683–697.

Kurklu A, Bilgin S. Cooling of a polyethylene tunnel type greenhouse by means of a rock bed. Renew Energy 2004; 29:2077–86.

Kuznik, F., David, D., Johannes, K., & Roux, J. J. (2011). A review on phase change materials integrated in building walls. Renewable and Sustainable Energy Reviews, 15(1), 379–391.

Kyritsis, S., Mavrogianopoulos, G., 1987. Passive system for heating greenhouses. In: von Zabeltitz, C. (Ed.), Energy Conservation and Renewable Energies for Greenhouse Heating. REU Technical Series 3. FAO, ENEA, Roma, pp. 111–117.

LBNL, 2013, WINDOW 6.3, Lawrence Berkeley National Laboratory: https://windows.lbl.gov/software/window/6/.

Löf, G. O. G. and R.W. Hawley, Ind. Eng. Chem., 40, 1061 (1948), "Unsteady states heat transfer between air and loose solids.''

Low-e glass in buildings, Impact on the environment and on energy savings, Groupement Europeen des Producteurs de Verre Plat, 2000.

MacCullagh, J. C., Ruttle, J., MacCullagh, R. H., & MacKinnon, D. J. (1978). The solar greenhouse book. Emmaus, PA: Rodale Pr.

Malone, P. (2011). Web Energy Logger (WEL) User Guide : Rev 4 . 0 . 3 Table of Contents :, 1–39.

Martinović G, Simon J. Greenhouse microclimatic environment controlled by a mobile measuring station. NJAS – Wageningen J Life Sci 2014;70–71:61–70.

Maxim Integrated Products, I. (2015). SDS2438 Smart Battery Monitor, 1–29.

Maxim Integrated Products, I. (2015a). DS18B20 Programmable Resolution 1-Wire Digital Thermometer DS18B20 Programmable Resolution 1-Wire Digital Thermometer Absolute Maximum Ratings, 92, 1–20.

Maxim Integrated Products, I. (2015b). SDS2438 Smart Battery Monitor, 1–29.

Mihalakakou, G. (2002). On the use of sunspace for space heating / cooling in Europe, 26, 415–429.

Mongkon, S., Thepa, S., Namprakai, P., & Pratinthong, N. (2013). Cooling performance and condensation evaluation of horizontal earth tube system for the tropical greenhouse. Energy & Buildings, 66, 104–111.

Molina-Aiz, F. D., Valera, D. L., & Álvarez, A. J. (2004). Measurement and simulation of climate inside Almería -type greenhouses using computational fluid dynamics. Agricultural and Forest Meteorology, 125(1–2), 33–51.

Monge-barrio, A., & Sánchez-ostiz, A. (2015). Energy efficiency and thermal behaviour of attached sunspaces , in the residential architecture in Spain . Summer Conditions. Energy & Buildings, 108, 244–256.

Nash, R., Williamson, J., 1978. Greenhouse heating using solar energy. In: Bilgen, E., Hollands, K.G.T. (Eds.), Proceedings of ISES Solar World Congress, Hamburg, pp. 64–69.

O. Ercan Ataer, (2006), STORAGE OF THERMAL ENERGY, in Energy Storage Systems, [Ed. Yalcin Abdullah Gogus], in Encyclopedia of Life Support Systems (EOLSS), Developed under the Auspices of the UNESCO, Eolss Publishers, Oxford ,UK.

OSRAM Opto Semiconductors GmbH (2015). Silicon PIN Photodiode SFH 203 P, 5, 1–9.

Owrak, M., Aminy, M., Jamal-abad, M. T., & Dehghan, M. (2015). Experiments and simulations on the thermal performance of a sunspace attached to a room including heat-storing porous bed and water tanks. Building and Environment, 92, 142–151.

Ozgener, O., & Ozgener, L. (2011). Determining the optimal design of a closed loop earth to air heat exchanger for greenhouse heating by using exergoeconomics. Energy & Buildings, 43(4), 960–965.

Öztürk, H.H., 2005. Experimental evaluation of energy and exergy efficiency of a seasonal latent heat storage system for greenhouse heating. Energy Conversion and Management 46, 1523–1542.

Öztürk, H. H., & Başçetinçelik, A. (2003). Energy and Exergy Efficiency of a Packed-bed Heat Storage Unit for Greenhouse Heating. Biosystems Engineering, 86(2), 231–245.

Ozturk, H.H., Bascetincelik, A., (2003b). Effect of thermal screens on the microclimate and overall heat loss coefficient in plastic tunnel greenhouse. Turkish Journal of Agriculture and Forestry 27 (3), 123–134.

Papadopoulos, A. P., & Hao, X. (1997). Effects of three greenhouse cover materials on tomato growth , productivity , and energy use, 70, 165–178.

Paula A. Claudino. (2016). EXPERIMENTAL AND MODELLING STUDY OF A GEODESIC DOME SOLAR GREENHOUSE SYSTEM IN OTTAWA. McMaster University.

Rick, B. (2014). Measuring Forecast Accuracy. Retrieved from https://www.slideshare.net/steelwedgesoftware/forecast-accuracy-webinar-may-2014.

Rodgers, J. L., & Nicewander, W. A. (1988). Thirteen Ways to Look at the Correlation Coefficient. The American Statistician, 42(1), 59.

Sanford, S. (2009). Reducing greenhouse energy consumption — An overview, 1–16.

Santamouris, M., Balaras, C. A., Dascalaki, E., & Vallindras, M. (1994). Passive solar agricultural greenhouses: A worldwide classification and evaluation of technologies and systems used for heating purposes. Solar Energy, 53(5), 411–426.

Santamouris, M., Mihalakakou, G., Balaras, C. a., Lewis, J. O., Vallindras, M., & Argiriou, a. (1996). Energy conservation in greenhouses with buried pipes. Energy, 21(5), 353–360.

Santamouris, M., Argiriou, A., & Vallindras, M. (1994). Design and operation of a low energy consumption passive solar agricultural greenhouse. Solar Energy,52(5), 371-378.

Santamouris, M., Balaras, C. A., Dascalaki, E., Vallindras, M., 1994b. Passive solar agricultural greenhouses: A worldwide classification and evaluation of technologies and systems used for heating purposes. Solar Energy 53 (5), 411–426.

Santamouris, M., 1993. Active solar agricultural greenhouse. The state of art. International Journal of Solar Energy 14, 19–32.

Seem, J.E., "Modeling of Heat in Buildings," Ph. D. thesis, Solar Energy Laboratory, University of Wisconsin Madison (1987).

Seginer, I., 1997. Alternative design formulae for the ventilation rate of greenhouses. Journal of Agricultural Engineering Research 68 (4), 355‐365.

Sethi, V. P., & Sharma, S. K. (2008). Survey and evaluation of heating technologies for worldwide agricultural greenhouse applications. Solar Energy, 82(9), 832–859.

Sethi, V. P. (2009). On the selection of shape and orientation of a greenhouse: Thermal modeling and experimental validation. Solar Energy, 83(1), 21–38.

Sharon M. Rudnitski (Ed.). (1987). Energy-conserving urban greenhouses for Canada. Canada: Minister of Supply and Services Canada.

Sharma, A., Tyagi, V. V, Chen, C. R., & Buddhi, D. (2009). Review on thermal energy storage with phase change materials and applications, 13, 318–345.

Sharma PV (2002) Environmental and engineering geophysics. Cambridge University Press, Cambridge.

Simone Rudge, A. M. F. (n.d.). Greenhouses for the Northern Climate, 1–41. Retrieved from,http://www.emr.gov.yk.ca/agriculture/pdf/Greenhouses_for_the_Northern_Climate.pdf

Singh RD, Tiwari GN. Energy conservation in the greenhouse system: a steady state analysis. Energy 2010;35:2367–73.

Solar Energy Laboratory, University of Wisconsin–Madison. (2012). TRNSYS: A Transient Systems Simulation Tool. Accessible online at http://sel.me. wisc.edu/trnsys/.

Solar Energy Laboratory. (2009). TRNSYS 17: A TRaNsient SYstem Simulation program – Multi zone building modeling .Solar Energy Laboratory, University of Wisconsin-Madison., 5.

Solar greenhouses-Canada. I. Canada. Agriculture Canada. Research Branch. II. Series: Publication (Canada. Agriculture Canada). English; 1814E.

Stanghellini C, Kempkes FLK, Knies P (2003). Enhancing Environmental Quality in Agricultural Systems. Acta Horticulturae, 609: 277-283.

Stanghellini, C, Meurs, W. V. (1992). Environmental control of greenhouse crop transpiration. Journal of Agricultural Engineering Research, 51, 297-311.

Statistics Canada. Table 001-0047 - Estimates of specialized greenhouse operations, greenhouse area, and months of operation, annual, CANSIM (database). (accessed: 2017-04-26).

Statistics Canada. Table 001-0052 - Greenhouse producers' operating expenses, annual (dollars), CANSIM (database). (accessed: 2017-04-26)

Stanciu, C., Stanciu, D., & Dobrovicescu, A. (2016). Effect of greenhouse orientation with respect to E-W axis on its required heating and cooling loads, 85(November 2015), 498–504.

Tyagi, V. V., Pandey, A. K., Buddhi, D., & Kothari, R. (2016). Thermal performance assessment of encapsulated PCM based thermal management system to reduce peak energy demand in buildings. Energy and Buildings, 117, 44–52.

Vadiee, A. (2013). Energy Management in Large scale Solar Buildings: The Closed Greenhouse Concept.

Vadiee, A. (2011). Energy Analysis of the Closed Greenhouse Concept. Stockholm: KTH, 1–154.

Van Kooten, O., Heuvelink, E. and Stanghellini, C. 2008. New developments in greenhouse technology can mitigate the water shortage problem of the 21st century. Acta Hort. 767: 45-52.

Waples, D. W., & Waples, J. S. (2004). A Review and Evaluation of Specific Heat Capacities of Rocks , Minerals , and Subsurface Fluids . Part 1 : Minerals and Nonporous Rocks, 13(2).

Wikipedia contributors. (2019, January 29). Quebec. In Wikipedia, The Free Encyclopedia. Retrieved 17:44, January 29, 2019, from https://en.wikipedia.org/w/index.php?title-=Quebec&oldid=880798410.

Willits, D. H., Chandra, P., & Peet, M. M. (1985). Modelling solar energy storage systems for greenhouses. Journal of Agricultural Engineering Research, 32(1), 73–93.

Yildiz, A., Ozgener, O., & Ozgener, L. (2011). Exergetic performance assessment of solar photovoltaic cell (PV) assisted earth to air heat exchanger (EAHE) system for solar greenhouse cooling. Energy & Buildings, 43(11), 3154–3160.